PROCESS SYNTHESIS AND OPTIMIZATION OF BIOREFINERY CONFIGURATIONS

A Dissertation

by

VIET PHAM

Submitted to the Office of Graduate Studies of
Texas A&M University
in partial fulfillment of the requirements for the degree of

DOCTOR OF PHILOSOPHY

August 2011

Major Subject: Chemical Engineering

Process Synthesis and Optimization of Biorefinery Configurations

PROCESS SYNTHESIS AND OPTIMIZATION OF BIOREFINERY CONFIGURATIONS

A Dissertation

by

VIET PHAM

Submitted to the Office of Graduate Studies of
Texas A&M University
in partial fulfillment of the requirements for the degree of

DOCTOR OF PHILOSOPHY

Approved by:

Chair of Committee,	Mahmoud El-Halwagi
Committee Members,	Guy Curry
	Mark Holtzapple
	Sam Mannan
Head of Department,	Michael Pishko

August 2011

Major Subject: Chemical Engineering

ABSTRACT

Process Synthesis and Optimization of Biorefinery Configurations. (August 2011)
Viet Pham, B.S., University of Technology, Ho Chi Minh City, Vietnam;
M.S., Texas A&M University
Chair of Advisory Committee: Dr. Mahmoud El-Halwagi

The objective of this research was to develop novel and applicable methodologies to solve systematically problems along a roadmap of constructing a globally optimum biorefinery design. The roadmap consists of the following problems: (1) synthesis of conceptual biorefinery pathways from given feedstocks and products, (2) screening of the synthesized pathways to identify the most economic pathways, (3) development of a flexible biorefinery configuration, and (4) techno-economic analysis of a detailed biorefinery design.

In the synthesis problem, a systems-based "forward-backward" approach was developed. It involves forward synthesis of biomass to possible intermediates and reverse synthesis starting with desired products and identifying necessary species and pathways leading to them. Then, two activities are performed to generate complete biorefinery pathways: *matching* (if one of the species synthesized in the forward step is also generated by the reverse step) or *interception* (a task is determined to take a forward-generated species with a reverse-generated species by identifying a known process or by using reaction pathway synthesis to link to two species.)

In the screening problem, the Bellman's Principle of Optimality was applied to decompose the optimization problem into sub-problems in which an optimal policy of available technologies was determined for every conversion step. Subsequently, either a linear programming formulation or dynamic programming algorithm was used to determine the optimal pathways.

In the configuration design problem, a new class of design problems with flexibility was proposed to build the most profitable plants that operate only when economic

efficiency is favored. A new formulation approach with proposed constraints called disjunctive operation mode was also developed to solve the design problems.

In the techno-economic analysis for a detailed design of biorefinery, the process producing hydrocarbon fuels from lignocellulose via the carboxylate platform was studied. This analysis employed many state-of-the-art chemical engineering fundamentals and used extensive sources of published data and advanced computing resources to yield reliable conclusions to the analysis.

Case studies of alcohol-producing pathways from lignocellulosic biomass were discussed to demonstrate the merits of the proposed approaches in the former three problems. The process was extended to produce hydrocarbon fuels in the last problem.

DEDICATION

To my family: parents, wife, and daughter.

ACKNOWLEDGEMENTS

I owe my deepest gratitude to my academic advisor, Dr. Mahmoud El-Halwagi, for his consistently great support and encouragement that enable me to develop understanding of process system engineering and to achieve key successes in my life. This dissertation would not have been possible without his insightful and thoughtful guidance. I have been so lucky to have such a remarkable advisor in the college years for my master's and doctoral programs.

I am grateful to Dr. Mark Holtzaple for making every effort to provide data, guidance, thoughts, and edits to make Chapter IV possible with a high quality. I am also thankful to other members of the research committee: Dr. Sam Mannan, Dr. Guy Curry, and Dr. Carl Laird (who served as a member for most of the research). This dissertation has been significantly improved with the valuable help of the committee which ideally suited to the research area.

I would like to thank the students in the Process Integration and Systems Optimization group, some other fellow students in the Department of Chemical Engineering, and the departmental staff for making it a friendly academic environment.

I am indebted to my family who supported me with unconditional love and care.

Financial support by the U.S. Department of Energy is gratefully acknowledged.

NOMENCLATURE

Abbreviations

ABE	Acetone-Butanol-Ethanol
AIChE	American Institute of Chemical Engineers
ASPEN	Advanced Simulator for Process Engineering
CPDM	Continuum Particle Distribution Model
CS	Carbon Steel
CSTR	Continuous Stirred-Tank Reactor
DB	Declining Balance
DDB	Double Declining Balance
DOE	Department of Energy
DS&B	Direct Salaries and Benefits
DW&B	Direct Wage and Benefits
EIA	Energy Information Administration
FCI	Fixed Capital Investment
FOB	Free on Board
LRT	Liquid Residence Time
MACRS	Modified Accelerated Cost Recovery System
MINLP	Mixed-Integer Nonlinear Programming
MPSP	Minimum Product Selling Price
MS&B	Maintenance Salaries and Benefits
MW&B	Maintenance Wage and Benefits
NREL	National Renewable Energy Laboratory
PEA	Process Economic Analyzer
PPI	Producer Price Index
PSA	Pressure-Swing Adsorption
RAM	Random Access Memory
ROI	Return on Investment

SS	Stainless steel
TCI	Total Capital Investment
VS	Volatile Solid
VSLR	Volatile Solid Loading Rate
WCI	Working Capital Investment

Variables

content	component flow rate of feedstock
d	design variable
δ	fractional variation of uncertainty
f	flow rate to and from equipment
F	Flexibility level
λ	Kuhn-Tucker multipler
msize	maximum size of equipment
prod	product flow rate
r	value of objective function of the optimization problem
revenue	revenue of plant operation
s	slack variable
size	size of equipment
supply	flow rate of feedstock
tflow	total inlet flow rate of equipment
U	upper bound of the slack variable
waste	flow rate of waste streams
x	state variable
y	binary variable
z	control variable

Parameters

AVAIL	availability of feedstock
ΔT	temperature approach of latent heat exchangers without fouling

$\Delta T'$	temperature approach of latent heat exchangers with fouling
A	heat transfer area of latent heat exchanger without fouling
A'	heat transfer area of latent heat exchanger with fouling
A_0	base-case heat transfer area of latent heat exchanger
CAPCOEF	coefficient of capital cost function
COST	cost of feedstock
DEMAND	demand of product
FRACTION	composition of feedstock
LB	lower bound
M	big-M – a scalar whichis big enough to deactivate a contraint
m	fouling factor
n	number of control variable (Chapter III) or oversizing factor (Chapter IV)
OPCOEF	coefficient of operating costs
P	number of scenarios
PRICE	price of products
PROB	occurrence probability of scenarios
q	heat flux in latent heat exchangers
q'	fouling heat flux in latent heat exchangers
q_0	base-case heat flux in latent heat exchangers
Q	heat transfer load in latent heat exchanger in non-fouling conditions
Q'	heat transfer load in latent heat exchanger in fouling conditions
SCALE	power of capital cost functions
SIZECOEF	coefficient of sizing equations
θ	uncertainty variable
U	heat transfer coefficient of latent heat exchanger in non-fouling conditions
U'	heat transfer coefficient of latent heat exchanger with fouling

UB	upper bound
w	weighting factor of scenarios
x	design parameter

Indices

i	node in the synthesized branching trees (Chapter II) or feedstock (Chapter III)
j	node in the synthesized branching trees (Chapter II) or equipment (Chapter III)
k	product
m	component
m'	component
n	node adjacent to node *n'* in the synthesized branching trees
n'	node adjacent to node *n* in the synthesized branching trees
N	the final (product) node
p	scenario

Superscripts

flow	regarding flow rates
IN	inlet
k	vertex of polyhedron of uncertainty region
N	nominal value
OUT	outlet
p	scenario

Sets

D	set of design variables
J	set of equipment indices
R	feasible region of uncertainty realization
T	region of uncertainty

X	set of state variables
Z	set of control variables

Functional notations

f	function of objective values regarding constituent conversion steps (Chapter II) or general functions in constraints of flexibility-design problem (Chapter III)
g	function of mass and energy balances, and other equality relations
h	function of specifications and limitations in constraints of the optimization problems
Y	function of design parameters

Units

gal	gallon
GB	gigabyte
GHz	gigahertz
h	hour
kg	kilogram
m	meter
MJ	megajoule
MMBtu	million British thermal unit
MMGPY	million gallon per year
MW	megawatts
SCF	standard cubic foot
tonne	a metric weight unit, equal to 1,000 kilograms.
yr	year

TABLE OF CONTENTS

Page

CHAPTER Page

Page

LIST OF FIGURES

Page

Page

Page

LIST OF TABLES

Page

Page

CHAPTER I
INTRODUCTION

With the growing attention to sustainable development, the concept of biorefineries is gaining an increasing attention. A biorefinery is a processing facility that receives biomass feedstocks and produces one or more chemical products and/or biofuels through a system of physical/chemical/biological processes. The resurging interest in biorefineries has been motivated by the dwindling fossil-fuel resources and increasing attention to strategies that reduce greenhouse-gas emissions. Several lab-scale concepts have been developed to produce biofuels; however, there are still very few biorefineries that have been commercialized to meet the techno-economic criteria for biofuels.

Well-developed approaches to the synthesis of reaction pathways are not suitable for problems of biorefinery design which have specific characteristics. Recently, a certain processing platform is usually chosen based on developer's interest, preferences, and experience without a thorough analysis or systematic approach to determine the best option. Although the development of the chosen option can lead to feasible biorefineries, the economic may not be viable. More importantly, new biorefinery configurations with better performance may not be generated. There is a critical need to quickly and methodically generate cost-effective and innovative biorefinery configurations.

The objective of this research is to develop novel and applicable methodologies to systematically solve the problems along a roadmap of constructing a globally optimum biorefinery design. The roadmap consists of the following steps: (1) synthesis of conceptual biorefinery pathways from given feedstocks and products, (2) screening of the synthesized pathways to identify the most economic pathways, (3) development of a flexible biorefinery configuration, and (4) techno-economic analysis of a detailed biorefinery design. The approaches to first two steps will be developed in Chapter II. The third and fourth problems will be addressed in Chapters III and IV, respectively.

This dissertation follows the style of *AIChE Journal*.

CHAPTER II
PRELIMINARY SYNTHESIS AND OPTIMIZATION OF BIOREFINERY PATHWAYS

2.1 Introduction

Recently, there has been a growing interest in research and development activities to develop technologies leading to cost-effective renewable energy. Traditional approaches to the design of biorefinery configurations usually do not lead to a globally optimum solution whereas systematic approaches developed for similar process system engineering problems are not well suited for biorefinery design.

A common approach to the design of biorefinery configurations is to start with a core conversion technology, which is usually located at the front end of a biorefinery (e.g., pretreatment, hydrolysis, fermentation, digestion, gasification, and pyrolysis), then add pre-processing and post-processing units for feedstock preparation and product separation and upgradation. Another common approach is to scale up the same units developed at the laboratory scale and revise the process configuration based on the practical aspects of large-scale production. Although these approaches can lead to process configurations that work, their overall performance may not be attractive. Furthermore, they may severely hinder innovation of new configurations.

This chapter proposes a novel two-stage approach to the synthesis and optimization for the design of biorefinery configurations. In the synthesis work with specified feedstocks and products, possible pathways are created to include conversion steps that are based on proven reactions or available technologies. A pathway synthesis method referred to as the “forward-backward” approach is introduced. It involves forward synthesis of biomass to possible intermediates and reverse synthesis starting with desired products and identifying necessary species and pathways leading to them. In the optimization work to determine an optimal configuration from the synthesized pathways, a preprocessing step of selecting an optimal policy in every conversion step of the

pathways is performed. This preprocessing step reduces the size of the subsequent optimization calculations.

2.2 Problem description

The problem can be described as follows: Given a set of biomass feedstocks with known flowrates and characteristics and a desired final product with specifications, it is desired to develop a systematic methodology to generate optimal configurations from feedstocks to products. Available for service is a set of conversion technologies with known performance. Various objectives may be considered such as the highest yield, the highest energy efficiency, the shortest route (the least number of processing steps), the minimum-cost route, or the most sustainable route (as characterized by sustainability metrics). Figure 1 shows the inputs and outputs of the problem.

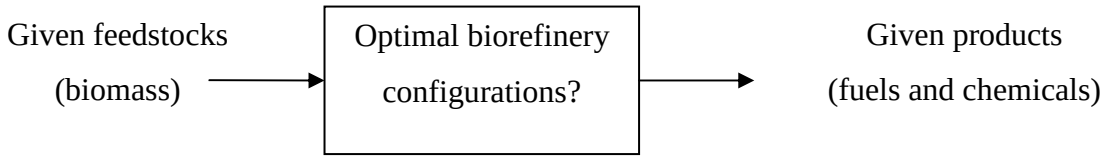

Figure 1. Schematic problem description.

2.3 Literature review

Several important pathways to produce transportation fuels and chemicals from biomass can be found in literature. Huber et al.[1] provided a review of current and possible future pathways for obtaining transportation fuels. Kamm and Kamm[2] and Fernando et al.[3] reviewed product trees of four biorefinery systems: lignocellulosic feedstock biorefinery, green biorefinery, whole-corn biorefinery, and biorefinery with integration of thermochemical and biochemical platforms. Fernando et al.[3] proposed an integration between biorefineries and petroleum refineries to produce 12 potential chemicals in addition to conventional fuels.

Databases of biomass-derived chemicals were developed at National Renewable Energy Laboratory. Werpy and Petersen[4] reported a large collection of chemicals that

can be derived from sugar and syngas. Holladay et al.[5] made a similar effort to find the most promising chemicals derived from lignin.

Various techniques have been developed for reaction pathway synthesis. The earlier work in the 1970's was reviewed by Agnihotri and Motard[6] and Nishida et al.[7] Proposed techniques in that period included matrix synthesis approach,[8] symbol triangle approach,[9] retro-synthesis approach,[10, 11] minimum Gibbs free energy approach,[12] and geometry synthesis approach.[13] The approach using Gibbs free energy was further developed in the 1980's.[6,14,15] In the 1990's, environmental aspects were incorporated in the synthesis of reaction pathways.[16-18] Recently, optimization-based approaches[19,20] and an evolutionary technique[21] for reaction path synthesis were introduced.

A systematic approach to the synthesis of optimal biorefinery pathways was reported by Bao et al.[22] The approach is based on developing a superstructure of conversion technologies and resulting intermediate chemicals then using a tree-branching and searching technique to determine candidate pathways.

Several papers have focused on the techno-economic analysis and optimization of specific production pathways such as ethanol,[23-27] biodiesel,[28,29] mixed alcohols and transportation fuels,[30-32] and energy.[33,34] There is also research to establish processing routes with minimum energy consumption prior to establishing the optimal products.[3,35-37] Elms and El-Halwagi[38] introduced an optimization routine for feedstock selection and scheduling for biorefineries and included the impact of greenhouse gas policies on the biorefinery design. Pokoo-Aikins et al.[39] included safety metrics along with process and economic metrics to guide the design and screening of biorefineries.

The optimization problem to determine the best pathway from the synthesized ones has been investigated by several researchers. Optimization has been performed based on yield,[22] entropy analysis,[40] optimization framework,[41] and modular platform.[42] Ng[43] used a pinch analysis for an automated targeting procedure to find the highest production rate and revenue without a detailed design of biorefineries. Alvarado-Morales et al.[35] applied principles of group-contribution to predict pure-component properties to simultaneously model, design, and synthesize biorefineries.

2.4 Proposed approach

The proposed approach involves synthesis and optimization tasks. The following are the main steps:

- Forward and backward branching
- Matching
- Screening
- Selecting optimal policies between each two consecutive nodes
- Optimizing pathways

These steps are explained in the ensuing sections.

2.4.1 The synthesis problem

To avoid generating complex (and potentially impractical) configurations, the number of conversion steps in the synthesis problem is limited to five. Each conversion step is a reaction system (a reactor or a set of reactors), followed by separation units necessary to purify the produced chemicals to appropriate levels for the next conversion steps. Pretreatment of lignocellulosic biomass is not counted as one of the conversion steps. The synthesis approach involves forward synthesis of biomass to possible intermediates and reverse synthesis starting with the desired products and identifying the necessary species and pathways leading to them. Once the feedstock-forward and the product-backward pathways are synthesized, two activities are performed: *matching* (which corresponds to direct connection of two species if one of the species synthesized in the forward step is also generated by the backward step) and *interception* (which refers to the addition of a conversion steps to convert a forward-generated species to a backward-generated species). The interception task may be detailed by identifying known processes to achieve such conversion or by using reaction pathway synthesis to link the two species.

Figure 2 illustrates an example of the branching trees. Each node represents an intermediate compound (i.e., a species) and each arc represents a conversion step. In the forward branching problem, the branching starts from the feedstock node. The nodes connecting to the feedstock node are compounds that can be directly produced from the

feedstock through one conversion technology. Two forward steps are allowed from the feedstock. For example, a carbohydrate feedstock can be converted into methane (by digestion), sugar (by enzymatic hydrolysis), syngas (which is a mixture of carbon monoxide and hydrogen, by gasification), etc. The next layer of nodes lists compounds that can be produced from the compounds at the previous nodes. For example, acetylene is produced from methane (by cracking). This is called the “forward problem" because the branching direction is co-current with the processing flows.

In the reverse problem, the branching originates from the final product node and is countercurrent to the processing flows. Two backward steps are taken from the final product. For example as shown by Figure 2, node Bromoethane (C_2H_5Br) connects to node Ethanol because bromoethane can be hydrolyzed into ethanol. One of the chemicals that can be used to produce bromoethane (by hydrobromination) is ethylene.

Next, nodes from the forward branching tree and from the backward branching tree are connected in one of two ways: *matching* or *interception*. An example of *matching* is when sugar appears as both a forward node and a backward node (see Figure 2). By connecting the two sugar nodes, a pathway is created from biomass to ethanol. An example of *interception* is the use of hydrogenation step (see Figure 2) to connect nodes Acetylene (C_2H_2) and Ethylene (C_2H_4), making another complete pathway from the biomass to the ethanol.

As a result of the synthesis problem, one or more complete pathways connecting a feedstock and products are found. Although based on known building blocks, the generated pathways can be novel because of their interconnections. The generated pathways can also be quickly constructed and screened. Figure 3a is an example of a superstructure of synthesized pathways. Lettered nodes represent intermediate compounds. Between each two nodes, there can be more than one pathway (e.g., the pathway from Feedstock to E) or arc (e.g., A-G, D-E, E-H, and F-I). It is useful to identify optimal pathways between nodes, which is described in the next section.

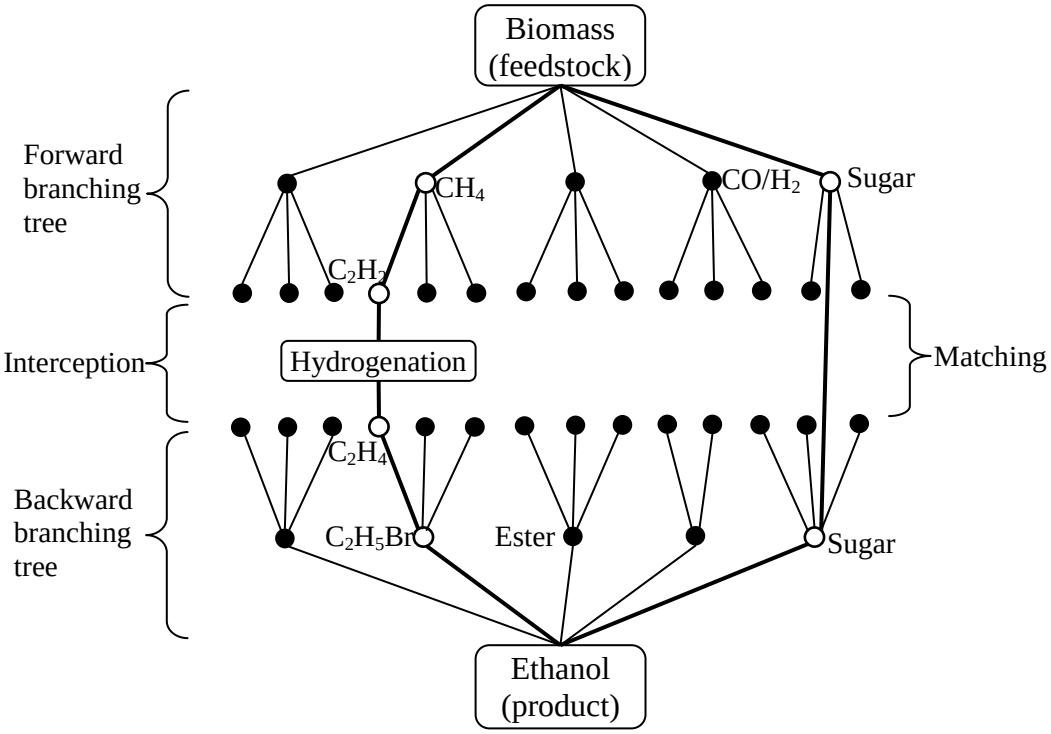

Figure 2. Forward and reverse branching trees.

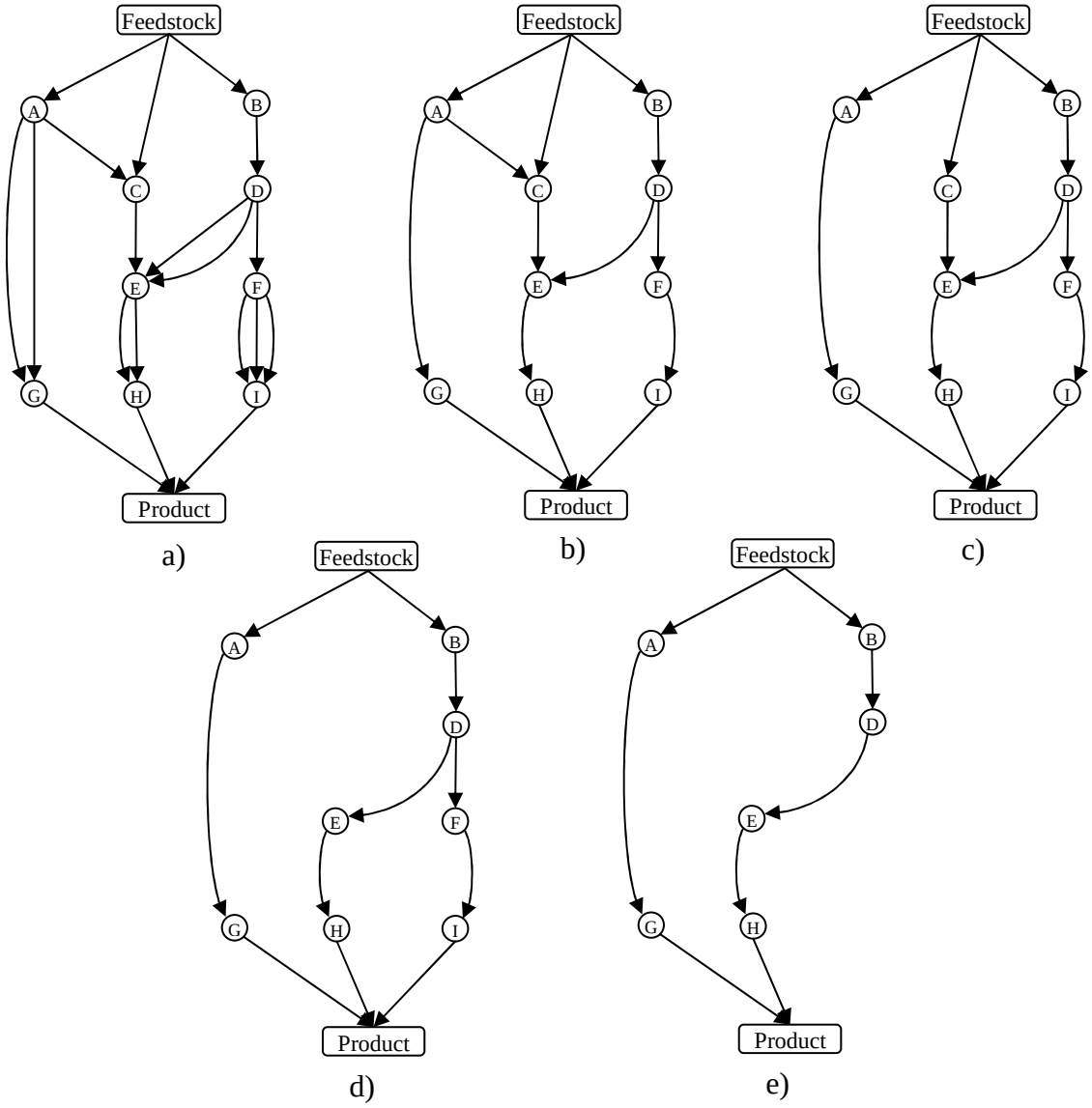

Figure 3. A superstructure of synthesized pathways representing conversion technologies (arcs) and intermediate chemicals (nodes),

(a) with all brainstormed arcs and nodes,

and after applying the principle of optimality to pathways connecting:

(b) every pair of adjacent nodes,

(c) Feedstock – C,

(d) Feedstock – E,

(e) D – Product.

2.4.2 Identifying optimal routes between nodes

In this proposed approach, a parameter-optimization step is performed first. In this step, a set of design parameters $\boldsymbol{x}_{ntn'}$ is designated for each conversion technology t that produces species n' from species n. The objective is to optimize the objective values $r_{ntn'}$ as follows:

Problem $P_{1.1}$:

$$r_{ntn'} = \min_{x} Y(x_{ntn'}) \text{ for every } t \tag{1}$$

$$\text{subject to } h(x_{ntn'}) \le 0 \tag{2}$$

$$g(x_{ntn'}) = 0. \tag{3}$$

The objective function of this optimization problem may be defined as the conversion step with the highest yield, the highest energy efficiency, the simplest, the minimum cost, the maximum profit, etc. The constraints of the formulation include:

- Key performances of processing technologies: yield, conversion, etc.
- Mass balances
- Energy balances
- Capital cost
- Operating cost

In this step, detailed analysis can be performed using available data and/or appropriate levels of simulation.

It is not uncommon to have multiple routes connecting two adjacent nodes. To reduce the complexity of the design problem, it is useful to determine optimal routes among the nodes. In this context, it is proposed to use Bellman's Principle of Optimality[44] to decompose the optimization problem into several sub-problems. The Principle of Optimality follows:[44] "An optimal policy has the property that whatever the initial state and initial decision are, the remaining decisions must constitute an optimal policy with regard to the state resulting from the first decision."

For network problems of the type addressed here in the biorefinery pathway synthesis, the principle of optimality may be stated as follows:[45] "There exists a policy that is optimal for every node."

Hence, an optimal policy is first identified for subproblems. Each subproblem corresponds to identifying the optimal conversion route between a pair of nodes. Specifically, two types of subproblems are considered:

- Arcs directly connecting two adjacent nodes (e.g., the three arcs connecting nodes F and I in Fig. 3a).

  Problem $P_{1.2}$:

  $$r_{nn'} = \min_{t} r_{ntn'} \tag{4}$$

  where $r_{nn'}$ is the objective value of the optimum arc connecting two adjacent nodes,

  $r_{ntn'}$ is the objective value of the arc using technology *t* and connecting the two adjacent nodes *n* and *n′*.

- Routes connecting two non-adjacent nodes through different intermediates (e.g., in Figure 3a, nodes Feedstock and E connected through the route Feedstock-C-E versus the route Feedstock-B-D-E).

  Problem $P_{1.3}$:

  $$r_{ij} = \min_{n,n'} f(r_{nn'}) \tag{5}$$

  where r_{ij} is the objective value of the optimum route connecting two non-adjacent nodes *i* and *j* by combination of adjacent acrs (*n*, *n′*),

  $r_{nn'}$ is the objective value of the optimum arc connecting two adjacent nodes *n* and *n′*.

As a result of solving Problems $P_{1.2}$ and $P_{1.3}$, optimal policies are determined and the superstructure is simplified to one of the levels as shown in Figure 3b – e. This is done prior to solving the superstructure-optimization problem.

Next, an optimal configuration from the synthesized and locally optimized pathways (the simplified superstructure) is determined by solving either a linear programming formulation or dynamic programming algorithm. As for the approach of linear programming formulation, the following problem is solved:

Problem $P_{1.4}$:

$$r_{1N} = \min_{i,j} f(r_{ij}) \tag{6}$$

where r_{1N} is the objective value of the optimum pathway connecting nodes Feedstock and Product,

r_{ij} is the objective value of the optimum route connecting two non-adjacent nodes i and j.

If the objective functions are non-linear, Problem P_{3a} is difficult to solve for global optima. In such cases, the following approach of dynamic programming is preferred because it is guaranteed to obtain the global optima. The approach of dynamic programming algorithm is based on the functional equation:

Problem $P_{1.5}$:

$$r_{1n'} = \min_{n} f(r_{1n}, r_{nn'}) \tag{7}$$

where r_{1n} and $r_{1n'}$ are the objective values of the optimum routes connecting nodes Feedstock – n and Feedstock – n' respectively,

n and n' are two adjacent nodes and the path direction is $n \rightarrow n'$.

Using the functional equation, $r_{1n'}$ can be determined once r_{1n} is known for every n and n' such that (n, n') is an arc. The algorithm starts from the first node (Feedstock) and ends at the last node (Product). This algorithm is called forward optimization in dynamic programming. The reverse algorithm that starts from the last node and is similarly developed is also applicable.

2.4.3 Framework

The proposed framework for the synthesis and optimization of biorefinery configurations is shown in Figure 4. Starting from the input information on feedstock and products, the following steps are performed in sequence:

1. *Forward* and *backward branching*. These two branching steps enumerate as many intermediate compounds (and associating conversion technologies) as possible. Those compounds can be produced from the feedstock (in forward branching problem) or converted into the final product (in reverse branching problem).
2. *Matching.* Some of the branches of the two trees are connected to yield complete pathways (from the feedstock to the final product) by identifying the identical intermediate compounds.
3. *Interception*. When two compounds on the edging layers of the branching trees are not connected, it is possible to identify known processes or reactions that will link the two compounds. This is referred to as “interception.”
4. *Screening*. Based on simple technical and economic analyses, this step eliminates the synthesized pathways that are too complex, thermodynamically infeasible, economically infeasible, or have too low yields. The elimination reduces the work load in the next steps without sacrificing optimal pathways.
5. *Optimizing parameters*. Before solving the superstructure-optimization problem, the design parameters are optimized for every synthesized pathway in this optimization step. Analyses (include simulation and techno-economic analysis) can be performed at different levels of details.
6. *Optimizing policies between two nodes*. Based on the connectivity between the nodes, two types of subproblems are solved: adjacent and non-adjacent. For the former subproblem, technologies that process the same nodes are compared for the identification of an optimal one. However, there can be cases in which a series of conversion steps are considered at the same time for a global optimum. For these cases, the latter subproblem is solved. Based on the principle of

optimality, this step reduces the number of synthesized pathways without affecting the final results of the optimization problem.

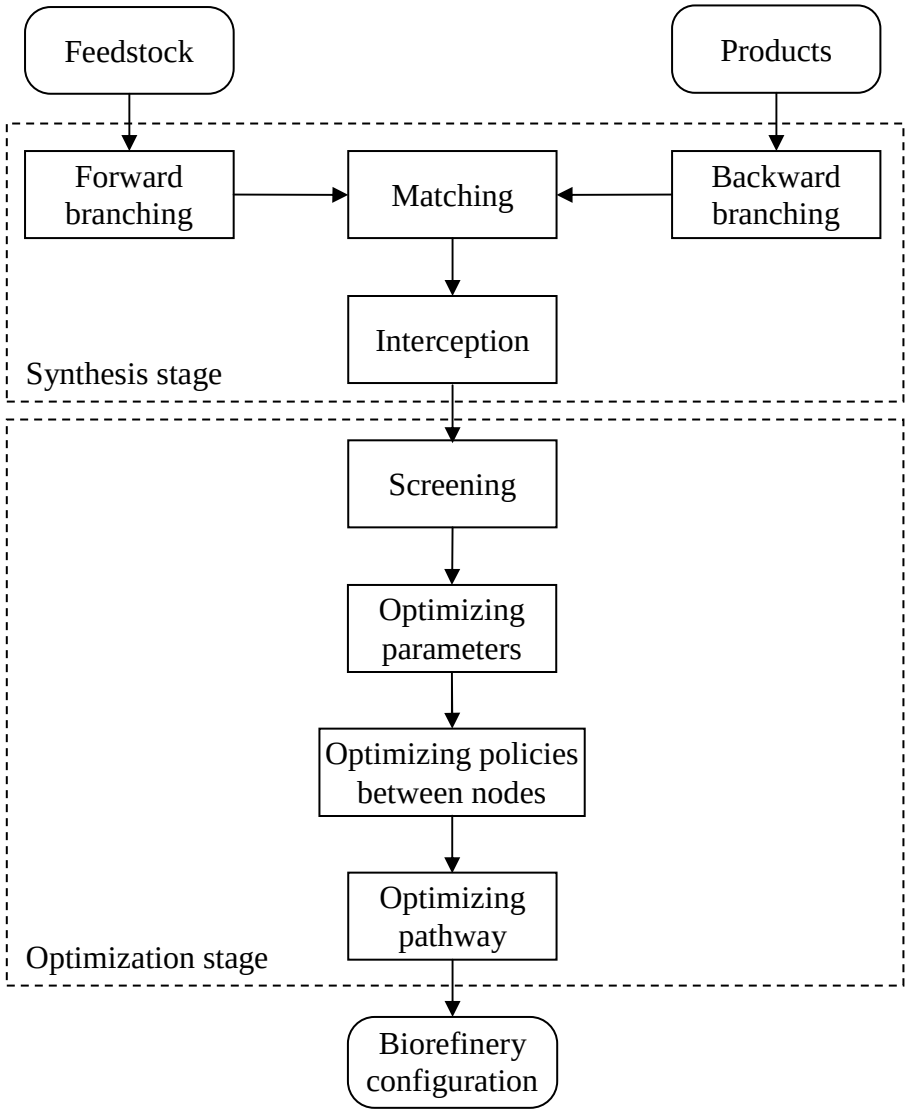

Figure 4. Framework for the synthesis and optimization of biorefinery configurations.

7. *Optimizing pathways*. Either a linear programming formulation or dynamic programming algorithm is used to determine the optimal configuration from the superstructure of synthesized pathways.

These steps are categorized into two stages: synthesis stage (which includes the first three steps) and optimization stage (which includes the remaining four steps). The output of the framework is a biorefinery configuration which is technically feasible and optimum according to the given data. The configuration comprises not only the optimized pathways between feedstock and final products, but also some open branches connecting to the pathways which represent by-product production.

2.5 Case study

It is desired to synthesize pathways that produce fuel-grade alcohols from lignocellulosic biomass and to determine the most cost-effective pathway. The proposed procedure for the solution is applied as described in the ensuing steps.

First, the branching and matching were performed. A tree of forward branching search from the feedstock was constructed. This tree tracks the compounds that can be produced from the lignocellulosic biomass within two conversion steps. Another tree starting from the bio-alcohol node was built to enumerate compounds from which the bio-alcohols can be derived. The enumeration in each direction is limited to two conversion steps to avoid an unnecessarily exhausting blind search. After the branching searches were done, the matching and interception steps were performed to identify complete pathways. Figure 5 shows a part of the two branching trees with identified complete pathways. Compounds, associating conversions, and unmatched branches are not presented for a clearer presentation. In the figures of synthesized pathways, it is not necessary to note to which layer a specific compound belongs. The left-hand side of Figure 5 collects biochemical pathways whereas the other side collects mostly thermochemical routes. The upper half (which is front-ends of biorefineries) includes biological conversions whereas the lower half involves chemical conversions.

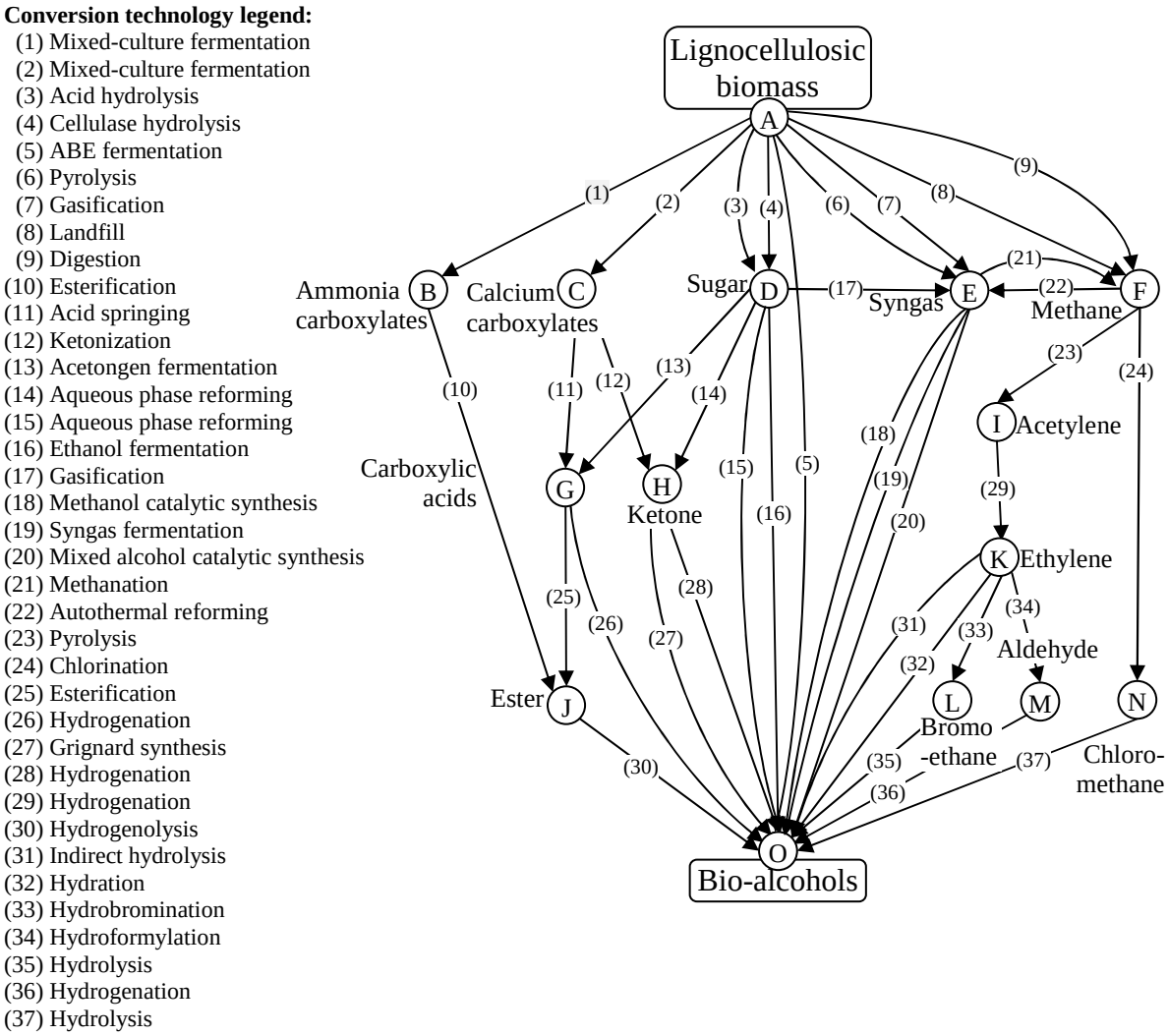

Figure 5. Part of the branching trees for the production of bio-alcohols from lignocellulosic biomass.

Table 1. Technology arcs eliminated due to their low yields.

Conversion steps	Feed	Product	Yield	Yield base	Reference
(6) Pyrolysis	Biomass	Syngas	Max 29.2%	Biomass weight	Goyal et al.[46]
(14) Aqueous phase reforming	Sugar	Ketones	23.7%	Fed carbon weight	Blommel and Cortright[47]
(15) Aqueous phase reforming	Sugar	Alcohols	8.7%	Fed carbon weight	Blommel and Cortright[47]
(19) Syngas fermentation	Syngas	Alcohols	53.1%	Carbon monoxide weight	Piccolo and Bezzo[48]
(24) Chlorination	Methane	Chloro-methane	Max 12%	Methane weight	Schmittinger[49]

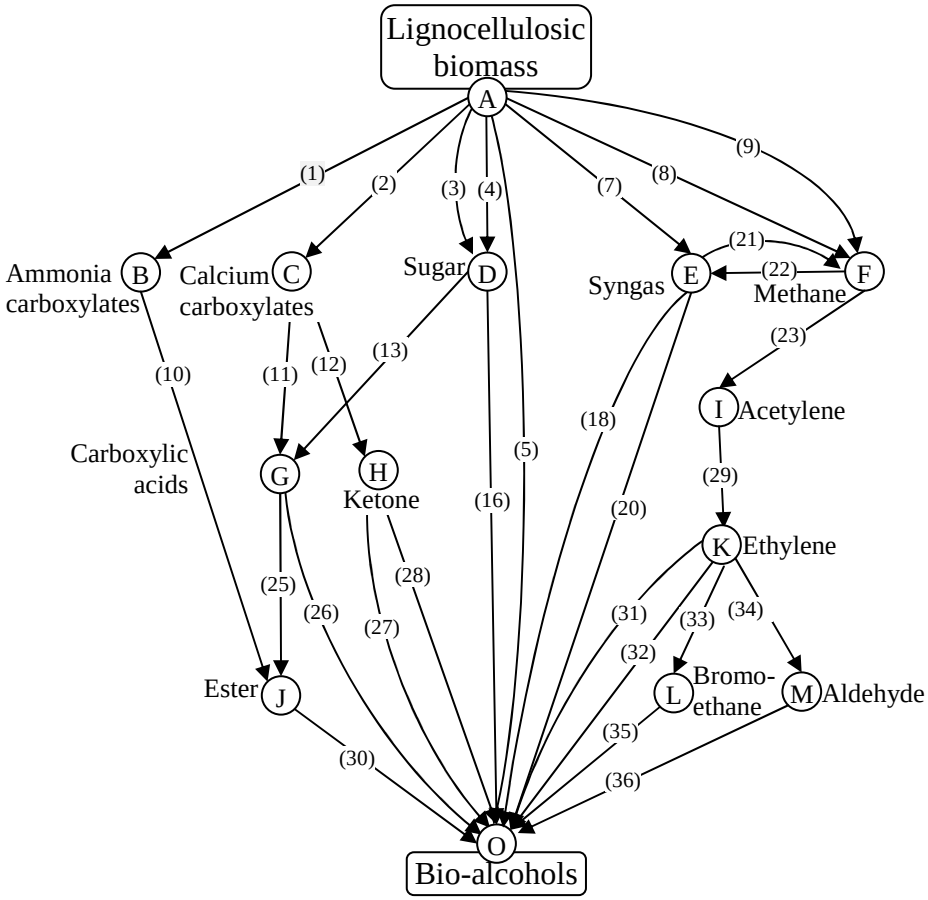

Figure 6. The superstructure of synthesized pathways after the screening step.

Next, the screening step was performed. Processing Technologies 6, 14, 15, 19, and 24 are eliminated because of their very low yields (Table 1). Arc 37 is disregarded despite its high theoretical yield because the associating pathway is incomplete after the elimination of Arc 24. In another case, Arc 17 is eliminated based on a simple economic analysis (it is not economically feasible to obtain syngas by performing expensive hydrolysis[50] (Arcs 3 and 4), then drying the sugar solution and gasifying the produced sugar (Arc 17). The direct gasification of the feedstock (Arc 7) is obviously more cost-

effective to produce the syngas because it employs less equipment, conversion, and separation steps. Note that although the routes involving Arcs 3 – 17 and 4 – 17 are eliminated, the Arcs 3 and 4 are kept because they are parts of other routes, for instance, through the one involving Arcs 3, 14, and 28. It is possible for an arc to connect the feedstock and the product to form a pathway. For example, the pathway via Arc 5 comprises only one conversion step which is acetone-butanol-ethanol (ABE) fermentation (pretreatment as well as other treatment and separation are not considered as conversion steps in this branching-tree presentation). Figure 6 shows the simplified superstructure after the screen step is performed.

In this case study, the parameter-optimization step to optimize the process designs (Problem $P_{1.1}$) was not performed because the overall objective values – production costs – of most of the pathways could be found from techno-economic analyses in the literature. In these techno-economic analyses, optimization of the process designs was done to some extent.

The next step is to optimize the policy between nodes. The technologies used for adjacent nodes were compared to find the most cost-effective ones (Problem $P_{1.2}$). These pairs of technologies were considered: (Arcs 27 vs. 28) and (Arcs 18 vs. 20). Then, another type of subproblems (Problems $P_{1.3}$) is solved to determine the optimal routes connecting the non-adjacent nodes: A → E, A → F, K → O, and G → O. The objective function of these subproblems is the minimization of the production costs, which has to be identical to that of the overall optimization problem. This work uses information of the production costs of these conversion steps from published data (with adjustments for the time value of money, location, and production capacity). In some cases where such economic information may not be available, simulation and heuristics can be used to determine the optimal ones. Table 2 summarizes the policy optimization between nodes. At the end of this step, the superstructure is simplified as shown in Figure 7.

Table 2. Problems of optimizing policy between two nodes.

Nodes	Feed	Product	Routes [a]	Key comments	References
A → F	Biomass	Methane	(7) Gasification & (21) Methanation	Production cost: $8.53/GJ of methane	Gassner and Maréchal[51]
			(8) Landfill	Production cost: $1.90 – $3.79/GJ of methane	EPA[52]
			(9) Digestion	Production cost: $0.20 – $0.55/GJ of methane	Gray[53]
A → E	Biomass	Syngas	**(7) Gasification**	Energy efficiency: 82.8%	Hamelinck and Faaij[54]
			(9) Digestion & (22) Autothermal reforming	Energy efficiency: 63%	Calculation
H → O	Ketones	Alcohols	(27) Grignard synthesis	Yield is 82 – 88%	Carey and Sundberg[55]
			(28) Hydrogenation	Yield is 100%	Chang[56]
K → O	Ethylene	Ethanol	(31) Indirect hydrolysis	Well developed and commercialized in 1960s but phased out because less economic than hydration.	
			(32) Hydration	Simple, direct, and most costly effective pathway	
			(33) Hydrobromination & (35) Hydrolysis	Involves many more steps than hydration pathway	
			(34) Hydroformylation & (36) Hydrogenation	Involves many more steps than hydration pathway	
G → O	Acid carboxylic	Alcohols	**(25) Esterification & (30) Hydrogenolysis**	Includes mild esterification (203 kPa and 50^{o}C) and hydrogenation (160^{o}C and 405 kPa)	Kiff and Schreck[57]
			(26) Hydrogenation	Involve furnace, intense hydrogenation (230 – 270^{o}C and 4.1 – 7.1 MPa), and expensive molecular sieve.	Kiff and Schreck[57]
E → O	Syngas	Methanol	**(18) Methanol synthesis**	Production cost ($2010): $19.98/GJ methanol [b]	Hamelinck and Faaij[54]
	Syngas	Alcohols	(20) Mixed alcohol synthesis	Production cost ($2010): $19.98/GJ methanol [c]	Bechtel[58]

Note: a. Bold routes are optimal ones; b. 20% was added to account for additional cost of processing municipal solid waste; c. An additional cost of $0.425/gal was added to account for biomass feedstock.[59]

Table 3. Problems of optimizing pathways.

Pathways	Description	Product	Base year			Year 2010				References
			Capacity	Product cost [b]	Energy density	Date	PPI [c]	Alcohols cost		
			MMGPY [a]	$/gal	MJ/gal			$/gal	$/GJ	
A→B→J →O	Mixed alcohols production via acid fermentation and esterification	Mixed alcohols	45	1.21	92	2007	213.7	1.39	15.14	Granda et al.[60]
A→C→ H→O	Mixed alcohols production via acid fermentation and ketonization	Mixed alcohols	35	1.44	101	2009	229.4	1.54	15.28	Pham et al.[61]
A→D→ G→J→O	Ethanol production via acetongen fermentation and ester synthesis	Ethanol	n/a	n/a	n/a	n/a	n/a	n/a	n/a	The Zeachem process
A→D→ O	Ethanol production via hydrolysis and yeast fermentation	Ethanol	50	1.03	79	2003	161.8	1.56	19.69	Hamelinck et al.[50]
A→O	Mixed butanol and ethanol production via ABE fermentation	Mixed alcohols	n/a	1.50	110	2007	214.8	1.71	15.47	Pfromm et al.[62]
A→E→ O	Methanol production via biomass gasification	Methanol	24	0.61	59	2001	151.8	1.18	19.98	Hamelinck and Faajj[54]
A→F→I →K→O	Ethanol production via syntheses of methane, acetylene, and ethylene	Ethanol	13	2.74	79	2008	245.5	2.73	34.43	Calculation

Note: a. MMGPY: Million gallons per year of products. Online operation is 8,000 hours per year

b. All the product costs exclude feedstock costs

c. PPI: Producer Price Index for Chemicals and Allied Products. PPI in 2010 (245.1) is the average from January 2010 to July 2010.

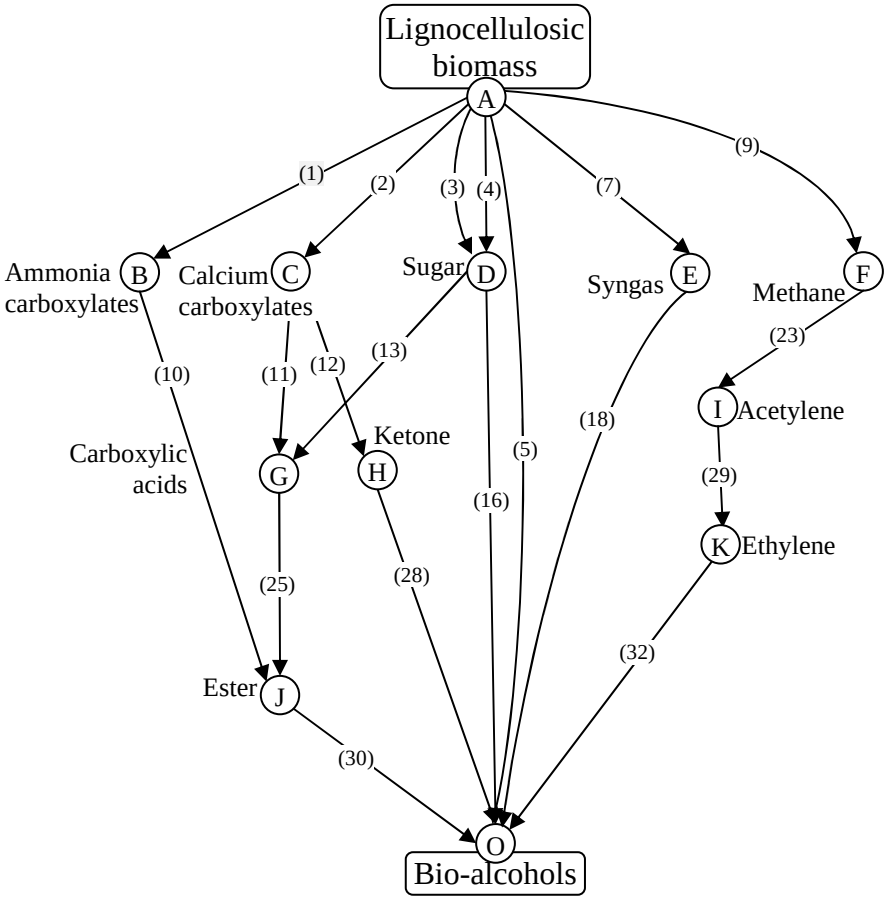

Figure 7. The synthesized superstructure after the step of optimization between nodes.

In the next step, the optimization problem $P_{1.4}$ is solved for an optimal pathway of the simplified superstructure. Most of the production costs of the biomass-to-alcohol pathways were available in published techno-economic analyses. The cost estimation from previous years was updated to year 2010 dollars using the Producer Price Index for Chemicals and Allied Products published by the U.S. Department of Labor.[63] As all pathways start with the given feedstocks, the feedstock costs were excluded for the comparison of production costs. Because different alcohols may be produced, the product price was calculated as $/GJ to have a consistent basis. The result of this optimization step is summarized in Table 3.

The calculations show that the following pathways are the most economically attractive routes: Mixed alcohols production via acid fermentation and esterification (A→B→J→O; $15.14/GJ of products). Mixed alcohol production via acid fermentation and ketonization (A→C→H→O; $15.28/GJ). Mixed butanol and ethanol production via ABE fermentation (A→O; $15.47/GJ).

Because the calculated costs of these three configurations are relatively close, additional analyses must be performed. This is consistent with the stated objective of the devised approach which is aimed at quick screening of pathways to generate a set of attractive configurations that can be later screened in more detail.

2.6 Summary

A common approach to the design of biorefinery configurations is to develop flowsheets around a core conversion technology or scale-up a laboratory-scale unit. Although feasible process configurations can be derived, their overall performance may not be attractive and the approach may severely hinder the innovation of new configurations.

A new methodology for the synthesis and optimization of biorefinery configurations was proposed in this chapter. The proposed forward and backward branching techniques – along with matching and interception steps – are used to synthesize the biorefinery pathways based on known conversion technologies. Bellman's Principle of Optimality can be applied to decompose the optimization problem into subproblems that can be readily solved to reduce the number of possible pathways from the synthesized ones without missing the globally optimal solution. The methodology is a systematic way to quickly synthesize and screen biorefinery pathways so as to generate promising pathways that can be assessed in more details.

The proposed methodology was demonstrated in a case study of producing fuel-grade alcohols from lignocellulosic biomass. The result indicated mixed alcohol production via acid fermentation and ABE fermentation as the most economically attractive pathways.

CHAPTER III
DESIGN OF BIOREFINERY CONFIGURATIONS WITH AN OPTIMAL LEVEL OF FLEXIBILITY

3.1 Introduction

Decisions on the design of chemical processes rely on input information, which generally has uncertainty or predictable variations in operation stage. The problem of accommodating these input changes in early design stage is referred to as design with flexibility. Based on sources of uncertainty, the input changes can be categorized into four types:[64]

- *Model-inherent uncertainties* – parameters in modeling equations to mathematically describe the process. They are obtained from experiments. Their changes are usually described in ranges possible realizations or in probability distribution functions.
- *Process-inherent uncertainties* – flowrates, temperatures, pressures, and stream qualities that normally disturb or fluctuate when the process is in operation. Their values can be obtained from measurement instruments and described by probability distribution functions.
- *External uncertainties* – availability, demand, prices, and qualities of raw materials, utility, and products. It also includes surrounding environmental conditions. The behaviors of these input changes depend on specific market or environmental conditions. They can be predicted (forecasted) from historical data.
- *Discrete uncertainties* – equipment availability and other random discrete events. An uncertainty of this type, for example, is an equipment failure of which probability (and frequency) can be retrieved from reliability databases.

Another classification of the input changes is based on the uncertainty nature and on how to describe it.[65] There are two categories of this classification: deterministic and stochastic. The deterministic uncertainties are described by a finite set of values

(scenarios) with given occurrence probabilities; therefore, they are preferred for the external and discrete uncertainties. The stochastic uncertainties have behavior of continuous random variations described by joint probability density functions; hence, they are more suitable for the model and process-inherent uncertainties.

Let θ be the uncertainty parameters, d be design variables, z be control variables, and x be state variables. The problem of flexibility design can be formulated in the following general forms:

Problem $P_{2.1}$:

$$\max_{d,z,x} P(d,z,x,\theta) \tag{8}$$

$$\text{subject to } f(d,z,x,\theta) \le 0 \tag{9}$$

$$d \in D,\ z \in Z,\ x \in X.$$

The objective function $P(d,z,x,\theta)$ is a cost function (e.g., revenue, profit, operation cost, capital cost). If the θ is described by (or discretized into) a set of scenarios with given probabilities (or weighting factors), $P(d,z,x,\theta)$ is an expected value of the cost function. The constraints represent specifications and process-modeling relations such as mass balance, energy balance, equilibrium, design equations, product qualities, etc. (Note that equality constraints are equivalent to a set of two inequality constraints with opposite signs; therefore, equality constraints are not shown in $P_{2.1}$ for simplification.) In the literature, design specifications were formulated in one of two constraint types: hard constraints and soft constraints. Hard constraints strictly restrict calculated variables in predefined ranges (e.g., $z \le 1$). On the other hand in soft constraints, violations are allowed with a penalty. For example, $(z-1)^2$ is a Taguchi loss function[66] to impose a penalty charge if value of z is not equal to 1, a desired value.

In design stage, process designers must anticipate the changes of input (θ) which may occur in operation stage and must decide on what strategies to respond. The response strategies can be categorized into three levels as shown in Figure 8. The quickest and easiest way to respond to the changes is manipulation of operation conditions (i.e., changing z values). If this strategy can not accommodate them (e.g., product specifications can not be met in any operation conditions), substitution of

feedstocks or products (changing other *z*) is considered. If the second-level strategy fails, the change of equipment sizes (i.e., changing *d* values) and/or of process structure (retrofitting) may need to be performed. The higher levels of the strategy pyramid require more effort, expense, and time to respond.

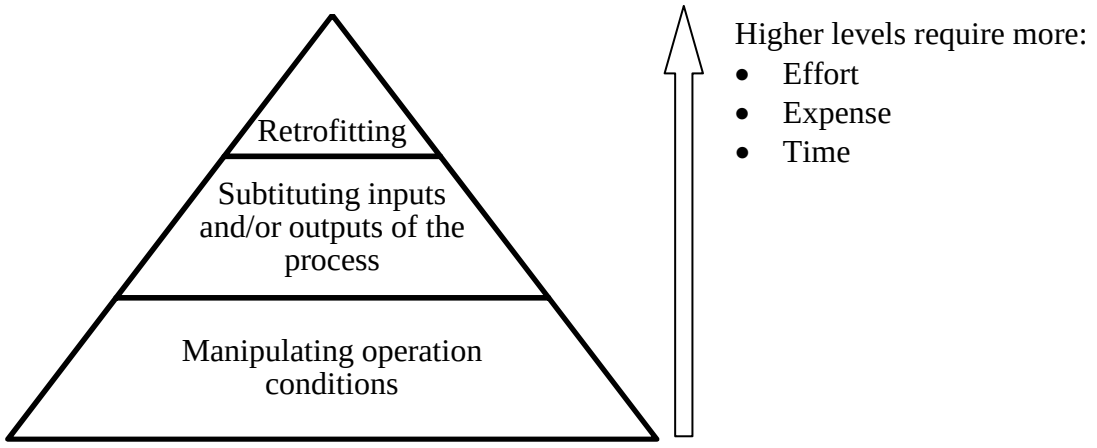

Figure 8. Strategies to respond to uncertainty changes.

3.2 Literature review of flexibility design

The solution approach to flexibility design has been studied for four decades. Well-known systematic approaches were mainly developed in 1980's and 1990's. Before the systematic tools were developed, the traditional approach in practice was to use nominal values of the uncertainties for the basic design and then apply empirical overdesign factors to equipment sizes to accommodate the uncertainties. The utilization of overdesign factors, which can be found in the literature,[67] is based on designer's experience. By using only nominal values, the traditional approach ignores other possible values of the uncertainties. Meanwhile, employing overdesign factors does not guarantee feasible operation in the whole uncertainty ranges due to lacks of insights on degree of flexibility and may result in unnecessary additional costs.

Based on design objectives, the systematic approaches have been usually grouped in two categories.[68] The first one is referred to as *optimal design for fixed degree of*

flexibility in which the design must be feasible at *all* values of uncertainties in a discrete set of realizations (multiperiod design problem) or in specified ranges (general design-under-uncertainty problem) – a semi-infinite set of realizations. These approaches are suitable for deterministic model of uncertainty.

In the multiperiod problems, solutions can be determined from the following one-stage formulation where the functions in program $P_{2.1}$ are rewritten for all periods:

Problem $P_{2.2}$:

$$\max_{d,z_p,x_p} \sum_{p=1}^{P} P(d, z_p, x_p, \theta_p) \tag{10}$$

$$\text{subject to } f(d, z_p, x_p, \theta_p) \le 0, \quad p = 1,...,P \tag{11}$$

$$d \in D,\ z_p \in Z,\ x_p \in X.$$

where P is the number of operation periods.

Multiperiod problems are usually easy to solve. However, the general design-under-uncertainty problems are much more difficult. Halemane and Grossmann[69] formulated the latter problem in a two-stage program:

Problem $P_{2.3}$:

$$\max_{d} \underset{\theta \in T}{\mathrm{E}} \left\{ \max_{z,x} P(d, z, x, \theta) \mid f(d, z, x, \theta) \le 0 \right\} \tag{12}$$

$$\text{subject to } \forall \theta \in T \left\{ \exists (z, x)[\forall j \in J(f_j(d, z, x, \theta) \le 0)] \right\}. \tag{13}$$

The outer stage is a design-stage problem where d is determined to optimize the expected value of the cost function. The inner stage, $\max_{z,x} P(d, z, x, \theta) \mid f(d, z, x, \theta) \le 0,$ is an operating-stage problem where values of design d are fixed and values of control z are determined to yield optimum values of the cost function for every $\theta \in T$.

The main difficulties of Problem $P_{2.3}$ are the need to solve a semi-infinite number of operating-stage problems because realizations of θ are (bounded) ranges and the flexibility tests (logical Constraint 13) must be verified. A common approach to the first difficulty, which was proposed by Grossmann and Sargent,[70] is to transform the formulation into a multiperiod program by discretizing θ space from the continuous

regions into discrete sets. As for the second difficulty, Halemane and Grossmann[69] reformulated the logical constraint with the following equivalent constraint:

$$\max_{\theta \in T} \min_{z,x} \max_{j \in J} f_j(d, z, x, \theta) \leq 0 \tag{14}$$

and proved that only vertices in the polyhedron of T (instead of continuous space of T) need to be verified with Constraint 14 if inequalities are convex, which significantly reduces computational expense.

The second category is *design with optimal degree of flexibility*. Its design objective is somewhere between the two extreme cases above (the traditional approach and the optimal design for fixed degree of flexibility) as the design is not necessary to be feasible at all value of uncertainties. Decision-making is based on a trade-off between a cost function and degrees of flexibility, which are quantified by a metric.

The key issue of the second-category is analysis of flexibility, i.e., quantification of flexibility level. Swaney and Grossmann[71] proposed a flexibility index to measure a partial region (of a given θ space) in which a fixed design d still satisfies feasible conditions. The feasible ranges of θ are expressed in terms of flexibility index F:

$$\theta^N - F \cdot \Delta\theta^- \leq \theta \leq \theta^N + F \cdot \Delta\theta^+ \tag{15}$$

where θ^N is the nominal value,

$\Delta\theta^-$ and $\Delta\theta^+$ are given negative and positive deviations.

Then, the program to determine flexibility index F can be mathematically formulated:

Problem $P_{2.4}$:

$$F = \max \delta \tag{16}$$

$$\text{subject to } \max_{\theta \in T(\delta)} \min_{z,x} \max_{j \in J} f_j(d, z, x, \theta) \leq 0 \tag{17}$$

$$T(\delta) = (\theta \mid \theta^N - \delta \cdot \Delta\theta^- \leq \theta \leq \theta^N + \delta \cdot \Delta\theta^+). \tag{18}$$

To solve Problem $P_{2.4}$, Swaney and Grossmann[72] assumed the critical points (solutions) lie at vertices of $T(\delta)$. Then Problem $P_{2.4}$ is equivalent to:

Problem $P_{2.5}$:

$$F = \min_{k \in V} \delta^k \tag{19}$$

$$\delta^k = \max_{\delta,z,x} \delta^k \tag{20}$$

subject to $f(d,z,x,\theta) \le 0$ (21)

$$\theta = \theta^N + \delta \cdot \Delta\theta^k \tag{22}$$

where V is the index set of vertices

$\Delta\theta^k$ is deviation of nominal value θ^N towards vertex k.

Alternatively, Grossmann and Floudas[73] proposed an approach to determine explicit solution of Problem $P_{2.4}$ without the assumption of critical point locations lying at vertices of $T(\delta)$. By analyzing properties of active constraints of feasible conditions (constraint 14), the authors formulated an equivalent mixed-integer minimization problem of the following forms:

Problem $P_{2.6}$:

$$F = \min_{\theta,z,x,\delta,s_j,\lambda_j,y_j} \delta \tag{23}$$

subject to $s_j + f_j(d,z,x,\theta) \le 0, \quad j \in J$ (24)

$$\sum_{j\in J} \lambda_j = 1 \tag{25}$$

$$\sum_{j\in J} \lambda_j \frac{\partial f_j}{\partial z} = 0 \tag{26}$$

$$\lambda_j - y_j \le 0, \quad j \in J \tag{27}$$

$$s_j - U(1-y_j) \le 0, \quad j \in J \tag{28}$$

$$\sum_{j\in J} y_j = n_z + 1 \tag{29}$$

$$\theta^N - \delta \cdot \Delta\theta^- \le \theta \le \theta^N + \delta \cdot \Delta\theta^+ \tag{30}$$

$$y_j = 0,1; \quad j \in J \tag{31}$$

where s_j is a slack variable for constraint j: $f(d,z,\theta) \le 0$,

λ_j is a Kuhn-Tucker multiplier for constraint j,

U is an upper bound for the slack,

n_z is the number of control variables z.

Problem $P_{2.6}$ has the advantage of not requiring the assumption of critical points on the vertices or exhaustive vertex search. Hence, it has been embedded in formulations to solve various types of retrofitting design problems. Pistkopoulos and Grossmann solved optimal retrofit design problems for increasing its flexibility to above a desired level in linear systems,[74] to exactly a desired level in nonlinear systems,[75] or to an optimum level that corresponds to a maximum profit with deterministic[76] and stochastic[77] uncertainty models.

Another way found in the literature to quantify flexibility levels is *stochastic flexibility*. Stochastic flexibility is defined as the probability that operation of a given design is feasible.[78] Thanks to probability nature, problems of determining optimal levels of flexibility with stochastic models of uncertainty parameters are best treated in this approach. In mathematical viewpoint, stochastic flexibility is the cumulative probability of the joint distribution $j(\theta)$ describing stochastic uncertainty over a feasible region, i.e., it is the integral of $j(\theta)$ over the feasible regions of θ:[78]

$$SF(d) = \int_{R(d)} j(\theta) d\theta \tag{32}$$

$$R(d) = \left\{ \theta \in T \left[\exists (z, x) \middle| \forall j \in J(f_j(d, z, x, \theta) \le 0) \middle| \right] \right\}. \tag{33}$$

Straub and Grossmann[79] embeded and handled this integral by discretization in design optimization problem of maximizing stochastic flexibility subject to a cost constraint. Pistkopoulos and Ierapetritou[80] solved the design problem with stochastic flexibility by optimizing a cost function while simultaneously measuring design feasibility.

Extensive reviews on the optimal flexibility design were reported by Grossmann et al.[68] and later by Grossmann and Straub.[81] Besides flexibility design, there are some other process system engineering problems that also encounter uncertainty and may share similar solution approaches. Some of them are controllability (ability of a control system to dynamically respond to disturbances), robustness, reliability (ability of a process to maintain normal operation when mechanical or electrical failures occur), value of perfect information, production planning, design and production of batch

processes. Reviews on these problems can be found in the publications of Pistkopoulos[64] and Bernardo et al.[65]

Above is a selective literature review of common formulation and solution approaches to process designs with flexibility under uncertainty. In gerneral, those methodologies are systematic but they share some common limitations. The optimal design for fixed degree of flexibility is conservative because it requires feasible operation in the whole ranges of unceratinty, which may result in unnecessary additional costs of oversizing and maintenance. On the other hand, the approaches to design with optimal degree of flexibility reduce those additional costs; however, they involve the issue of flexibility analysis, which requires complicated formulation and solution methodologies. The research objective is to propose a novel formulation approach that tackles these two limitations and is well suited for the design of flexible bio-refinery configurations.

3.3 Problem description

3.3.1 Motivation

Design of flexible biorefinery configurations involves external uncertainties and model-inherent uncertainties. External uncertainties usually include:

- Feedstock prices, availability, and composition
- Product prices, demand, and specifications
- Prices and availability of raw chemical and utility

Values of those parameters are uncertain because they depend on market conditions, which change with time and vary from one parameter to another. Most of their changes, for instance corn prices as shown in Figure 9, are arbitrary. But some of them, particularly availabilities of agricultural products, are seasonal and recurrent. For example, storage stocks of frozen corn in the United States are annually repeated due to weather conditions (Figure 10). (Note: Although frozen corn is not a biorefinery feedstock, its stocks reflect the availability change of corn crop used for fuel production).

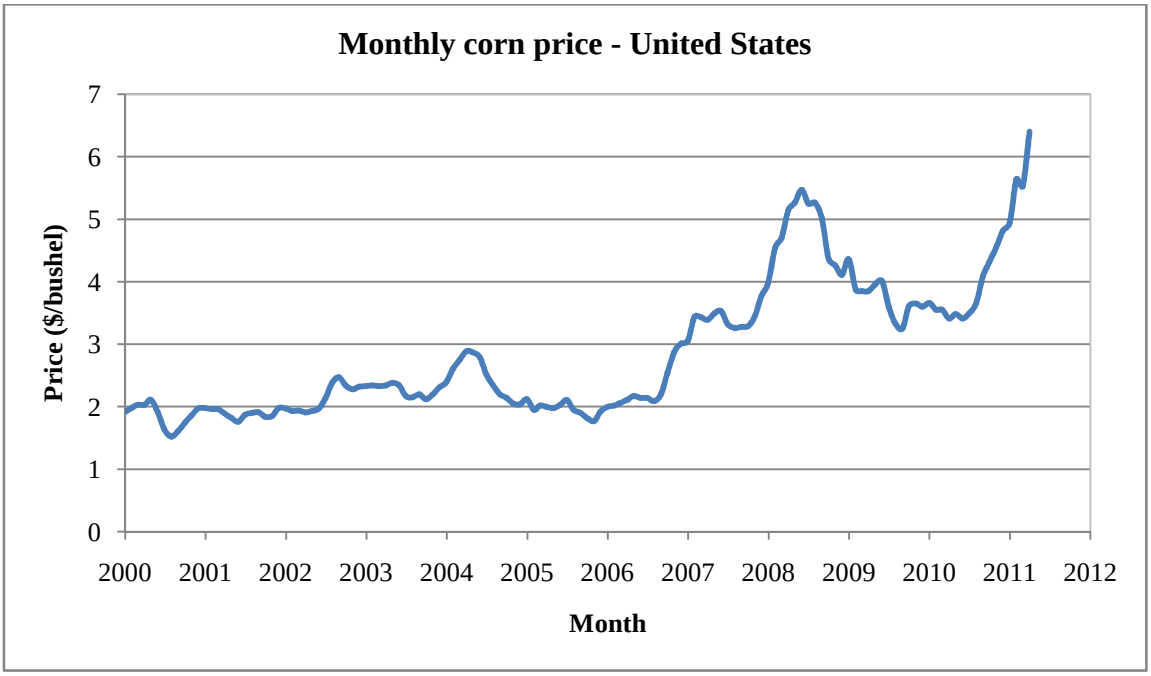

Figure 9. U.S. monthly corn price received by farmers.[82]

Some of the parameters depend on each other. For example, the price of hydrogen (as a raw material for an option to remove oxygen content out of biomass components) is proportional to the price of natural gas (as a common utility for heating) because hydrogen is mainly produced by reforming natural gas. The relationship is of the following form:[60]

$$\text{Hydrogen price (\$/kg)} = 0.172 \cdot \text{Natural gas price (\$/GJ)} \tag{34}$$

Such a relationship between uncertainties does not impose more difficulty on the solution approach; instead, it reduces the number of uncertainty scenarios to be investigated.

Uncertainty levels of the external uncertainties can be reduced by performing analysis of historical market data and predicting future trends based on data. However, uncertainty levels can not be further reduced because the uncertainties depend on external conditions.

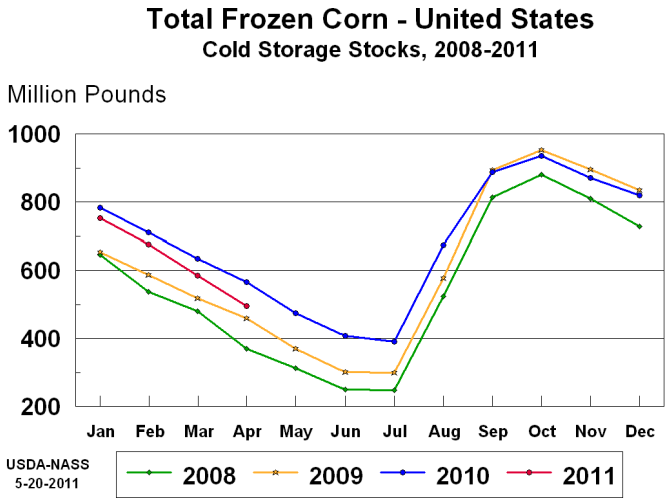

Figure 10. Cold storage stock of U.S. corn.[83]

On the other hand, model-inherent uncertainties have different characteristics. They are obtained from experiments; therefore, their uncertain levels can be further reduced with more experiments (yet requires more experimental costs).[65] In conceptual biorefinery configuration design, the uncertainties in interest are usually yields of being-developed conversion technologies. In detail process design, other process-modeling parameters such as kinetic constants, physical properties, efficiency, transfer coefficients, and so on should be also considered. They are uncertain because of tolerance of the models (e.g., models are linearized for simplification), discrepancy between operation in research scales and in commercial scales (e.g., ideal mixing might not be achieved in commercial-scale large vessel as in laboratory-scale small apparatus), and degradation in operation (e.g., heat transfer coefficient decreases due to fouling). The changes are usually described in ranges possible realizations or in probability distribution functions.

Let consider a simple example of corn-to-ethanol design with two uncertainties. For demonstration purpose, assume the future change of corn price (θ_1) will be the same as the historical monthly price shown in Figure 9. Between January 2000 and April 2011, the price reached a minimum at $1.52/bushel in August 2000 and a maximum of

$6.40/bushel at the latest data record (April 2011). The average value is $2.87/bushel and the time period when the price exceeds $5/bushel is short (9 months out of 137 months of the whole recorded data). Ignore the increasing trend of the price after the latest month. The second uncertainty is overall yield of the process (θ_2) defined as a fraction of theoretical yield ethanol from corn grain, which is 124.4 gallons/dry ton feedstock.[84] The actual yield is somewhere between 60% and 90% of theoretical, and expected at 85%.

Design strategies for this example using approaches available in the literature can be briefly described as follows. In traditional approach, the plant is designed with nominal values of θ, for example, $\theta_1 = 2.87$ and $\theta_2 = 85\%$; then, equipment sizes are overdesigned to accommodate the higher throughput when $\theta_2 = 90\%$. In the approaches to optimal design for fixed degree of flexibility, the plant operation must be feasible for any values of θ in the uncertain ranges $1.52 \leq \theta_1 \leq 6.40$ and $60\% \leq \theta_2 \leq 90\%$. Such design is conservative as the plant must be in operation in the whole ranges, which results in high capital cost and probably a negative revenue in operation in some scenarios (e.g., in scenarios $\theta_1 > 5$). In the approaches to design with optimal degree of flexibility, a flexibility index that is based on the bound and nominal value of θ is analyzed; expensive iterative calculation is usually required to construct a trade-off curve between values of a profit function and the flexibility index.

Alternatively, a new design strategy is proposed in this research. The design need not being feasible at any value of θ. Instead, the plant is designed such that it is in operation only when economic efficiency is favored (e.g., profit function is positive) and product qualities are met. During the operation stage, if these conditions are not satisfied, part of the plant is idle or the whole plant is shutdown to avoid economic loss. Hence, the design has an optimum level of flexibility. From a mathematical viewpoint, for every value of θ, design variables are calculated if those operation conditions are satisfied; otherwise, design variables have trivial values (zeros). In addition, non-iterative calculation is desired to reduce calculation effort. The problem of biorefinery configuration design is suitable for this strategy because it is not uncommon for part or

whole plant to be idle for economic reasons. Conversely in other design problems (for instance, design of flexible heat exchanger networks), the priority strategy is operation feasibility at various θ scenarios.

3.3.2 Problem statement

In this research, the term *flexibility* implies the ability of a process to be operable (i.e., feasible and profitable) in various scenarios of uncertainties. If the process is operable at any value of uncertainty, it is fully flexible. If the process is operable at some realizations of uncertainty, it is partially flexible. Figure 11 shows a sketch of trade-off curve between the profit and flexibility level. As flexibility level increases, higher capital costs are needed because equipment sizes are increased and more pieces of equipment are employed to accommodate wider ranges of uncertainty values. Also, revenue of the process increases as its online time increases because it operates in additional scenarios. As a result, the profit – which is a combination of the capital cost and revenue – has a maximum value at a certain flexibility level. The problem objective is to obtain the design with the maximum profit. In other words, the problem is design with an optimal level of flexibility.

The general problem, configuration design with an optimal level of flexibility, can be stated as follows. A superstructure of the flowsheet with modeling equations is given. Information on available rates, characteristics, and prices of feedstocks, utilities, products, and other raw materials is also given. Those inputs may contain uncertainty or predefined variations that are modeled as deterministic uncertainty, i.e., described in ranges or discrete sets with occurrence probabilities. The problem is then to design a configuration (i.e., determine equipment sizes) with a level of flexibility so as to maximize the expected value of profit which is derived from revenue and annualized capital costs. The process does not need to operate at any value of the inputs; instead, it is allowed to be idle in some scenarios if economics are not favored or if qualities are not met. Figure 12 summarizes the problem statement.

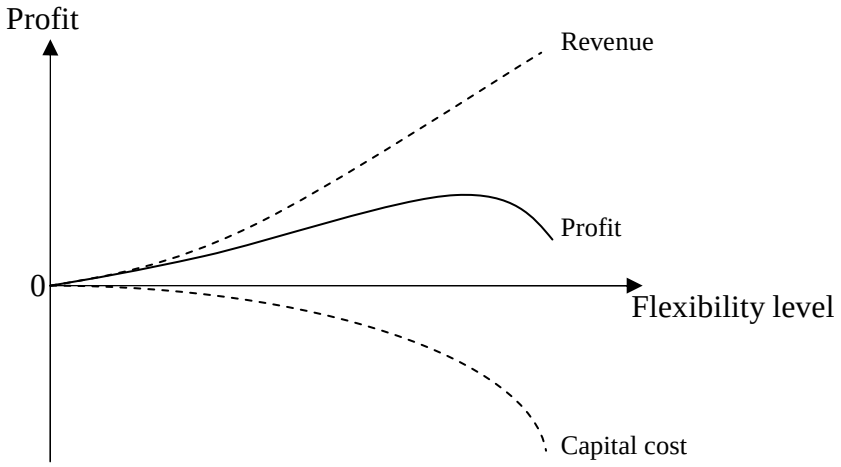

Figure 11. Trade-off curve of profit and flexibility.

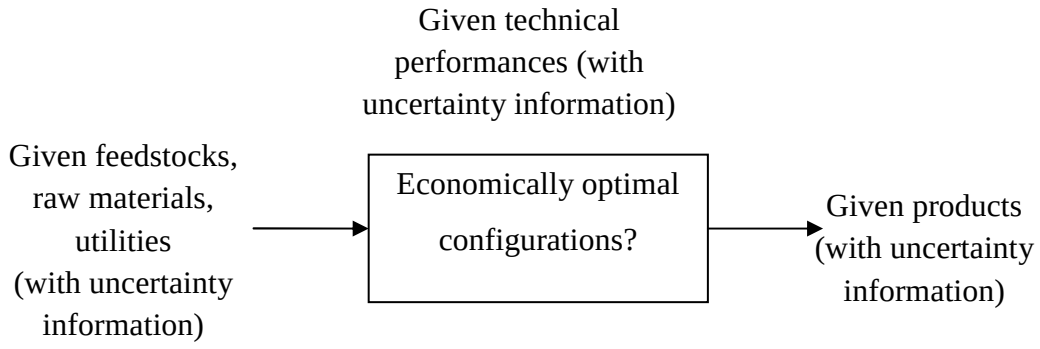

Figure 12. Schematic configuration design with an optimal level of flexibility.

Particularly for the problem of biorefinery configuration design with an optimal level of flexibility, given information is:

- Biomass (feedstock) availability, characteristics, and prices with uncertainty
- Biofuel (and other byproducts) demand, specifications, and prices with uncertainty

- Utility and other raw materials (e.g., hydrogen, acid, enzyme, lime, etc.) availability and prices with uncertainty
- Technical performances (yield, conversion, design equations) with uncertainty.

The profit function is of the following form:

[Profit] = [Product sale] – [Operating cost] – [Annualized capital cost] (35)

Product sale is the annual income from selling products, which is a function of product prices and rates. *Operating cost* includes annual costs of feedstocks, chemicals, utilities, and labor. This second term is a function of their prices and production rates. *Annualized capital cost* accounts for depreciation of the investment and depends on equipment sizes.

3.4 Approach

3.4.1 Disjunctive operation mode constraint

The constraint $f(d,z,x,\theta) \leq 0$ has been referred to as a general form of all constraints involving in the formulations. Let classify those constraints into three following types:

Equalities: $g(d,z,x,\theta) = 0$ (36)

Flow rate bounds: $LB \leq z^{flow} \leq UB$ (37)

Other inequalities: $h(d,z,x,\theta) \leq 0$ (38)

where LB and UB are lower bound and upper bound of flow rate z^{flow} going through equipment (z^{flow} is classified as control variables).

Constraint 36 is a set of process-modeling equations (mass and energy balance, equilibrium, design equations, etc.). Constraint 37 exists because ranges of operating flowrates are limited by equipment sizes which are fixed in operation. Constraint 38 represents other feasible conditions and specifications.

The unique design strategy of this work is to determine the process configurations and equipment sizes such that the process is not in operation when it is not profitable or when qualities are not met. To formulate this strategy, the following set of constraints is proposed to replace Constraints 37 and 38:

$$h(d,z,x,\theta) \leq M \cdot (1 - y) \quad (39)$$

$$LB \cdot y \leq z^{flow} \leq UB \cdot y \quad (40)$$

where M is a large scalar, called big-M, and y is a binary variable.

If the equipment is in operation, then its associating flow rate $z^{flow} > 0$. Constraint 40 imposes $y = 1$; therefore, $h(d,z,x,\theta) \leq 0$ must be satisfied because of Constraint 39. Otherwise, if $h(d,z,x,\theta) \leq 0$ is not met, then $y = 0$ (because of Constraint 39) and z^{flow} is forced to be 0 (because of Constraint 40). Solver will decide the operation mode, i.e., whether $y = 0$ or $y = 1$ to maximize the profit.

They are described as *disjunctive operation mode constraints*. These constraints can be considered as a general form of hard constraints because they become hard constraints when y is assigned 1 (before the formulation is solved). Figure 13 shows an example that using disjunctive operation mode constraints results in an equal or higher profit.

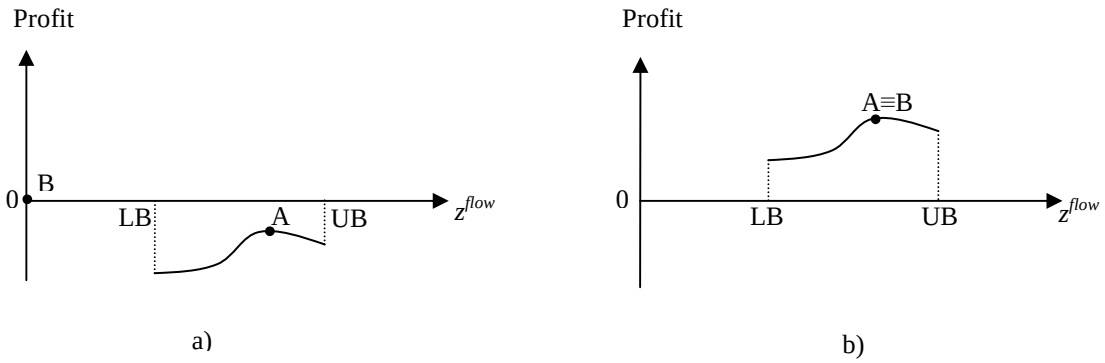

Figure 13. Comparison of solutions from two design strategies: using conventional hard constraints (A) vs. using disjunctive operation mode constraints (B), at two scenarios a) idle is economically favored and b) operation is economically favored.

3.4.2 Formulation

The problem of design with optimal level of flexibility can be formulated as follows:

Problem $P_{2.7}$:

$$\max_{d,z_p,x_p} \sum_{p=1}^{P} w_p \cdot P(d, z_p, x_p, \theta_p) \tag{41}$$

$$\text{subject to} \quad g(d, z_p, x_p, \theta_p) = 0, \quad p = 1,...,P \tag{42}$$

$$h(d, z_p, x_p, \theta_p) \le M_p \cdot (1 - y_p), \quad p = 1,...,P \tag{43}$$

$$LB \cdot y_p \le z_p^{flow} \le UB \cdot y_p \tag{44}$$

$$d \in D,\ z_p \in Z,\ x_p \in X$$

where w_p is a weighting factor. It is usually a probability of occurrence or fractional length of time periods in multi-period design problems.

When it comes to configuration design with optimal level of flexibility, Problem $P_{2.7}$ can be expanded to the following forms:

Problem $P_{2.8}$:

$$\underset{d_j, z_p^{flow}}{\text{Max}} \sum_{p=1}^{P} w_p \cdot R_p(z_p^{flow}, \theta_p) - \sum_{j=1}^{J} C_j(d_j, \theta_j) \tag{45}$$

subject to

Revenue function: $R_p(z_p^{flow}, \theta_p) = \theta_p^{\mathrm{T}} \cdot z_p^{flow}$ (46)

Capital cost function: $C_j(d_j, \theta_j) = \theta_j^{base} \cdot d_j^{\theta_j^{scale}}$ (47)

Availability of raw materials: $h_i(z_p^{flow}) \le M_i(1\text{-}y_i)$, $\forall i \in I,\ p \in P$ (48)

Product demand: $h_k(z_p^{flow}) \le M_k(1\text{-}y_k)$, $\forall k \in K,\ p \in P$ (49)

Mass balance of equipment:

$$g_j(d_j, z_{jp}^{flow\ in}, z_{j'p}^{flow\ out}, \theta_{jp}) = 0, \quad \forall j,\ j' \in J,\ j \ne j',\ p \in P \tag{50}$$

Mass balance between equipment (which defines the process structure):

$$g(z_{jp}^{flow\ in}, z_{j'p}^{flow\ out}) = 0, \quad \forall j,\ j' \in J,\ j \ne j',\ p \in P \tag{51}$$

Equipment sizes in every scenario: $g(d_{jp}, z_{jp}^{flow}) = 0, \quad \forall j \in J,\ p \in P$ (52)

Equipment sizes designed: $d_j \ge d_{jp}$, $\forall j \in J, p \in P$ (53)

Disjunctive operation mode: $\mathrm{LB} \cdot y_{jp} \le z_{jp}^{flow} \le \mathrm{UB} \cdot y_{jp}$, $\forall j \in J,\ p \in P$ (54)

Variable domains: $y_{jp} = 0,1\,, \quad \forall j \in J,\ p \in P$ (55)

$$d,\ z \geq 0 \tag{56}$$

where $R_p(z_p^{flow}, \theta_p)$ is a revenue function for scenario *p* of flow rate variables and parameters of raw materials, product, and operating costs;

$C_j(d_j, \theta_j)$ is a capital-cost function of equipment *j* depending on variables of equipment sizes d_j and parameters to scale capital costs at various sizes.

$P_{2.8}$ is a mixed-integer nonlinear programming problem. The nonlinearity results from the annualized capital cost term (a power function) in the objective function. Additionally, it results from the disjunctive operation mode constraints if the bounds (LB and UB) contain variables, for instance size d_j of associating equipment. In most of the cases, a local optimal solution is also the global optimal solution. (In Lingo,[85] it can be verified when upper and lower bounds are found matched in solution report.)

3.4.3 Solution algorithm

Figure 14 summaries the solution approach to configuration design with an optimum level of flexibility, which consists of the following steps:

- *Transformation of uncertainty models*. As discussed in Section 3.3.1, input information with uncertainty is described in various forms. In this step, they are transformed into a discrete set of scenarios. If the variations are given in continuous ranges, the ranges are discretized into multiple segments. The segments with identical values can be combined into one scenario with summation of their occurrence probabilities. Similarly, if information is available in forms of continuous (long) time periods, they are discretized into multiple equal small periods of which each is assigned a scenario. (Note: This problem objective is flexibility, rather than scheduling.)
- *Formulation*. The problem is formulated as Problem $P_{2.8}$. It is a mixed-integer nonlinear program (MINLP). The nonlinear terms appear in the objective function. They may also appear in constraints if nonlinear models are used. If

all the constraints are linear, global optimum is likely obtained using conventional solution methods.

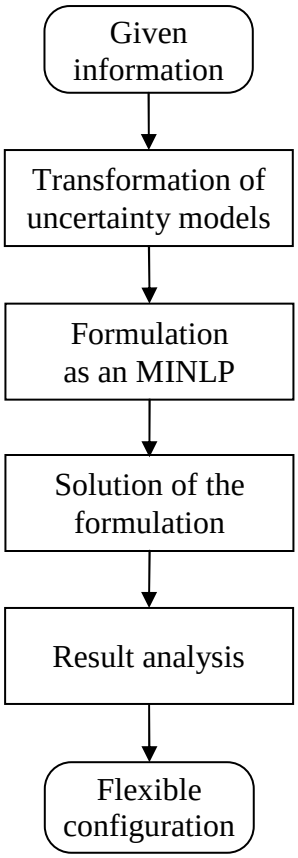

Figure 14. Solution framework to configuration design with an optimum level of flexibility.

- *Solution of the formulation*. The optimization program can be solved using optimization software for the (local) optimum solution. Whether the found solution is the global optimum might be verified in calculation reports.
- *Result analysis*. The solution of the formulation is analyzed for a practical configuration. For example, if a part of the process is assigned idle in most of

scenarios that are expected not to occur in the near future, then that part needs not to be constructed at the beginning of the project. It helps to reduce initial capital cost and to avoid maintenance costs during the idle period.

As a result, a flexible configuration with a maximum expected value of profit is obtained. Also, operation modes in every scenario of uncertainties are available in the solution.

3.5 Case study

3.5.1 Problem description

In Chapter II, the case study of synthesizing lignocellulosic-biomass-to-alcohols pathways showed that mixed alcohol production via acid fermentation and ketonization is one of the most promising pathways. In this chapter, a case study of configuration design with an optimum level of flexibility, based on the mixed alcohol production pathway, is investigated to demonstrate the merits of the proposed approach.

The problem is stated as follows. Given is information on raw materials and products, and a superstructure of processing units with technical performances for the conversion of lignocellulosic biomass to mixed alcohols. It is desired to determine the configuration and sizes of the main processing units that give a maximum expected value of profit.

The information on raw materials (including two lignocellulosic sources and hydrogen) is availability, costs, and components compositions. There are two products: fuel-grade mixture of alcohols as the main product with given demand and prices, and lime as a value-added byproduct with given prices.

The superstructure as shown in Figure 15 has an optional set of processing units (gasification, cogeneration, water-gas shift, and pressure-swing adsorption) to produce power, steam, and hydrogen from fermentation residue. If those units are not employed, the process must import the utilities and hydrogen from external sources and the fermentation residue is considered as waste with a charge of $22/tonne. For simplification in the superstructure, some raw materials (e.g., natural gas, fermentation nutrient source, steam for water-gas shift) and byproducts (e.g., water from vapor

compression system and crystallization, carbon dioxide from lime kiln, solid waste from gasification, steam and power from cogeneration, flue gas from PSA) are not considered in the model because they are accounted for in the operating cost of associating units. Detailed description of the process is available in Section 4.3.1.

Input information is reported in Appendix A. The technical performances are yields, which are based on component rates (instead of total flow rates). Some of the input data have variations with probabilities of occurrence.

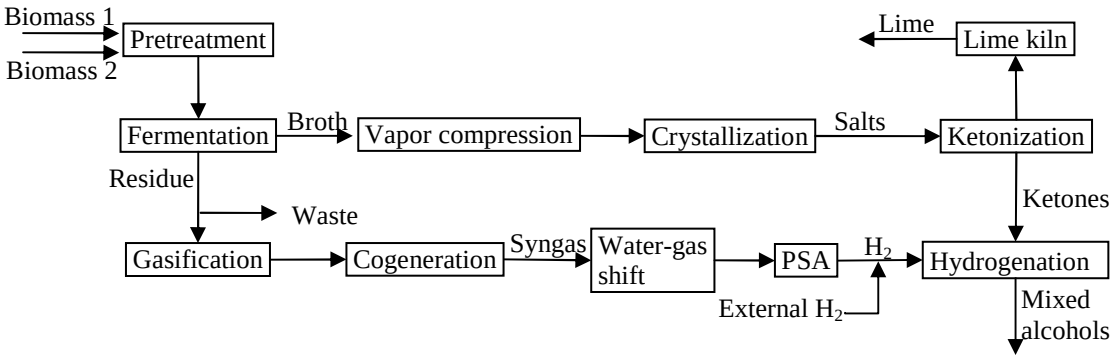

Figure 15. A superstructure of the biomass-to-alcohols configurations.

The capital and operating costs of processing units are modeled in the following forms:

$$\text{Capital cost} = (\text{Capital-cost coefficient}) \cdot (\text{Size of the unit})^{\text{Scaling factor}} \quad (57)$$

$$\text{Operating cost} = (\text{Operating-cost coefficient}) \cdot (\text{Flow rate}) \quad (58)$$

where *size of the unit* is a characteristic size of the associating unit. For example, it is the pile volume in pretreatment unit or it is the total heat transfer area of latent heat exchangers in vapor compression system. *Flow rate* is a characteristic flow rate of associating units, for example, inlet wet biomass rates in the pretreatment and fermentation units (i.e., excluding lime, fresh water, nutrient rates). For this reason, one should not compare operating and capital costs based on the coefficient because the bases of characteristics sizes and flow rates are different. The lists of characteristic sizes

and flow rates of all the units are given in tables on pages 107 and 108. The operating-cost coefficient as well as the operating cost of the cogeneration unit is negative in the model (i.e., making positive profit to the plant) because of credits from power and steam produced from this unit.

3.5.2 Solution

The solution starts with a transformation of models describing input variations. However, for simplification and a clearer presentation the variations are given in six scenarios with probabilities of occurrence (see Appendix A).

The problem can be then formulated in the following forms:

Problem $_{2.9}$:

$$\max \sum_{p=1}^{6} \text{PROB}_p \cdot \text{revenue}_p - \frac{1}{7} \sum_{j=1}^{11} \text{CAPCOEF}_j \cdot \text{msize}_j^{\text{SCALE}_j} \tag{59}$$

subject to

$$\textit{revenue}_p = \sum_{k=1}^{2} \text{PRICE}_{kp} \cdot \text{prod}_{kp} - \sum_{i=1}^{3} \text{COST}_{ip} \cdot \text{supply}_{ip} - \sum_{j=1}^{11} \text{OPCOEF}_{jp} \cdot \text{tflow}_{jp} - 22 \sum_{j=1}^{11} \sum_{m=1}^{10} \text{waste}_{jpm}, \quad \text{for } p = 1,...,6 \tag{60}$$

Availability of raw materials: $\text{supply}_{ip} \le \text{AVAIL}_{ip}$, for $i = 1,...,3,\ p = 1,...,6$ (61)

Compositions of raw materials:

$$\text{content}_{ipm} = \text{FRACTION}_{im} \cdot \text{supply}_{ip} \ , \quad \text{for } i = 1,...,3,\ m = 1,...,10,\ p = 1,...,6 \tag{62}$$

Product demand: $\text{prod}_{kp} \le \text{DEMAND}_{kp}$, for $k = 1,2;\ p = 1,...,6$ (63)

Total inlet flow rate of equipment: $\text{tflow}_{jp} = \sum_{m=1}^{10} f_{jpm}^{IN}$, for $j = 1,...,11,\ p = 1,...,6$ (64)

Mass balance of equipment:

$$f_{jpm}^{OUT} = \sum_{m'=1}^{10} f_{jpm'}^{IN} \cdot \text{YIELD}_{jpm'm}, \quad \text{for } j = 1,...,11,\ m = 1,...,10,\ p = 1,...,6 \tag{65}$$

Mass balance between equipment:

- Raw materials – Pretreatment:

$$\sum_{i=1}^{2} \text{content}_{ipm} = f_{1pm}^{IN} \quad , \quad \text{for } m = 1,...,10,\ p = 1,...,6 \tag{66}$$

- Pretreatment – Fermentation: $f_{1pm}^{OUT} = f_{2pm}^{IN}$, for $m = 1,...,10,\ p = 1,...,6$ (67)

- Fermentation – Vapor compression system & Gasification:

$$f_{2pm}^{OUT} = f_{3pm}^{IN} \quad , \quad \text{for } m = 4,...,10,\ p = 1,...,6 \tag{68}$$

$$f_{2pm}^{OUT} = f_{7pm}^{IN} + \text{waste}_{2pm} \quad , \quad \text{for } m = 1,...,3,\ p = 1,...,6 \tag{69}$$

$$0 = f_{7pm}^{IN} \quad , \quad \text{for } m = 4,...,10,\ p = 1,...,6 \tag{70}$$

$$0 = f_{3pm}^{IN} \quad , \quad \text{for } m = 1,...,3,\ p = 1,...,6 \tag{71}$$

- Vapor compression system – Crystallization:

$$f_{3pm}^{OUT} = f_{4pm}^{IN} \text{ , for } m = 1,...,10,\ p = 1,...,6 \tag{72}$$

- Crystallization – Ketonization: $f_{4pm}^{OUT} = f_{5pm}^{IN}$, for $m = 1,...,10,\ p = 1,...,6$ (73)

- Ketonization & Pressure swing adsorption – Hydrogenation & Lime kiln:

$$f_{3p10}^{OUT} = f_{11p10}^{IN} \quad , \quad \text{for } p = 1,...,6 \tag{74}$$

$$f_{5p7}^{OUT} = f_{11p7}^{IN} \quad , \quad \text{for } p = 1,...,6 \tag{75}$$

$$0 = f_{11pm}^{IN} \quad , \quad \text{for } p = 1,...,6,\ m = 1,...,6,8, \text{ and } 9 \tag{76}$$

$$f_{5p6}^{OUT} + f_{10p6}^{OUT} + \text{supply}_{3p} = f_{6p6}^{IN} \quad , \quad \text{for } p = 1,...,6 \tag{77}$$

$$f_{5pm}^{OUT} = f_{6pm}^{IN} + f_{11pm}^{IN} \quad , \quad \text{for } p = 1,...,6,\ m = 1,...,5 \text{ and } 7,...,10 \tag{78}$$

$$f_{10p6}^{OUT} + \text{supply}_{3p} = 0.055\, f_{5p5}^{OUT} \quad , \quad \text{for } p = 1,...,6 \tag{79}$$

- Gasification – Cogeneration: $f_{7pm}^{OUT} = f_{8pm}^{IN}$, for $m = 1,...,10,\ p = 1,...,6$ (80)

- Cogeneration – Water-gas shift: $f_{8pm}^{OUT} = f_{9pm}^{IN}$, for $m = 1,...,10,\ p = 1,...,6$ (81)

- Water-gas shift – Pressure-swing adsorption:

$$f_{9pm}^{OUT} = f_{10pm}^{IN}, \quad \text{for } m = 1,...,10,\ p = 1,...,6 \tag{82}$$

- Hydrogenation – Main product: $prod_{1p} = f_{6p9}^{OUT}$, for $p = 1,...,6$ (83)

- Lime kiln – Byproduct: $\text{prod}_{2p} = f_{11p10}^{OUT}$, for $p = 1,...,6$ (84)

Equipment sizes in every scenario:

$$\text{size}_{jp} = \text{SIZECOEF}_j \cdot \text{tflow}_{jp}, \text{for } j = 1,...,11,\ p = 1,...,6 \quad (85)$$

Equipment sizes designed: $\text{msize}_j \geq \text{size}_{jp}$, for $j = 1,...,11,\ p = 1,...,6$ (86)

Disjunctive operation mode constraints:

$$0.5 \cdot y_{jp} \cdot \text{msize}_j \leq \text{size}_{jp} \leq 10,000 \cdot y_{jp} \ , \quad \text{for } j = 1,...,11,\ p = 1,...,6 \quad (87)$$

$$y_{jp} \leq 10 \cdot \text{msize}_j \ , \quad \text{for } j = 1,...,11,\ p = 1,...,6 \quad (88)$$

Variable domains: $y_{jp} = 0,1$, for $j = 1,...,11,\ p = 1,...,6$ (89)

$$f_{jpm}^{IN},\ f_{jpm}^{OUT},\ \text{msize}_j,\ \text{size}_j,\ \text{prod}_{kp},\ \text{supply}_{ip},\ \text{tflow}_{jp} \geq 0,$$
$$\text{for } i = 1,...,3,\ j = 1,...,11,\ k = 1,2,\ m = 1,...,10,\ p = 1,...,6 \quad (90)$$

where *i*, *j*, *k*, *m*, and *p* are indices for raw materials, equipment, products, components, and scenarios, respectively; UPPERCASES notates given parameters (corresponding to θ) and lowercases are variables (corresponding to *d*, *z*, and *x*) to be determined; indices for processing units are numbered in the following order: (1) Pretreatment, (2) Fermentation, (3) Vapor compression system, (4) Crystallization, (5) Ketonization, (6) Hydrogenation, (7) Gasification, (8) Cogeneration, (9) Water-gas shift, (10) Pressure swing adsorption, and (11) Lime kiln.

In the objective function, the total capital cost is divided by 7 to account for straight-line 7-year depreciation with a discount rate of 0%. In the disjunctive operational mode constraints, equipment is forced to operate at least 50% of designed capacity; otherwise, it is not in operation. The upper limit is 100% of designed capacities, which is imposed by Constraint 86. Big-M is not needed in the inequality constraints of raw material availability (Constraint 61) and product demand (Constraint 63) in this particular case study because they are automatically satisfied when associating flow rates are zeros. The coefficients (which are 10,000 and 10) in the disjunctive operational mode constraints are arbitrary big numbers to impose $y = 1$ when size > 0 and $y = 0$ when msize = 0, respectively.

Lingo[85] software version 10.0 was used to solve this optimization program. Formulation codes in Lingo are reported in Appendix B. A global optimum was found in 207 seconds on a personal computer with the processor Intel Core i3 M350@2.27GHz and with 4.0 GB RAM. The global optimum was obtained with aid of the default built-in Global-Solver tool in Lingo 10.0.

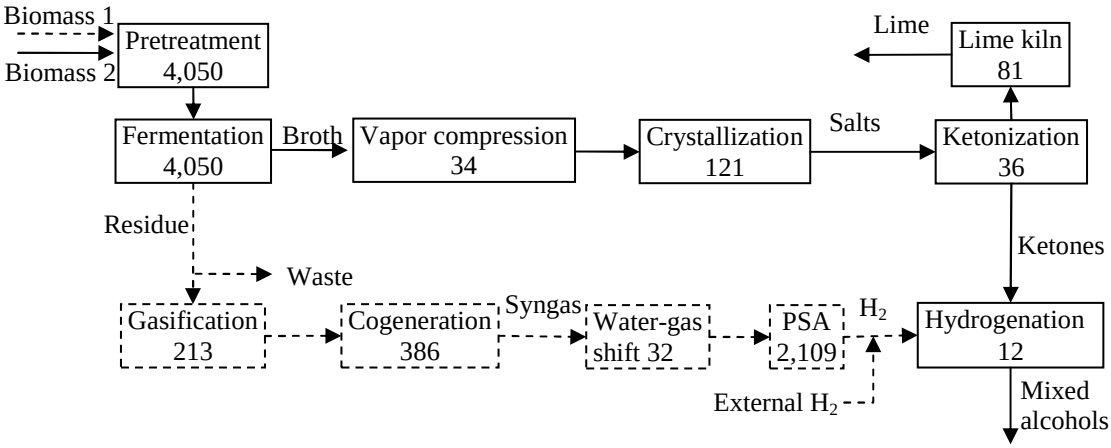

Figure 16. Designed flexible biorefinery with characteristic sizes.

A detailed report of calculated variable values is attached in Appendix C. The result shows that all the processing units in the super structure are employed in the optimum design. Figure 16 depicts the design of the biorefinery with characteristic sizes of all the processing units. In the figure, the units and streams with dash lines are invested but not employed in all scenarios. The result (Table 4) also gives the operation modes in every scenario as follows:

- *Scenario 1* – This is the scenario with the highest occurrence probability (50%). All of the processing units are designed to operate at full capacities in this scenario. The plant only uses Biomass 2 (i.e., no Biomass 1) because Biomass 2 has significantly lower cost although it has higher content of lignin. The plant needs external hydrogen because hydrogen from processing

residue is not enough for the Ketone Hydrogenation unit. Let refer to this scenario as a base case. Other scenarios are compared to this scenario to clarify the difference of operation mode.

- *Scenario 2* – External hydrogen ($200/tonne) in this scenario is much cheaper than in Scenario 1 ($4,000/tonne). For economic reason, the plant uses only external source for the hydrogen demand. As a result, the residue processing section (including gasification, cogeneration, water-gas shift, and PSA) is idle. Other sections are in operation with full capacities. All fermentation residue (142 tonne/h) is discharged as waste.
- *Scenario 3* – The prices of the two biomass feedstocks are higher ($90 and $40 versus $30 and $5/wet tonne). These prices are too high for the plant to be profitable. Therefore, the whole plant is shutdown. In other words, the highest profit in this scenario is 0. (Note that in practice a plant still loses money if it is not in operation because of some fixed costs such as wages, debt interest, etc.)
- *Scenario 4* – The situation of this scenario is the limited availability of favorable Biomass 2. In addition to using all Biomass 2 availability, the plant intakes some amount of Biomass 1. The mixed feedstock has lower content of lignin which is a source for internally producing hydrogen. Total yield of the main product is higher. As a result, pretreatment and fermentation operates under capacities whereas the downstream processing units operate at limitation (full capacities). Furthermore, more external hydrogen is needed.
- *Scenario 5* – The fermentation yield is assumed dropped for some reason, e.g., the yield in a commercial-scale plant is lower than that in the laboratory scale. The results show that the plant production rate is reduced although pretreatment and fermentation operate at full capacities. The good point is that no external hydrogen is needed because demand of hydrogen in the

Ketone Hydrogenation unit is reduced and fermentation residue is more than enough (a small portion of the residue, 18 tonne/h, is discharged as waste).

- *Scenario 6* – Demand of all products is increased. For economic reasons, production rate should be increased because the operation is profitable as seen in Scenario 1. However, the production rate is kept as in Scenario 1 because of capacity limitation of the designed sizes. Occurrence probability of Scenario 6 is lower than Scenario 1. Therefore, solver chooses the equipment sizes to be best suitable for Scenario 1. In other words, increasing equipment sizes is favored for operation in Scenario 6 but it is not favorable in a big picture considering all the scenarios.

Table 4. Summary of the case study result.

Operational mode	Scenario					
	1	2	3	4	5	6
Main processing chain	On	On	Off	On	On	On
Residue processing chain	On	Off	Off	On	On	On
Biomass 1 usage (tonne/h)	0	0	0	168	0	0
Biomass 2 usage (tonne/h)	450	450	0	250	450	450
External H_2 usage (tonne/h)	0.41	2.11	0	0.60	0	0.41
Sign of profit value	+	+	0	+	+	+

In general, the result analysis shows that the operation in some scenarios is not optimum. If designers know for sure that a certain scenario will occur, the design will be different to suit that scenario. Because of uncertainty, however, the final design must accommodate all scenarios (i.e., be flexible) with an optimum of expected profit value. Although the design is not economical in Scenario 3, it is still worth building the plant because occurrence probability of Scenario 3 is very low (5%).

3.6 Summary

Input information for the design of chemical processes has uncertainty or variations. In the design stage, process designers must anticipate the changes of input, which may

occur in the operation stage and must decide on what strategies to respond. This is the problem of design with flexibility.

The traditional approach, which employs overdesign factors, does not guarantee feasible operation and results in unnecessary additional costs. Developed systematic approaches are conservative, result in robust yet expensive design and non-profitable operation, or involve the issue of complicated flexibility analysis.

This chapter proposes a new class of design problems with flexibility and a new formulation approach that is well suited for the design of flexible bio-refinery configurations. The design strategy is to build the most profitable plants that operate only when economic efficiency is favored and product qualities are met. If these conditions are not satisfied, part of the plant is idle or the whole plant is shutdown to avoid economic loss. Hence, the design has an optimum level of flexibility. The formulation approach is to include *disjunctive operation mode constraints*. The solution to the formulation is a mixed-integer nonlinear program and solvable for a global optimum in a regular optimization software.

A case study of configuration design for the mixed-alcohol production pathway successfully demonstrated the merits of the proposed approach. The design shows its level of flexibility in operational modes in various scenarios of input changes. The expected profit value was maximized.

This research has investigated the new concepts in deterministic flexibility problems. Future work is recommended to consider applicability of the proposed approach to stochastic flexibility problems and other process system engineering problems.

CHAPTER IV
TECHNO-ECONOMIC ANALYSIS OF A LIGNOCELLULOSE-TO-HYDROCARBONS PROCESS VIA THE CARBOXYLATE PLATFORM

In Chapter II, a methodology to quickly synthesize and screen biorefinery pathways was developed. From a promising pathway, flexible conceptual biorefinery configurations that can accommodate uncertainty and variations of inputs were designed using the novel design strategy and solution approach in Chapter III. This chapter is a further step in the process of biorefinery design.

In this chapter, a technical and economic analysis of a biofuel process was performed. Data were obtained from sources that are as much reliable as possible to the authors. The biofuel process has additional downstream units to convert mixed alcohols into hydrocarbon fuels. The ensuing sections are organized in a similar order to the sequence of the techno-economic analysis: (1) overview of the process, (2) technical analysis, (3) economic analysis, and (4) sensitivity analysis.

4.1 Introduction

Technologies for renewable fuels from biomass are being developed to reduce dependence on imported petroleum, decrease greenhouse gas emissions, and improve national security. Many biochemical and thermochemical pathways have been proven technically; however, high production costs have prevented many pathways from being economically viable without government subsidies. Figure 17 summarizes typical pathways to produce hydrocarbon fuels from biomass via alcohols.

- The sugar-to-alcohol pathway represents industrial production of bioethanol from sugarcane in Brazil.
- The starch-to-alcohol pathway uses amylase enzymes to produce intermediate sugars, which is exemplified by the corn-to-ethanol industry in the United States.
- The lignocellulose-to-alcohol pathway uses cellulase enzymes to produce intermediate sugars, which is in the process of being commercialized.

- The thermochemical pathway gasifies biomass into syngas ($CO + H_2$), which is then catalytically converted into methanol or ethanol.
- The lignocellulose-to-alcohol pathways use mixed cultures of acid-forming micro-organisms to produce intermediate carboxylates (ammonium carboxylates in Path A, calcium carboxylates in Paths B and C), which are described as carboxylate platforms. Via pure-culture fermentation, the carboxylate platform is described by Agler et al.[86]

The first three biochemical platforms require aseptic fermentations, which is expensive. Further, because of its recalcitrance to enzymatic hydrolysis, lignocellulose requires high cellulase loadings. The carboxylate pathways produce fuels and chemicals from biomass without encountering those problems.

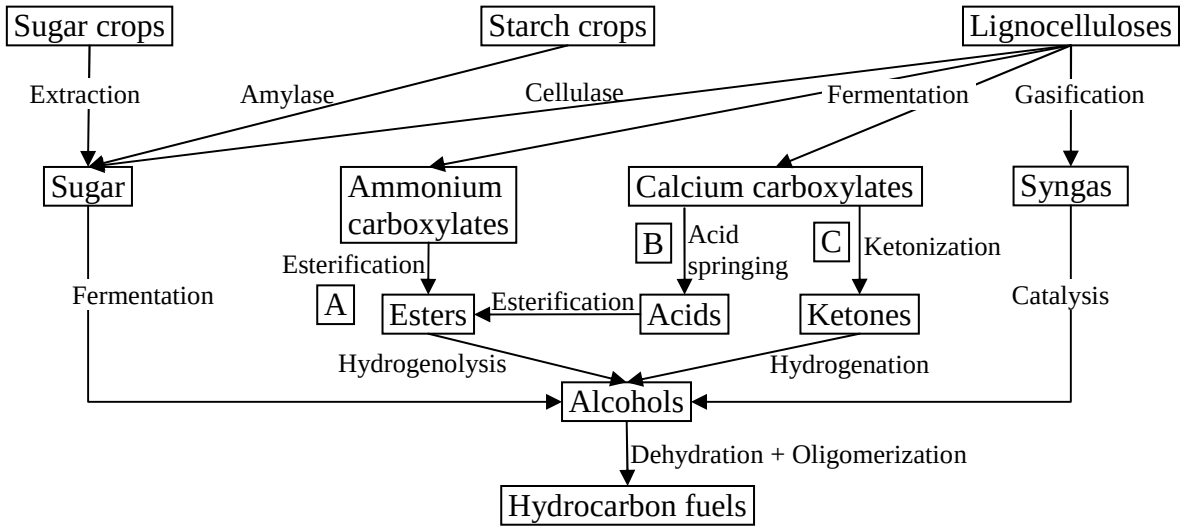

Figure 17. Pathways for converting biomass to hydrocarbon fuels.

In terms of intermediate chemicals, the pathways shown in Figure 17 employ three platforms: sugar, carboxylate, and syngas. Holtzapple and Grand[31]a[31] showed that the carboxylate and sugar platforms give the highest theoretical yield of lignocellulosic biomass to hydrocarbon fuels when the three platforms were compared using the same ideal biomass feedstock. The biomass composition was assumed to consist of 31.7%

lignin and 68.3% polysaccharides on an ash-free basis, which is similar to compositions found in hardwood biomass. The theoretical energy efficiency of the carboxylate platform is equal to that of the sugar platform and higher than that of the syngas platform.

When producing hydrocarbons from alcohols, dehydration causes a mass loss of 30% (isopropanol), 39% (ethanol), and 56% (methanol). The theoretical loss of energy is 2% (isopropanol), 5% (ethanol), and 10% (methanol). Based on these examples, the pattern is clear: higher alcohols have greater retention of mass and energy when converted to hydrocarbons. The carboxylate platforms can produce higher alcohols (propanols and higher) than the other platforms.

A key feature of the carboxylate platform is the fermentation, which employs a mixed culture of acid-forming microorganisms to convert biomass components (carbohydrates, proteins, fats) to carboxylate salts. The process does not require aseptic conditions, which lowers capital costs and improves operability. The microorganisms produce their own enzymes – a type of consolidated bioprocessing – which reduces operating costs compared to traditional enzymatic pathways. Depending on the choice of buffer, the salts are ammonium carboxylates (buffered by NH_4HCO_3) or calcium carboxylate (by $CaCO_3$). Via Pathway A (Figure 17), ammonium carboxylates are processed by esterification and hydrogenolysis, which produces a mixture of primary alcohols. Because there is almost no carbon loss from biomass to final products, this pathway has a high theoretical overall alcohol yield. Via Pathway B (acid springing), the calcium carboxylates are converted to the corresponding carboxylic acids. From the acids, mixed alcohols are produced by esterification and hydrogenolysis. Via Pathway C, calcium carboxylates are thermally converted into ketones, which subsequently are hydrogenated into a mixture of secondary alcohols. In the latter route, the overall alcohol yield is lower than that of the former, but it does not demand as much hydrogen.

Biomass-to-fuel pathways via the carboxylate platform have been researched and developed for 20 years in Dr. Mark Holtzapple’s research group at the Department of

Chemical Engineering, Texas A&M University. The technologies have been further developed and licensed by Terrabon, Inc. under the trademarked name MixAlco™.

Previous work on MixAlco™ process economics includes a study by Holtzapple et al.[87] who estimated the economics of the calcium carboxylate platform (Pathway C) using municipal solid waste or sugarcane bagasse as feedstocks. For the dewatering process, they employed water extraction with amines and multi-effect evaporation. Lau et al.[88] evaluated the production of ethanol from sweet sorghum via the acid springing platform (Pathway B) using various scenarios of plant location, capacity, and incentives. Granda et al.[60] analyzed the process economics of the ammonium carboxylate pathway (Pathway A) using municipal solid waste as feedstock in different scenarios of hydrogen sources and prices.

This chapter performs a techno-economic analysis for the lignocellulose-to-hydrocarbons pathways using the calcium carboxylate platform (Pathway C) with vapor-compression dewatering, which is a version of the MixAlco™ process. Pham et al.[89] performed a similar techno-economic analysis at a different plant capacity. Compared to previous efforts, this work emphasizes process synthesis, integration, and analysis with simulation in Aspen Plus,[90] equipment cost estimation from Aspen Process Economic Analyzer,[91] and the most updated experimental data and cost basis.

4.2 Approach

The techno-economic analysis was performed in five key steps as shown in Figure 18.

- Development of process flow diagrams: From experimental data on key conversion and separation steps, designs for a plant at commercial scale were developed. All equipment necessary for conversion, separation, transportation, treatment, and storage is identified.
- Simulation and calculation of mass and energy balance: Process simulation software Aspen Plus90 was used to simulate the process. Some biofuel components (e.g., lignin, xylan, xylose) are not available in the Aspen Plus database. They were added to the simulator in a user-defined database, called

Inhouse Database (INHSPCD) in Aspen Plus, using estimated properties from NREL.[92,93] A few reactions (for example, pretreatment, waste treatment) and separation (filtration, drying, crystallization) were difficult to simulate in Aspen Plus and therefore were treated as a "black box" simulation. Mass balances of these units were given from experimental data or estimated by heuristics. As a result of this step, flow rates of every stream, utility demand, and energy generation were available in the simulation results.

- Process integration: In this integration step, the process design was modified to minimize overall consumptions of resources: chemicals, fresh water, external energy demand, make-up solvent, etc. Two types of process integration problems were performed: (1) heat integration of heat exchanger networks using pinch analysis to target simultaneously the minimal heating and cooling utility demand[94] and (2) recycle water and other chemicals to minimize fresh usage.[95] After the targets were identified, integrated heat exchanger networks and recycle strategies were synthesized so the overall consumption of fresh resources was close to the target values, subject to the constraint that the processes be practical and readily controlled. The integration results were then used to update the simulation models, mass balance, and energy balance.
- Equipment sizing and costs: Most of the simulation models in Aspen Plus calculated the equipment size, which were detailed enough to estimate equipment costs in Aspen PEA software.91 For unconventional equipment that is not available in Aspen PEA, their costs were obtained from vendor quotes or estimated from the literature. For example, some equipment common in biofuel process – but not found in the software – are bale transport and unwrapping conveyers, truck scales, belt filters, clarifiers, and large digestion tanks. A good source of literature references for such equipment is the techno-economic analysis reports of NREL.[23,27,96] If an equipment cost is referred to the literature, the reference cost is scaled to appropriate capacity with scaling exponents

reported by Wallas[97,98] and is updated to year 2010 dollars using the Chemical Engineering's Plant Cost Index.[99]

- Project economic and sensitivity analysis: The estimated equipment costs account for equipment only, i.e., the costs of equipment materials and fabrication. Other project costs (e.g., equipment installation, instruments and piping, construction, building, contingency) were assumed proportional to the equipment costs by predefined factors. For biochemical processing equipment, the factors are employed from the NREL method.[23] For traditional chemical processing equipment, the factors are employed from the Lang method.[98] Cash flow analysis was performed to evaluate project economics in a base case. After that, sensitivity analysis was performed to investigate how the project economics were sensitive to technical performance (e.g., yields, concentrations, capacity, heat transfer coefficient, temperature approach of latent heat exchangers) and economic assumptions (e.g., raw material prices, after-tax discount rate, cost estimation uncertainty).

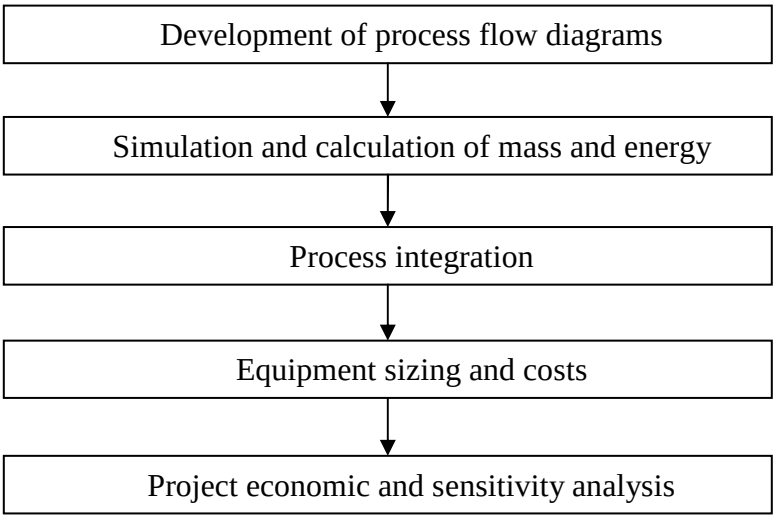

Figure 18. Major steps of the techno-economic analysis.

These are five essential steps; however, a biofuel techno-economic analysis is not limited to these steps. In addition, the following issues must be considered:

- Plant capacity, location, and logistic systems to collect biomass feedstock
- Type of feedstock
- Life cycle assessment and greenhouse gas emission
- Technology alternatives of key conversion steps

These issues are out of the scope this work, but they are interesting topics for future work.

4.3 Technical analysis

4.3.1 Process description

Figure 19 depicts biomass-to-hydrocarbons via the MixAlco^{TM} process. To make hydrocarbon fuels, the MixAlco^{TM} process has the following steps: (1) pretreatment with lime, (2) fermentation with a mixed culture of acid-forming microorganisms to obtain carboxylate salts, (3) dewatering with a high-efficiency vapor-compression evaporator, (4) thermal conversion of salts to ketones, (5) hydrogenation of the ketones to mixed alcohols, and (6) oligomerization of alcohols to hydrocarbons using zeolite catalysts.

The biomass feedstock must contain a source of energy and a source of nutrients. Examples of energy sources include sorghum, bagasse, municipal solid waste, office paper, paper fines, rice straw, water hyacinths, pineapple waste, and aloe-vera pulp. Examples of nutrient sources include food scraps, sewage sludge, or manure. In addition, chemical nutrients (e.g., urea, ammonia, ammonium bicarbonate) can be added to supply essential minerals. In this techno-economic analysis, forage sorghum and manure are used as the feedstock in a recommended ratio of 80:20 sorghum:manure.[100] Sorghum is an energy crop that has been well studied and developed at Texas A&M University.

If the biomass has significant lignin content, it is pretreated with lime, which can be recycled using downstream processes. In the fermentation, the nutrient source is mixed with the pretreated biomass. From the ketonization reactor, calcium carbonate is recycled to buffer the fermentation, which produces a broth of mixed calcium carboxylates. In the descumming and dewatering unit, the broth is concentrated to obtain

solid salts, which are then thermally converted into ketones and calcium carbonate in the ketonization unit. Then, the ketones are hydrogenated into mixed alcohols. Potential sources of hydrogen include fermentation broth, gasified fermentation residue, reformed methane, and water electrolysis. In the base case, hydrogen is recovered in the plant from fermentation gas and shifted syngas. The recovered hydrogen is sufficient to meet the demands of ketone and olefin hydrogenation. To make hydrocarbons, the mixed alcohols are dehydrated and oligomerized to produce olefins, *n*-paraffins, iso-paraffins, and aromatics with boiling ranges of gasoline and kerosene depending upon reaction conditions employed in the oligomerization reactor. The light fraction can be used for gasoline and the heavy fraction used as jet fuel. To improve product quality, the olefins can be saturated.

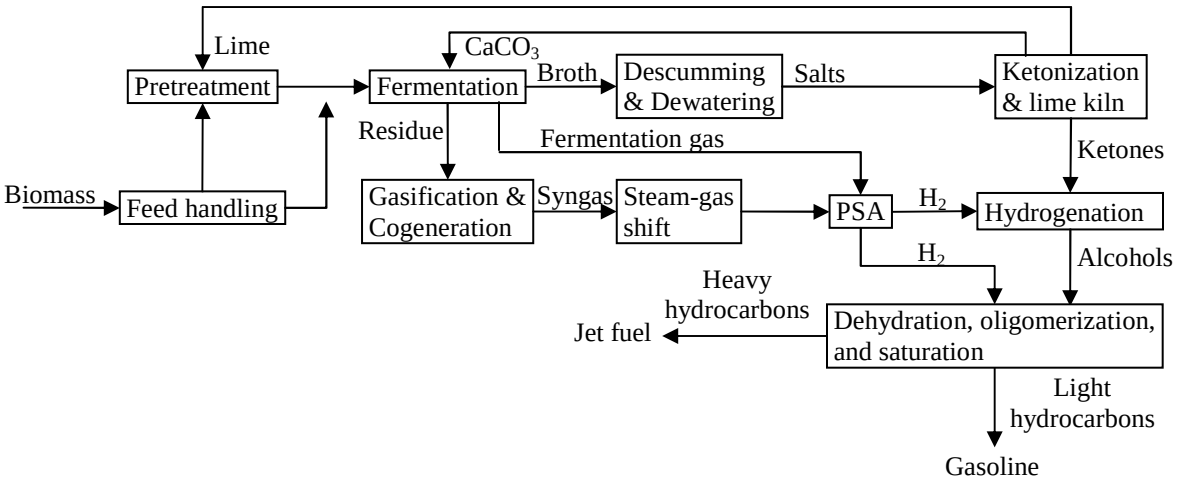

Figure 19. Simplified process block diagram of the analyzed MixAlco^{TM} process (Pathway C).

In one process option, the undigested fermentation residues (about 20% of the biomass feed) is gasified and processed via cogeneration, steam-gas shift, and pressure-swing adsorption (PSA) units to generate steam, power, and hydrogen for the plant.

Using Pathway C, hydrogen from gasified biomass residue and fermentation gas are sufficient to supply the hydrogen needs of the plant.

In the MixAlco™ process, the fermentation broth contains 2 – 6% salts, which is concentrated using vapor-compression and crystallization units. The recovered distilled water is recycled to the fermentation and pretreatment. Water entering with the biomass feed is purged as distilled water, which can be sold as a by-product.

Pretreatment and Fermentation

In principle, any chemical or physical pretreatment method can be used in the MixAlco™ process; however, lime pretreatment is the best choice for purposes of mass integration, reactor design, and operation. Recycled lime from the lime kiln is assumed to contribute 65% of lime demand in the pretreatment with the 35% make-up lime purchased from external vendors. Using lime, the pretreatment can be performed in simple inexpensive pile reactors.[31] Pile pretreatment integrates with fermentation piles in a round-robin system, in which biomass solids are held in the same pile for both pretreatment and fermentation. Although the residence time of pretreatment (6 weeks) and fermentation (up to 8 weeks) is long, the round-robin system results in steady flowrate and product concentration in the broth.

Using a mixed culture of microorganisms is the key feature of the MixAlco™ process. These microorganisms not only digest carbohydrates, but also proteins and fats. For food wastes, this advantage gives a significantly higher overall yield than other common fermentation methods. The MixAlco™ process does not require sterilization or external enzymes, which reduces capital and operating costs. Consequently, reactors do not require stainless steel, and can be constructed using low-cost materials (e.g., concrete or plastic) that support piles or submerged fermentation. Holtzapple et al.[87] discuss the design of submerged fermentation ponds.

Figure 20 depicts a pile reactor. Shredded biomass is piled up on 1-meter-thick gravel bed which is used to filter water draining from the pile. The water is pumped back to the top. Underneath the gravel layer is a geo-membrane layer to isolate the system from surrounding soil. The pile, which is up to 30 m high, can be used for pretreatment

and fermentation. In pretreatment mode, air is blown through a scrubber to remove carbon dioxide and discharged to the bottom of the pile. In fermentation mode, the pile must be covered by a geo-membrane and air is not introduced to maintain anaerobic conditions. To remove odors, fermentation gases are discharged through a biofilter.

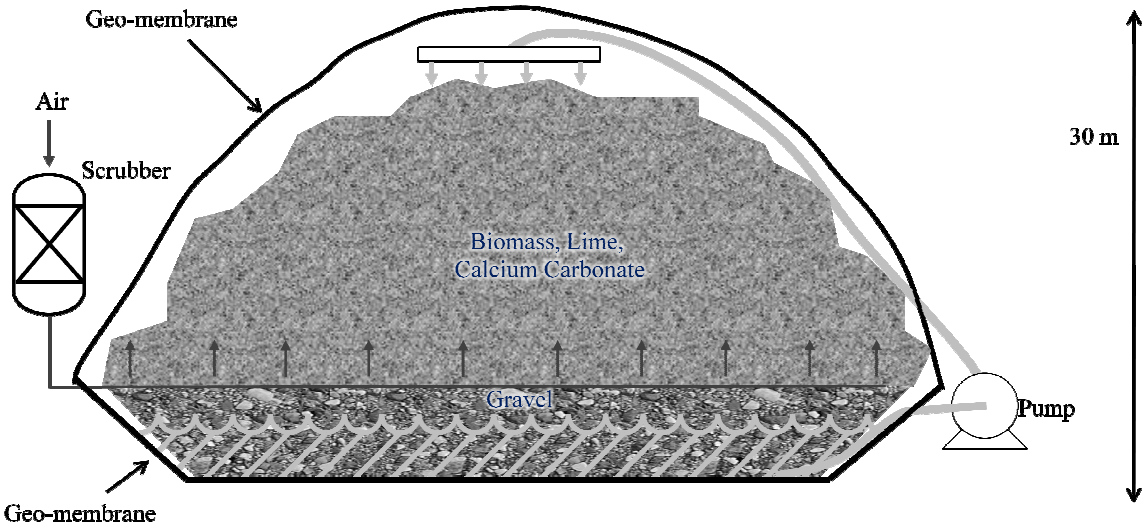

Figure 20. Pretreatment and fermentation pile reactor.

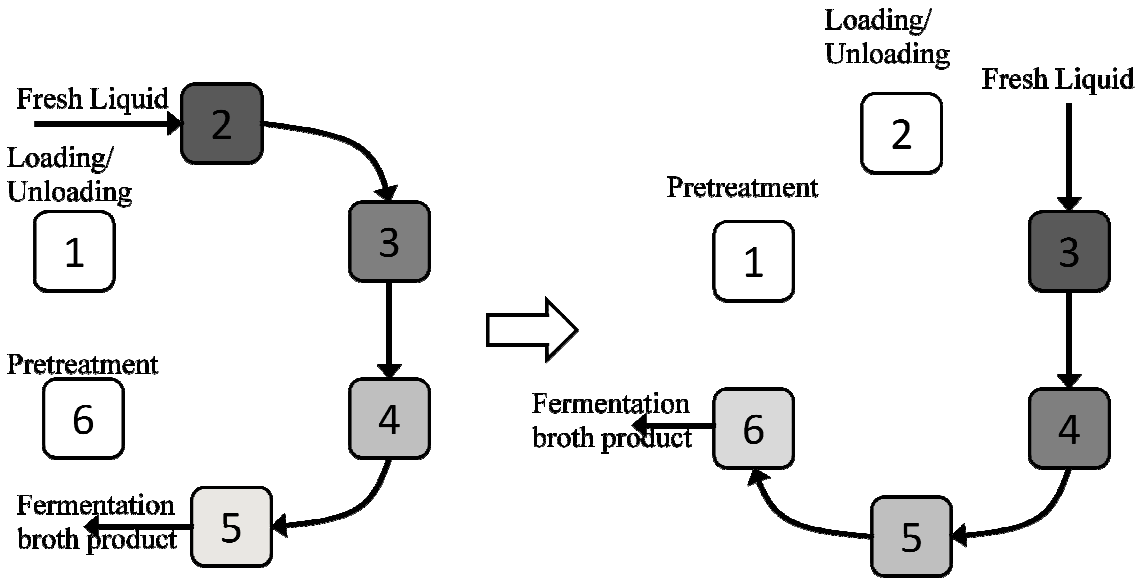

Figure 21. Round-robin operation (darker boxes represent older fermenting piles).

The pretreatment and fermentation piles are in batch operation with a total residence time of up to 11 weeks. In contrast, the downstream sections operate in continuous mode. The pretreatment and fermentation configuration was designed to operate in a round-robin system to minimize fluctuation of outlet fermentation concentration and flow rate. Figure 21 delineates a round-robin system of six pile reactors. A reactor can be in pretreatment mode and later in fermentation mode. At a given time, one of the reactors is being loaded or unloaded, one is in pretreatment mode, and the other four are in fermentation mode but at different extents of conversion. Reactor 2 is the oldest and Reactor 5 is the newest fermentation. Although solid biomass does not move, water flow is countercurrent with fermentation maturity. Fresh water is pumped to the oldest fermenting pile, circulated internally, and pumped to the next newer pile. As a result, the most dilute broth contacts the most digested biomass and the most concentrated broth contacts the freshest biomass. This countercurrent arrangement allows for both high product concentrations and conversions.

Dewatering

In the base-case scenario, calcium carboxylate concentration in the fermentation broth is assumed to be 5% weight. Other components (e.g., dissolved carbon dioxide, microorganisms, undigested biomass, and other unknowns) are impurities and must be removed along with water. To purify the carboxylate salts, the broth is degassed by stripping, descummed using flocculant, evaporated with vapor compression, and crystallized (Figure 22).

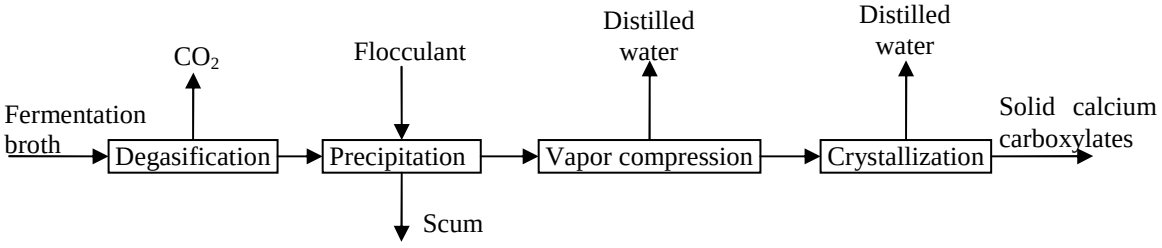

Figure 22. Simplified process block of the descumming and dewatering unit.

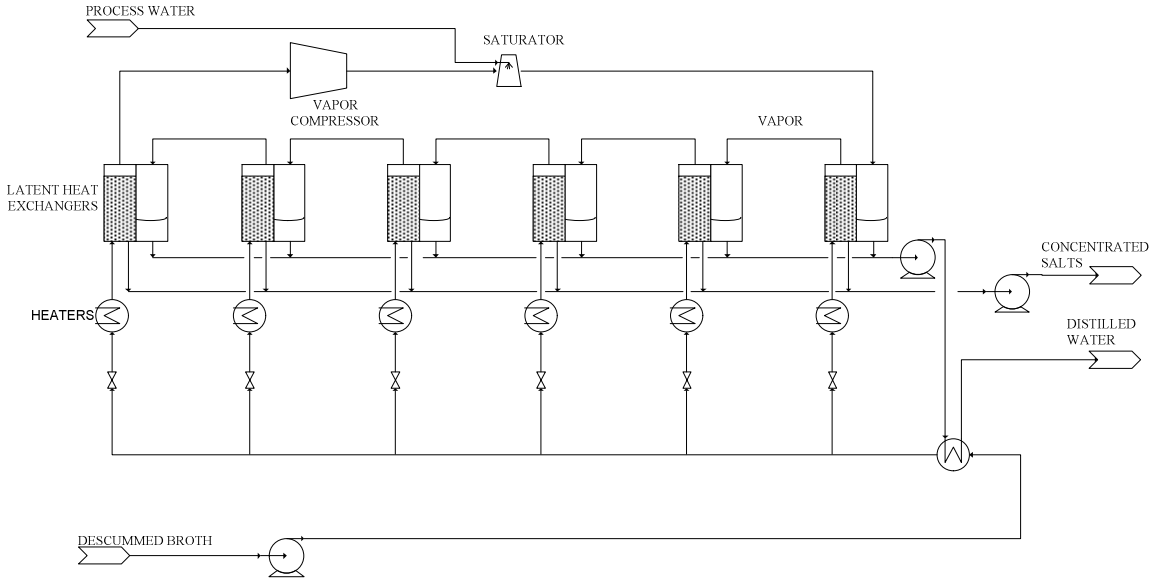

Figure 23. A parallel configuration of multi-effect vapor-compression evaporator.

The key to efficiently vaporizing water is the novel design and optimized operating conditions of the vapor-compression unit. Figure 23 is a simplified process flow diagram of the vapor-compression unit. At high pressure (8 bars), the descummed broth is preheated by countercurrent exchange of heat from product streams (which contain condensed water), and then is evenly split into many stages. The figure shows six stages, but there can be tens of stages in practical plants. In this work, six stages were chosen. In every stage, the inlet streams pass through a valve and a heater to be adjusted to saturation conditions. After that, they enter latent heat exchangers and use heat from the condensing vapor of an adjacent stage to vaporize water from the fermentation broth. The vapor from the first stage is compressed to a higher temperature and pressure, and then is saturated so it readily condenses and transfers heat to the last stage. In Figure 23, the pressure profile of the latent heat exchangers increases from left to right. With this profile, vapor from the right adjacent stage has higher temperature than the salt solution in the left adjacent stage; hence, heat transfer occurs. Using copper plates with a hydrophobic coating to promote dropwise condensation, an extremely high overall heat

transfer coefficient of 240 kW/(m^2·K) (42,200 Btu/(h·ft^2·F)) was achieved using ΔT = 0.2 K at the laboratory scale.[101,102] This allows a very small temperature approach of only 0.20 K (0.36°F) while maintaining a high heat flux of 48 kW/m^2. As a result, the compression ratio of the compressor is small, which saves both associated capital and operating costs. The net energy consumption of this vapor compression unit is only 1.45 kWh per m^3 (18.8 MBtu/1,000 gallons) of water vaporized, equal to 0.14% of the latent heat vaporization of the same amount of water.

Ketonization

The solid salts are sent to a dryer to remove residual moisture (Figure 24). At high temperatures (430°C) in the ketonization reactor, calcium carboxylates are thermally converted into ketones and calcium carbonate

R-COO Ca COO-R' → R-CO-R' + $CaCO_3$

where R and R' represent hydrocarbon groups. The reactor is kept under vacuum (30 mm Hg) which reduces residence time to avoid decomposing the produced ketones. The ketone vapor is quickly removed from the reactor, quenched, and condensed. Part of the calcium carbonate is directly recycled to the fermentors and the remaining portion is converted into quick lime (CaO) in a kiln. The quick lime is recycled to the pretreatment reactors. Unlike conventional lime kilns that are fed coarse limestone, this kiln processes fine calcium carbonate powder; thus, some processing steps (grinding, drying) are not needed.

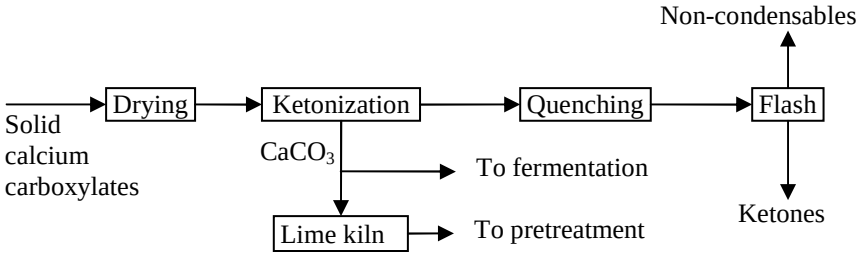

Figure 24. Simplified block diagram of the ketonization and lime kiln unit.

Ketone hydrogenation

In this conversion step (Figure 25), the ketone carbonyl groups react with hydrogen to form alcohol groups in an exothermic reaction:

$$R\text{-}CO\text{-}R' + H_2 \rightarrow R\text{-}CH(OH)\text{-}R'$$

The reaction is performed at high pressure (55 bars) and at isothermal (130^{o}C) conditions. The optimal design was found to be three CRTRs in series.[103] In each CSTR, liquid ketones, solid Raney nickel catalyst, and hydrogen bubbles are well mixed. The heat of reaction is recovered by a pump-around system. Hydrogen is fed to every CSTR in 20% excess to maximize the ketone conversion. The net demand of hydrogen is 0.0225 kg H_2/kg mixed alcohol (25.0 SCF per gallon of mixed alcohols) or 0.00687 kg H_2/kg dry ash-free biomass (1.30 SCF per dry ash-free pound of biomass). The produced mixture of secondary alcohols can be directly used as a transportation oxygenated fuel like bioethanol, but it has higher energy content (net heating values are 34.6 and 26.8 MJ/kg, respectively).

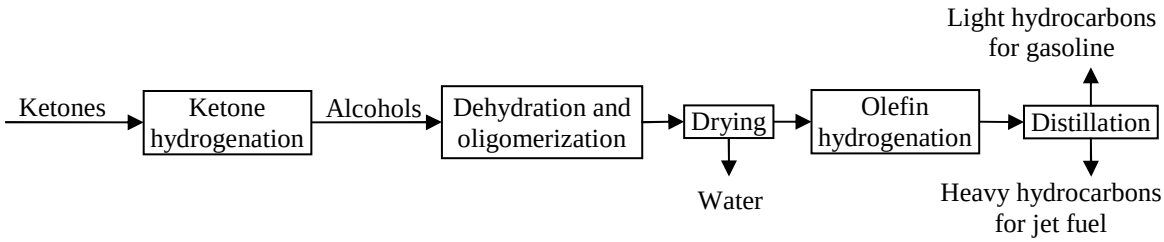

Figure 25. Simplified block diagram of ketone hydrogenation, dehydration & oligomerization, and olefin hydrogenation units.

Dehydration and oligomerization

The mixed alcohols are further processed to produce hydrocarbon fuels (Figure 25). Using H-ZSM-5 catalyst in a reactor at 300^{o}C and 3 bars, the alcohols are dehydrated:

$$R\text{-}CH(OH)\text{-}CH_2\text{-}R'' \rightarrow R\text{-}CH{=}CH\text{-}R'' + H_2O \quad (91)$$

In the same reactor, the produced olefins are oligomerized as shown in the following simplified reaction:

$$C_mH_{2m} + C_nH_{2n} \rightarrow C_{m+n}H_{2m+2n} \quad (92)$$

Depending upon the specific reaction conditions (time, pressure, temperature), the products are very complex and include olefins, *n*-paraffins, iso-paraffins, aromatics, and cyclics. Water dissolved in the hydrocarbon products is removed in a drying unit using a salt filter.

Olefin hydrogenation

To improve fuel quality, the olefins can be hydrogenated to make corresponding paraffins (Figure 25). Similar to the design of the ketone hydrogenation, this conversion unit employs CSTRs in series with Raney nickel catalyst. The carbon double-bond C=C is saturated to stabilize the hydrocarbon product:

$$C_xH_{2x} + H_2 \rightarrow C_xH_{2x+2} \quad (93)$$

In this step, the net demand of hydrogen is 0.0139 kg H_2/kg hydrocarbon fuels (15.4 SCF per gallon of hydrocarbon fuel) or 0.0034 kg H_2/kg dry ash-free biomass (0.64 SCF per dry ash-free pound of biomass). Out of the reactor, the mixed hydrocarbons are distilled into C_{8-} and C_{9+} fractions. The light fraction and heavy components can be used as blending components for gasoline and jet fuel, respectively.

Hydrogen source

Hydrogen is required to produce alcohols and saturate hydrocarbons. Two scenarios of hydrogen sources were analyzed.

In the first scenario, hydrogen is produced by gasifying undigested biomass from the fermentors. The investment includes not only gasification, but also cogeneration, steam-gas shift, and pressure-swing adsorption (PSA, next section) to supply hydrogen, steam, and power for the plant. Figure 26 shows the gasification and cogeneration processes in this scenario. First, the small amount of the biomass suspended in the pretreatment liquor is recovered in filtration. Then, that filtered biomass is mixed with fermentation residue and dried in a rotary dryer using flue-gas heat. After drying, the moisture content in the biomass is about 10%. In the next step, the dried biomass is gasified to generate syngas

and byproduct char. Energy from the hot syngas is used to make high-pressure steam, which is expanded in a steam turbine to generate power.

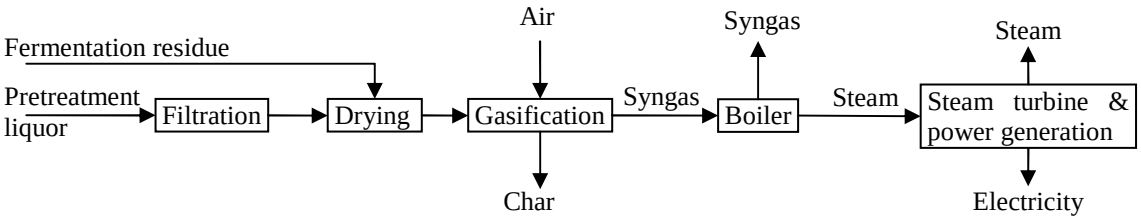

Figure 26. Simplified block diagram of gasification and cogeneration unit.

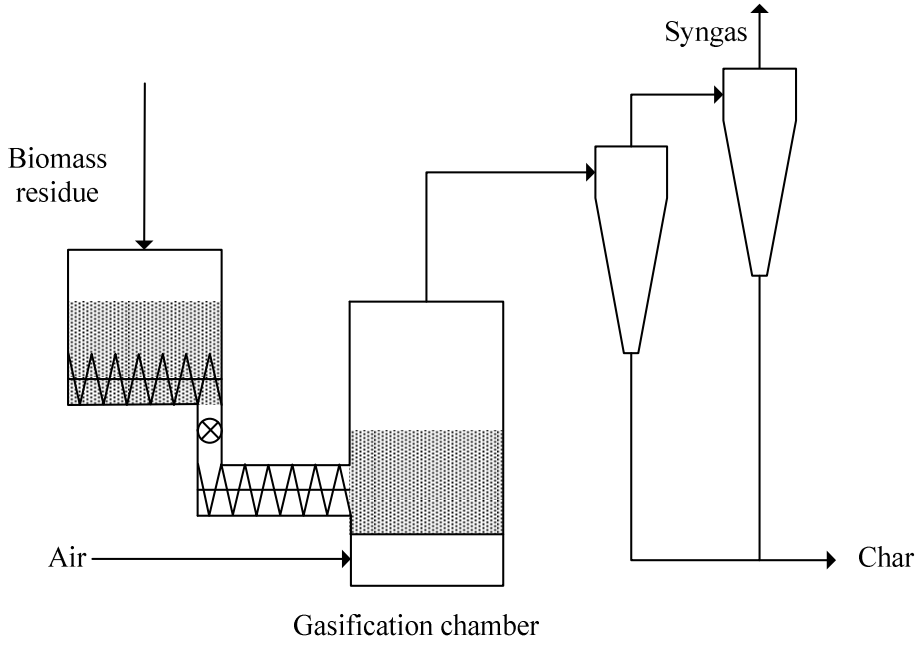

Figure 27. Schematic of the atmospheric biomass gasifier.

Figure 27 shows the gasifier, a fluidized-bed followed by two cyclones that effectively remove particulates (char, ash) from the syngas.[104] Atmospheric-pressure air, but no steam, is introduced to the gasifier, which requires only a simple control system

and low-cost cyclones. The capital cost of this gasifier is only 25% of commercial pressurized gasifiers that use steam.[104] There are multiple uses for the char recovered from the cyclones: (1) add to soil to sequester carbon and improve fertility, (2) sell to coal-fired power plants to provide "green" fuels, and (3) burn at the plant to recover alkaline ash that can be used to replace lime in the pretreatment.

In the second scenario, hydrogen is not produced in the plant but is purchased from external sources, such as pipelines or oil refineries. In this scenario, the gasification and cogeneration unit is retained to use biomass residues to generate steam and power, but an additional combustion chamber is installed after the cyclones to completely burn the syngas and produce more steam and power.

Steam-gas shift and pressure-swing adsorption

This section is only needed when hydrogen is produced in the plant (as described in Scenario 1). More hydrogen is made using the shift reaction between steam and carbon monoxide:

$$H_2O + CO \rightarrow H_2 + CO_2 \quad (94)$$

Because of the compositional characteristics of the syngas, a one-stage shift is sufficient for high conversion and low residence time. The hydrogen-rich syngas, along with fermentation gas, is passed through molecular sieve beds in the pressure-swing adsorption unit, which purifies hydrogen. Both of these technologies are well developed.

4.3.2 Maximal theoretical yields

Theoretical yields in biofuel processes can be simply calculated from the stoichiometry of the representative reactions; however, identification of representation reactions is difficult in some cases. The ensuing equations are representative reactions of the key conversion steps of the carboxylate platform. In practice, because of the mixed-culture fermentation, there are no pure intermediate chemicals. Instead, there are many chemicals with the same functional groups at each conversion step. Nonetheless, the lowest molecular weight chemicals are used to represent intermediates so the maximal theoretical yields can be determined. For example, acid acetic is considered as the only intermediate in the acid-forming fermentation products, acetone is the only intermediate

ketone, and isopropanol is the only intermediate alcohol. The final product was represented by a compound that has the physical properties close to the real final product (e.g., octane, C_8H_{18}, is used to represent gasoline).

If feedstock is assumed pure cellulose ($C_6H_{10}O_5$), the ideal conversions follow:

- Fermentation: $2\ C_6H_{10}O_5 + 2\ H_2O + 3\ CaCO_3 \rightarrow 3\ Ca(CH_3COO)_2 + 3\ CO_2 + 3\ H_2O$ (95)
- Thermal conversion: $Ca(CH_3COO)_2 \rightarrow CH_3COCH_3 + CaCO_3$ (96)
- Ketone Hydrogenation: $CH_3COCH_3 + H_2 \rightarrow CH_3CHOHCH_3$ (97)
- Dehydration: $CH_3CHOHCH_3 \rightarrow CH_3CH{=}CH_2 + H_2O$ (98)
- Oligomerization: $8\ CH_3CH{=}CH_2 \rightarrow 3\ C_8H_{16}$ (99)
- Olefin hydrogenation: $C_8H_{16} + H_2 \rightarrow C_8H_{18}$ (100)

The overall reaction is $16\ C_6H_{10}O_5 + 33\ H_2 \rightarrow 9\ C_8H_{18} + 24\ CO_2 + 32\ H_2O$ (101)

where the molecular weights of cellulose and gasoline (C_8H_{18}) are 162 and 114 kg/kmol respectively. The mass yield of the final product is

$$\frac{9\times 114}{16\times 162} = 0.396 \text{ tonne of gasoline per tonne of cellulose.} \quad (102)$$

Assuming the specific gravity of the gasoline is 0.74 tonne/m^3, the theoretical volumetric yield of the final product is:

$$0.396\frac{\text{tonne gasoline}}{\text{tonne cellulose}}\times\frac{\text{m}^3}{0.74\text{ tonne}}\times 264\frac{\text{gallon}}{\text{m}^3} = 141 \text{ gallons of gasoline per tonne of cellulose.} \quad (103)$$

The overall reaction shows that about 25% of the carbon is lost as carbon dioxide in the fermentation step. Other theoretical yield losses result from oxygen removal as carbon dioxide and water produced in the fermentation and dehydration steps.

The maximal theoretical yields from specific biomass feedstocks are lower than 141 gallons per tonne because there is no practical biomass feedstock containing pure cellulose. (Note: Waste office paper has a composition of 87.4% cellulose, 8.4% hemicellulose, 2.3% lignin, and 1.9% ash,[105] which is very close to pure cellulose.) In addition, in the carboxylate platform, the optimal biomass feedstocks consist of 80% carbohydrate source and 20% nutrient source. In this analysis, the plant uses forage

sorghum (77.1% carbohydrates, 15.2% lignin, and 7.7% ash) for carbohydrate source and manure (48.0% carbohydrate, 16.6% lignin, and 35.4% ash) for nutrient source in a ratio of 80:20 respectively. The maximal theoretical yield of the plant is

$$141 \times \frac{4 \times 77.1\% + 1 \times 48.0\%}{5} = 101 \text{ gallons of gasoline per dry tonne of biomass} \quad (104)$$

Lignin and ash are not fermentable and all carbohydrates are assumed to be cellulose.

Table 5. Key process performances.

Unit	Parameter	Value
Pretreatment	Make-up lime demand	0.054 g CaO/g biomass
	Total lime loading	0.15 g CaO/g biomass
	Reaction time	6 weeks
Fermentation	Conversion	0.8 g digested/g volatile solids fed
	Selectivity	0.62 g carboxylic acids/g volatile solids digested
	VSLR	3.00 g VS/(L liquid · day)
	LRT	28 days
	Product concentration	40 g acids/L liquid
	Reaction time	32 days
	Substrate concentration	10%
Dewatering	Carboxylate recovery	95%
	Heat transfer coefficient	240 kW/(m^2·K)
	Temperature approach	0.20 K
	Cost of latent heat exchangers	\$155/m^2
Ketonization	Conversion	99.5%
	Yield	0.583 g ketones/g carboxylic acids
Ketone hydrogenation	Conversion	98.4%
Dehydration & Dimerization	Light hydrocarbon yield	0.6 g light hydrocarbon/g alcohols
	Heavy hydrocarbon yield	0.2 g heavy hydrocarbon/g alcohols
Olefin hydrogenation	Conversion	98.4%
Gasification & Cogeneration	Gasification temperature	760°C
	Solid-to-air ratio	0.625
Steam-gas shift & PSA	Steam-gas shift temperature	254°C
	Hydrogen recovery	95%
The whole plant	Gasoline yield	57 gallons/dry-ash-free tonne biomass
	Jet fuel yield	19 gallons/dry-ash-free tonne biomass

4.3.3 Process performance

Table 5 summarizes key process performance parameters used to calculate mass and energy balances in the base case. The performance of units in the main route (i.e., excluding units that process fermentation residue), has been proven at the laboratory scale. A yield of more than 70 gal hydrocarbon fuel per tonne of municipal solid waste was reportedly achieved at the demonstration scale.[106] The performances of residue-processing units were typical values from literature discussed above. In this techno-economic analysis, these performances are assumed to be achieved in commercial scale of the n^{th} plant.

The pretreatment unit consumes a significant amount of lime, most of which is available from recycle. In fermentation, the mass of carboxylic acid products is half the mass of volatile solids fed. The long residence time of pretreatment and fermentation requires large piles, which have a volume of 600,000 m^3 each. In a practical plant, the yield losses result from by-products (see previous section), but also incomplete chemical conversions and partial recovery of main products in separation steps. The final products, hydrocarbon fuels, are fractions of gasoline and jet fuel produced in a ratio of 3:1.

4.3.4 Process simulation

In Aspen Plus simulations of biofuel processes, physical properties of some key biomass components and biochemical reactions are not available from standard software databases. Most of them are unconventional compounds and their properties are difficult to estimate using available property prediction methods.Wooley and Putsche[92] at NREL has built a database of some biofuel components that are present in lignocellulose-to-ethanol processes. The components are cellulose, glucose, xylan, xylose, lignin, zymo (bacterium), cellulase (enzyme), soluble solids, and gypsum. The authors collected their physical properties from the literature and estimated missing ones when necessary. The properties were coded in appropriate format to be recognized as an in-house database[107] by Aspen Plus and are called whenever needed.

Based on the key performance data (Table 5) from experiments, the entire process was simulated in Aspen Plus to calculate detailed mass and energy balances. Table 6 summarizes the types of Aspen Plus models used to simulate key processing units. In general, the conversion steps with well-defined reaction stoichiometry and yields (hydrogenation and dehydration) were simulated by the RStoic model. The RGibbs model simulated the conversions in which multiple reactants randomly react in the same types of reactions to yield multiple products with the same functional groups (ketonization and dimerization).

Table 6. Aspen Plus models for key processing units.

Processing units	Aspen Plus models	Calculated parameters
Pretreatment reactor	RStoic	Heat of dissolving lime in water
Fermentation reactors	RStoic	Heat of reactions
Latent heat exchangers	HeatX	Heat transfer area
Ketonization reactor	RGibbs	Yields and heat of reactions
Hydrogenation reactors	RStoic	Heat of reactions
Dehydration reaction	RStoic	Heat of reactions
Dimerization reaction	RGibbs	Yields and heat of reactions
Drum dryer	Flash	Heating utility consumption

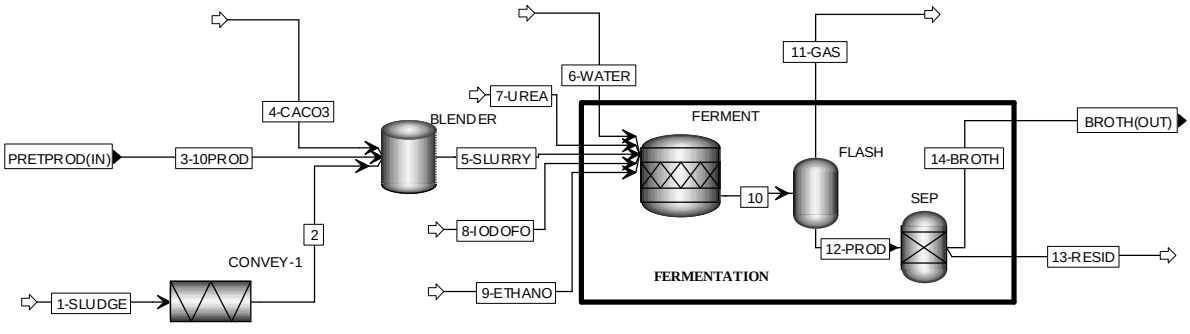

Figure 28. Simulation of the fermentation unit in Aspen Plus.

The pretreatment and fermentation reactions are difficult to simulate because of their complexity. The RStoic model was used to simulate partially what happened in the reactors. For the pretreatment, only the heat of dissolving quick lime in water was estimated; lignin degradation was treated as a "black box," i.e., no simulation was done. For fermentation, the experimental yields and assumed mechanism were used to calculate the conversion of intermediate reactions in a preprocessing step without aid from Aspen Plus; then, the reactions with calculated conversions were simulated by the RStoic model in Aspen Plus to reproduce the yields and estimate energy balance. Figure 28 shows the simulated process of the fermentation section in Aspen Plus.

Other processing units that are difficult to simulate in Aspen Plus (for example, waste treatment, filtration, drying, crystallization) were treated as "black boxes." Mass balances of these units were available from experimental data or estimated by heuristics.

4.3.5 Process integration

In the simulation, the heat exchanger network was integrated by identifying opportunities to save heating and cooling utility consumption. Pinch analysis[94] was applied to determine the savings target. Figure 29 depicts a grand composite curve of the heat exchanger network. Below the pinch point is no curve, which indicates that if the network is ideally integrated, no cooling utility is needed and the heating utility consumption is significantly reduced. Table 7 shows the reduction is 60% as compared to the scenario of no-integration or heat recovery. However, in a practical design, some hot and cold streams should not be integrated to avoid a complex control system, even though it is possible. For example, process streams through condenser, reboiler, and heat exchangers used to finely tune temperatures were not considered in the integration. So, the expected integration needs some more cooling and heating utility, which are reported in the last column of Table 7.

Water balance is another process integration problem in biochemical processes. As in other biochemical platforms, the carboxylate platform demands a large amount of water in the fermentors. Water needs to be removed from the main fermentation products in followed-up separation units. In other biochemical platforms, the recovered

water is usually treated to meet the required fermentation conditions. In contrast, water in the carboxylate platform is distilled by energy-saving vapor compression. The high quality of vaporized water and low quality requirements for fermentation broth allows water recycling without treatment, which slightly reduces production costs (Table 8) and significantly makes the process more sustainable. In net balance, the plant generates surplus distilled water, which is about equal to the moisture content in the biomass feedstock.

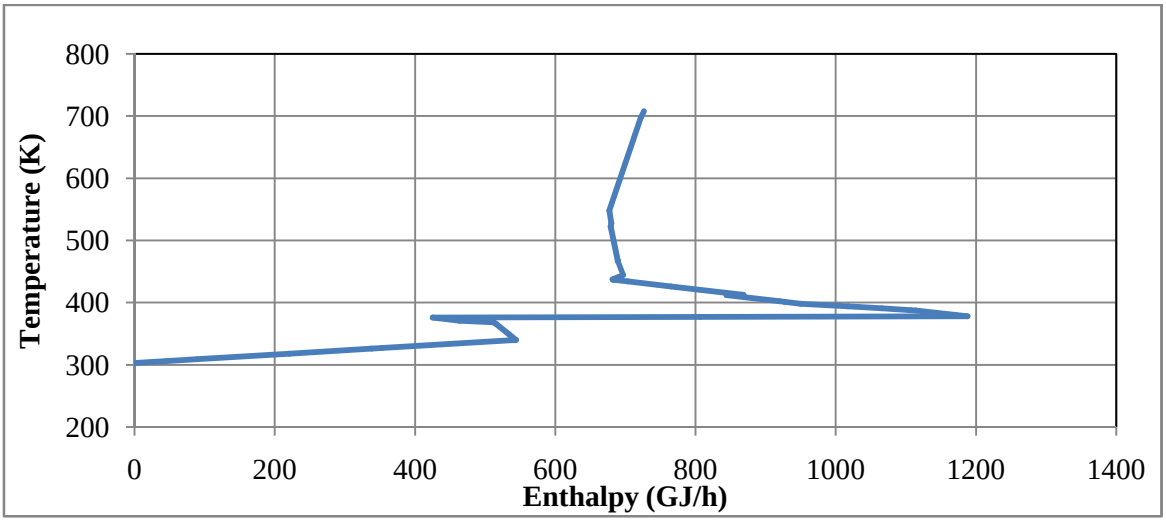

Figure 29. Grand composite curve for heat integration of the heat exchanger network.

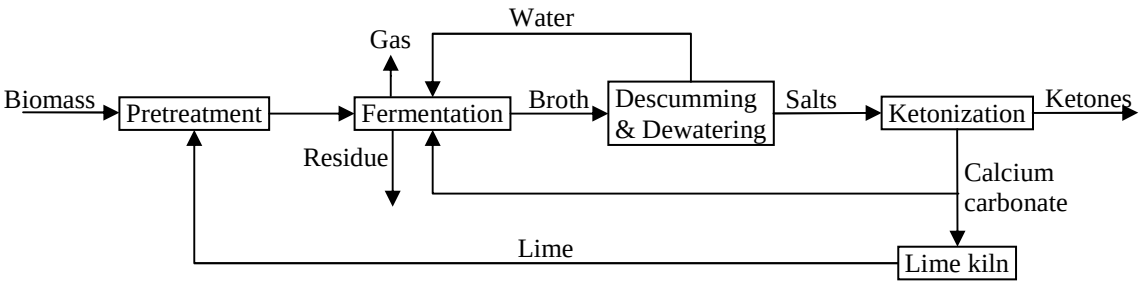

Figure 30. Recycle of water and chemicals.

Table 7. Utility consumption in targeted and expected scenarios of heat integration.

Utility	No integration	Targeted integration	Expected integration
Heating utility (GJ/h)	1,720	726	616
Cooling utility (GJ/h)	994	0	110

Recycling lime and calcium carbonate is another advantage of the carboxylate platform compared to other biochemical platforms, which allows lime pretreatment to be applied very effectively. The pretreatment unit requires 1.5 tonnes of lime for every 10 dry tonne biomass fed (Table 5). The calcium flows through the pretreatment, fermentation, descumming, and dewatering units along with the main products, and is finally recovered in the ketonization unit as calcium carbonate. Part of the calcium carbonate is directly recycled to the fermentors as buffer. The remaining calcium carbonate is conveyed to the lime kiln (Figure 30) to produce lime, which is recycled to the pretreatment unit. As a result, a significantly smaller amount of make-up lime is needed (Table 5) and operating costs were significantly reduced (Table 8).

Table 8. Savings from the recycle of chemicals.

Chemicals	Fresh water	Fresh calcium carbonate ($CaCO_3$)	Fresh lime (CaO)
Consumption without recycle (tonne/h)	1,840	45.7	30.2
Consumption with recycle (tonne/h)	0	0	10.7
Reduction (%)	100	100	65
Prices ($/tonne)	0.13	66	70
Saved costs ($MM/year)	1.91	24.1	10.9
Saved costs ($/gal product)	0.016	0.198	0.090

4.3.6 Energy efficiency analysis

The maximal theoretical energy efficiency of cellulose-to-gasoline conversion via the carboxylate platform is 89.4%. It can be derived from the overall reaction (see

Section 3.2) given the higher heating values of cellulose (17.6 MJ/kg),[108] hydrogen (141.8 MJ/kg),[90] and gasoline (as C_8H_{18}, 47.9 MJ/kg.)[90]

For the analyzed plant, 80% of the biomass feedstock is forage sorghum (77.1% carbohydrates, 15.2% lignin, and 7.7% ash) and the remaining 20% is manure (48.0% carbohydrates, 16.6% lignin, and 35.4% ash). With the higher heating value of lignin (29.5 MJ/kg),[109] and ash (assume 0 MJ/kg), the higher heating value of the feedstock is 17.1 MJ/kg. The maximal theoretical energy efficiency of the plant is calculated to be 81.0%.

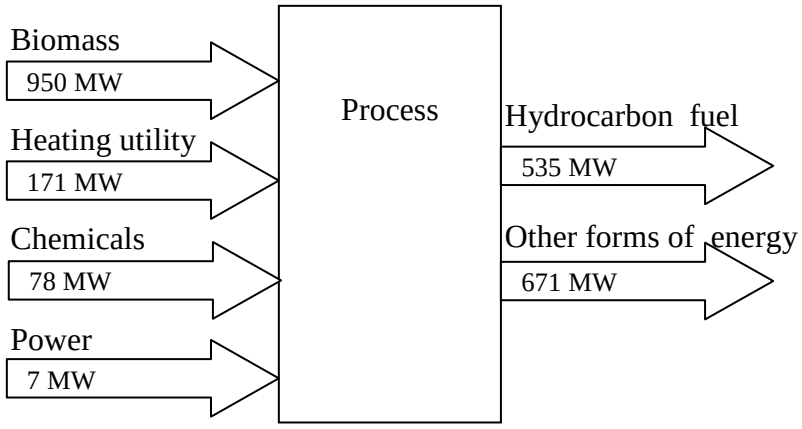

Figure 31. Energy balance of the plant.

In the above calculations of the two maximal theoretical energy efficiencies, it was assumed that the process had no input source of energy other than the biomass and hydrogen. To operate the process in practical plants, more energy inputs are needed in the form of chemicals, heating utility, and electricity. All sources of energy inputs for the analyzed plant are summarized in Figure 31. For biomass, chemicals, and hydrocarbon fuel, the energy loads are based on higher heating values at the standard condition (i.e., sensible heating values are negligible). The total input energy and energy contained in the products are is 1,206 MW and 535 MW, respectively. The energy efficiency of the plant is therefore 44.4%.

4.4 Economic analysis

4.4.1 Analysis procedure and basis

The economic analysis starts by estimating purchased equipment costs in Aspen Icarus Process Evaluator,[91] which are based on the equipment size. Some equipment sizes (e.g., compressor power, heat exchanger area, distillation column diameter and height) were reported in the simulation results in Aspen Plus whereas others (e.g., sizes of crystallizer, drum dryer, and clarifier) were estimated by using reliable heuristics and assumptions.[97,98] If package quotes were available from the literature or vendors, those quotes were used instead of estimating the costs from individual pieces of equipment. Scaling factors for estimating equipment costs at various capacities are referred to NREL,[23] which in turn took most of the scaling factors from Wallas.[97] These scaling factors are summarized in Table 9 and are defined as follows:

$$\text{Equipment cost B} = (\text{Equipment cost A}) \times \left(\frac{\text{Capacity B}}{\text{Capacity A}}\right)^{\text{Scaling factor}} \quad (105)$$

After that, other relevant costs to build the plant were estimated as factors of the purchased equipment cost. For pretreatment, fermentation, and support units (waste water treatment, storage, and utilities), this work employs the modified factor method of NREL[23] (which is suitable to aqueous-based processes. This modification has a five-fold higher contingency factor than the original NREL method. Lang factors[98] for fluid processing were applied for other units, which are similar to chemical and petrochemical processes. The factor values of those two methods are compared in Table 10. The total capital investment costs are 3.5 and 6 times the purchased equipment costs, using the modified NREL method and the Lang factor, respectively. The main difference comes from the installation factors.

Subsequently, cash flow and financial models were constructed to evaluate the project economics. The basis and assumptions of the base-case models are presented in Table 11. The federal income tax rate, the depreciation method and period were recommended by NREL after a review on Modified Accelerated Cost Recovery System (MACRS)[110] issued by Internal Revenue Service. No subsidies or incentives were applied.

After the financial model for the base case was built, the minimum product selling price (MPSP) was determined. It is the hydrocarbon fuel price that results in a net present value of zero in the cash flow with a predefined after-tax discount rate. To simplify the economic analysis, the gasoline and jet fuel prices were assumed to be identical.

Finally, to perform sensitivity analysis, the following key parameters in the simulation and financial models were varied: fermentor operating conditions, overall yield, plant capacity, sources of hydrogen supply, prices of feedstock and raw chemicals, and after-tax discount rate of the cash flow.

Table 9. Scaling factors to estimate equipment costs at various sizes.

Equipment type	Installation factors	Scaling factor	Scaling base
Agitators: CS; SS	1.3; 1.2 [a]	0.51 [d]	Flow
Blenders	1.3 [a]	0.49 [b]	Flow
Blowers	1.4 [a]	0.59 [b]	Flow
Centrifuges, CS	1.3 [a]	0.67 [b]	Flow
Clarifiers, thickeners	1.51 [c]	0.60 [c]	Flow
Columns, distillation, CS; SS	3.0; 2.1 [a]	0.62 [b]	Diameter squared
Compressors, motor driven	1.3 [a]	0.69 [b]	Flow
Conveyers and elevators	1.4 [a]	0.60 [c]	Flow
Crystallizers	1.9 [a]	0.37 [b]	Flow
Dryers	1.4 [a]	0.40 [b]	Flow
Evaporators, thin film, CS	2.5 [a]	0.54 [b]	Flow
Filters, belt press	1.25 [c]	0.60 [c]	Solid flow
Filters, pneumapress	3.34 [c]	0.60 [c]	Solid flow
Heat exchangers, shell-tube	2.1 [a]	0.44 [b]	Heat transfer area
Pumps, centrifugal, CS	2.8 [a]	0.79 [d]	Flow
Reactors, kettle	2.1 [a]	0.54 [b]	Flow
Reactors, multi-tubular, SS	1.6 [a]	0.56 [b]	Flow
Shredders,	1.38 [c]	0.60 [c]	Flow
Tanks, field erected, CS	1.4 [c]	0.57 [b]	Flow
Truck scale	2.47 [c]	0.60 [c]	Flow
Vessels, pressure, CS	1.7 [a]	0.51 [d]	Flow

Note: a. Wallas,[97]
b. Peters et al.[98]
c. Aden et al.[23]
d. Garrett.[111]

Table 10. Factors in estimation of project costs.

Lang method [a]		Modified NREL method [b]	
Cost items	Factor	Cost items	Factor
Direct cost		Direct cost	
Purchased equipment	**100**	Purchased equipment	**100**
Equipment installation	47	Installation	70 [c]
Instrumentation & control	36	Ware house	2.55
Piping	68	Site development	15.3
Electrical systems	11		
Buildings	18		
Yard improvements	10		
Service facilities	70		
Total direct costs	**360**	Total direct costs	**188**
Indirect costs		Indirect costs	
Engineering and supervision	33	Prorateable costs	18.8
Construction expenses	41	Field expenses	18.8
Legal expenses	4	Office & construction	47.0
Contractor's fees	11	Contingency	28.2
Contingency	44	Other	18.8
Total indirect costs	**144**	Total indirect costs	**132**
Fixed capital investment (FCI)	**504**	FCI	**320**
Working capital investment (WCI=15%FCI)	89	WCI = 10% FCI	32
Total capital investment (TCI)	**593**	TCI	**352**

Note: a. Peters et al.,[98]

b. Aden et al.[23]

c. In the NREL report,[23] this cost item ranges from 20 from 200 depending on types of equipment (see Table 9 for details), 70 is the mean value.

Table 11. Basis and assumptions of the financial models for the base case.

Parameters	Values
Plant life	20 years
General plant depreciation	200% DDB for 7 years
Steam generation unit depreciation	150% DB for 20 years
Financing	100% equity
After-tax discount rate	10%
Income tax rate	39%
Dollar year value	2010
Subsidy	No
Plant capacity	160 dry tonnes/h of forage sorghum (8.1% ash) and 40 dry tonnes/h of manure (35.4% ash)
Construction period	1.5 years
Start-up time	6 months
Revenues	50%
Variable Costs	75%
Fixed Costs	100%
Operating season	8,000 hours per year
Delivered prices of raw materials:	
Forage sorghum	$60/dry tonne
Manure	$10/dry tonne
Hydrogen source	From the processing of fermentation residue

4.4.2 Base-case economic analysis

For the base-case plant in which all the parameter values shown in Tables 1 and 7 were applied, the fixed capital investment (FCI) is $331 MM. Figure 32 shows how the capital is distributed in the plant. The steam-gas shift and PSA units contribute most to the FCI followed by gasification and cogeneration, dewatering unit, and ketonization. The high capital costs of water-gas shift, PSA, and gasification indicate that producing hydrogen from fermentation residue is expensive. Most of the dewatering costs come from the expensive crystallization equipment. Because of the low-cost pile design, pretreatment and fermentation require only 7.2% of the investment.

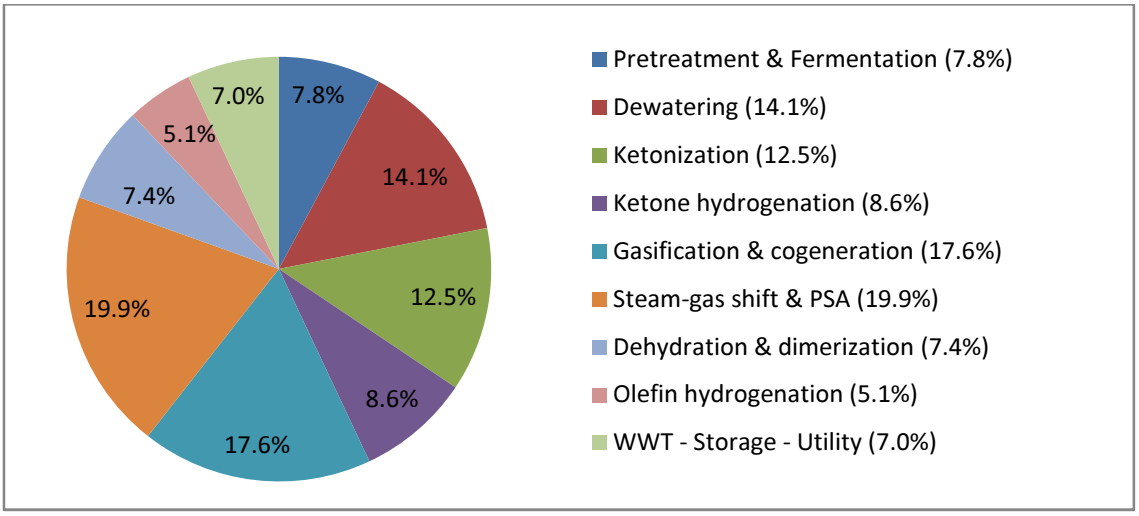

Figure 32. Breakdown of the fixed capital investment (FCI) for the base case.

Table 12. Variable operating costs.

Cost items	Rate	Price	Annual cost $1,000/yr	Unit cost $/gal product
Feedstock				
Forage sorghum	160 tonne/h	$60/tonne	76,800	0.630
Manure	40 tonne/h	$10/tonne	3,200	0.026
Chemicals				
Lime	10.7 tonne/h	$70/tonne	6,006	0.049
Ethanol	9.47 tonne/h	$2.2/tonne	167	0.001
Flocculant	208 kg/h	$991/tonne	1,650	0.014
Iodoform	7.17 kg/h	$25/kg	1,434	0.012
Utility				
High-pressure steam	14.1 tonne/h	$10.1/tonne	1,142	0.009
Low-pressure steam	476.3 tonne/h	$5.50/tonne	20,955	0.173
Natural gas	1.6×10^3 m^3/h	$0.113/$m^3$	1,469	0.012
Electricity	6.58 MW	$0.062/kWh	3,244	0.027
Cooling water	18,838 m^3/h	$0.013/$m^3$	1,959	0.017
Boiler water	117 m^3/h	$0.13/$m^3$	121	0.001
Waste disposal	32.5 tonne/h	$18/tonne	4,681	0.038

Variable and fixed operating costs are presented in Tables 12 and 13. The variable operating cost is dominated by the main feedstock cost ($60/tonne forage sorghum), followed by the cost of low-pressure steam that is primarily consumed by the crystallizer. The key contribution of the fixed operating costs is maintenance-related costs, which were estimated as a factor of the capital costs.

The MPSP of the base case was estimated to be $1.83 per gallon hydrocarbon fuels at an after-tax discount rate of 10%. Table 14 shows the components of this selling price. The biomass feedstock is the highest cost component; it contributes 36% to the MPSP. It implies that using low-cost waste feedstocks will significantly reduce the product cost. Other high-cost components are capital depreciation (13.2%), utilities (12.2%), and maintenance (11.9%). It indicates the significant contributions of the capital investment and the low-pressure steam consumption to the selling price.

Table 13. Fixed operating costs.

Cost items	Annual cost ($1,000/yr)	Calculation (*)
Labor		
Direct wage and benefits (DW&B)	4,481	For operators
Direct salary and benefits (DS&B)	672	15% of DW&B
Operating supplies and services	269	6% of DW&B
Technical assistance to manufacturing	747	$52,000/(operator/shift)-year
Control laboratory	409	$57,000/(operator/shift)-year
Maintenance		
Wage and benefits (MW&B)	11,576	4.5% of FCI
Salaries and benefits (MS&B)	2,894	25% of MW&B
Materials and services	11,576	100% of MW&B
Maintenance overhead	579	5% of MW&B
Operating overhead		
General plant overhead	1,393	7.1% of DW, DS, MW, MS, & B
Mechanical department services	471	2.4% of DW, DS, MW, MS, & B
Employee relations department	1,158	5.9% of DW, DS, MW, MS, & B
Business service	1,452	7.4% of DW, DS, MW, MS, & B

(*) Followed the instruction of Seider et al.[112]

Table 14. Cost components of MPSP in the base case.

Cost component	Contribution	
	$/gallon of product	Percentage (%)
Biomass	0.656	35.8
Chemicals and waste disposal	0.114	6.3
Utility	0.237	12.9
Labor	0.054	2.9
Maintenance	0.218	11.9
Operating overhead	0.037	2.0
Average capital depreciation	0.241	13.2
Average income tax	0.140	7.7
Average return on investment (ROI)	0.134	7.3
Total	1.832	100.0

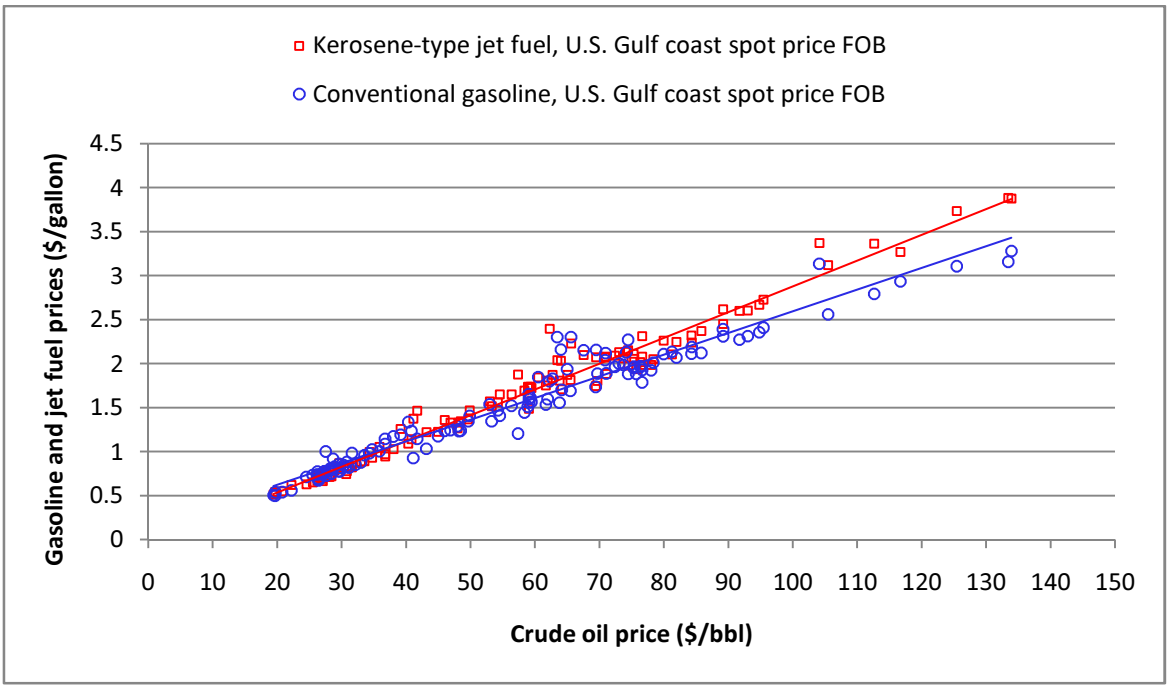

Figure 33. Historical monthly prices of crude oil, gasoline, and jet fuel (EIA, 2011).[113]

Economic viability of biofuel processes depends on how the biofuel competes with petroleum-derived fuels. During the 10-year period from January 2001 to January 2011, Figure 33 tracks the historical monthly spot prices (FOB) of conventional gasoline and kerosene-type jet fuel (at U.S. Gulf coast) produced from crude oil (priced at Cushing, Oklahoma). Petroleum refineries sell gasoline and jet fuel at $1.83/gal when the crude oil price is about $65 – $70 per barrel.

4.5 Optimization and sensitivity analysis

4.5.1 Optimization of yield and fermentation operating conditions

Process economics are strongly affected by the practical overall yield of the plant, which is controlled by fermentor operating parameters: volatile solid loading rates (VSLR), liquid residence times (LRT), and carboxylate product concentration. These parameters along with other relevant terms are defined as follows:

$$\text{Volatile solid fed (VS)} = \text{Dry biomass} - \text{Ash in biomass} \tag{106}$$

$$\text{Conversion} = \frac{\text{VS digested}}{\text{VS fed}} \tag{107}$$

$$\text{Selectivity} = \frac{\text{Total carboxylate produced (based on weight of acids)}}{\text{VS digested}} \tag{108}$$

$$\text{Overall yield} = \frac{\text{Total volume of hydrocarbon fuel produced}}{\text{Dry biomass weight fed}} \tag{109}$$

$$\text{Volatile solids loading rate (VSLR)} = \frac{\text{Weight of VS fed}}{\text{Total liquid volume in all fermentors} \cdot \text{time}} \tag{110}$$

$$\text{Liquid residence time (LRT)} = \frac{\text{Total liquid in all fermentors}}{\text{Flow rate of liquid out of fermentor train}} \tag{111}$$

$$\text{Fermentation concentration} = \frac{\text{Total carboxylate produced (based on acid weight)}}{\text{Flow rate of liquid out of fermentor train}} \tag{112}$$

$$\text{Fermentation time} = \frac{\text{Dry biomass weight in all fermentors}}{\text{Dry biomass rate}} \tag{113}$$

$$\text{Substrate concentration} = \frac{\text{Dry biomass weight in all fermentors}}{\text{Dry biomass weight} + \text{Liquid weight in all fermentors}} \tag{114}$$

In this sensitivity analysis, VSLR, LRT, and fermentation product concentration were considered as independent variables. All others were calculated accordingly (yield, selectivity, fermentation time, total carboxylate produced, VS fed, VS digested, and rates of liquid) or specified as unchanged inputs (dry biomass, ash content, conversion, and substrate concentration). Table 5 reports their values in the base case.

The overall yield is proportional to total acids produced in the fermentation, which assumes that individual yields of all other steps are fixed. From the equations above, the overall yield relates to the three independent variables as follows:

$$\text{Overall yield} \sim \frac{\text{Fermentation product concentration}}{\text{VSLR}\cdot\text{LRT}} \tag{115}$$

This relation indicates that overall yield favors higher fermentation product concentration and lower multiplication of VSLR and LRT.

In fact, the three parameters (VSLR, LRT, and fermentation product concentration) interact as documented in previous work.[114-117] The interactions were predicted using the Continuum Particle Distribution Model (CPDM). However, to investigate the effect of operating ranges on process economics in this work, the parameters were arbitrarily varied in predefined ranges (Table 15).

Table 15. Ranges of fermentation operation parameters.

Parameter	Unit	Base case	Investigated range
Fermentation product concentration	g acids/L	40	10 – 60
Volatile solids loading rate (VSLR)	g/(L·day)	3.0	3 – 10
Liquid residence time (LRT)	day	28	5 – 30

To perform the sensitivity analysis, the MPSP was estimated in a number of scenarios of various combinations of the three independent parameters. Because the parameters affect fermentation outlet flow rates and compositions, mass and energy balance of the whole plant were changed in every scenario. The capital and operating costs were updated accordingly before the MPSP was recalculated.

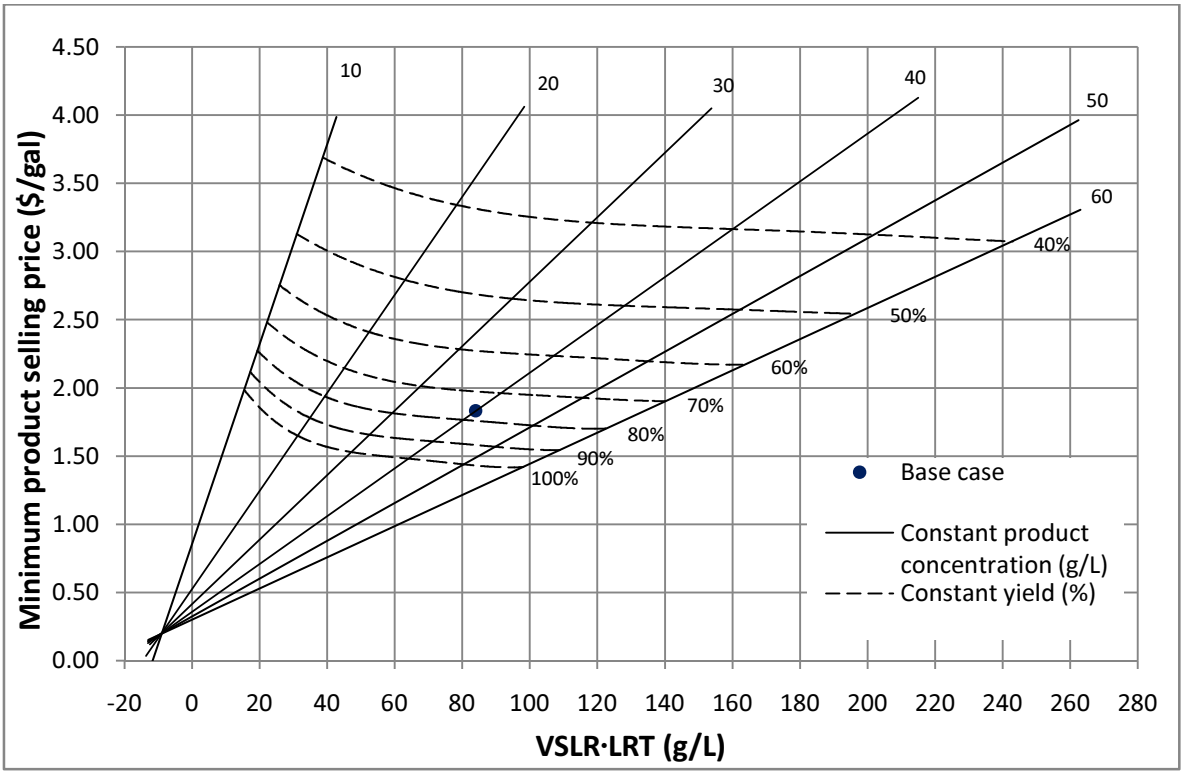

Figure 34. Minimum product selling prices with respect to multiplication of volatile solid loading rate and liquid residence time at various concentrations of carboxylic acids in fermentation broth (forage sorghum cost $60/dry tonne, after-tax discount rate 10%, hydrogen produced from gasification of fermentation residue, plant capacity 200 dry tonne/h, plant life 20 years).

Figure 34 shows the calculation results that cover the whole parameter ranges. Some characteristics follow:

- For constant fermentation product concentration, MPSP is linear with VSLR·LRT. The MPSP decreases as VSLR·LRT decreases. The reason is VSLR·LRT is inversely proportional to yield (as discussed above) and MPSP is generally smaller at higher yields. The value of VSLR·LRT can be reduced until

the yield is equal to the theoretical yield. In Figure 34, the yield (in percentage) is defined as

$$\text{Yield (\%)} = \frac{\text{Practical overall yield}}{\text{Theoretical overall yield}} \times 100\% \quad (116)$$

- Straight lines of constant fermentation product concentration (solid lines) converge to one point outside the operable region, which is the upper part of the 100% yield curve (dashed curve).
- For constant yield (along the dashed lines), MPSP decreases as the fermentation product concentration increases. In the investigated ranges, the increased concentration results in lower fermentation costs because of reduced fermentation time (with constant yield) and lower dewatering costs because less water must be vaporized. In Figure 34, yields of 40, 50, 60, 70, 80, 90, and 100% are reported.

Figure 34 can be used to predict quickly the overall yield and MPSP, given the fermentation operating parameters (VSLR, LRT, and product concentration). In a reverse problem, it can be used to indicate what fermentation parameters are required to reach a desired yield or MPSP. The result shows that the minimum MPSP in the investigated ranges is $1.42/gal, which would be achieved at an acid concentration of 60 g/L and a VSLR·LRT of 98 g/L (with a yield of 100%).

4.5.2 Vapor compression system

The vapor-compression system (Figure 23) is the key dewatering unit that concentrates the calcium carboxylate solution in an energy-efficient way. There is a need to optimize the operating conditions and perform sensitivity analysis because (1) the system is highly integrated with the fermentation and (2) although excellent performance has been achieved at the laboratory scale, it has not yet been demonstrated at commercial scale. This section investigates the effects of temperature approach, fouling, and fabrication costs of the latent heat exchangers on the MPSP. Table 16 shows the parameter ranges.

Table 16. Ranges of latent heat exchanger parameters.

Parameter	Notation	Unit	Base case	Investigated range
Temperature approach	ΔT	K	0.20	0.20 – 3.0
Heat transfer coefficient	U	kW/(m^2·K)	240	10 – 300
Equipment cost	C	\$/m^2	155	0 – 400

Temperature approach

Temperature approach is the temperature difference (ΔT) between vaporizing salt solution and condensing vapor in a stage of the latent heat exchangers. It is related to heat transfer in the ensuing equation:

$$Q = q \cdot A = U \cdot A \cdot \Delta T \tag{117}$$

where Q = heat transfer (kW), q = heat flux (kW/m^2), ΔT = temperature approach (K), U = overall heat transfer coefficient (kW/(m^2·K)), and A = heat transfer area (m^2).

For 0.203-mm-thick copper plates with lead-containing Ni-P-PTFE hydrophobic coatings, saturated steam pressure of 722 kPa, and forced convective saturated liquid,[102] experimentally found that U depends on ΔT in non-fouling conditions as follows:

$$U = 61.1(\Delta T)^{-0.915} \tag{118}$$

Therefore,

$$q = 61.1(\Delta T)^{0.085} \tag{119}$$

$$Q = 61.1 \cdot A \cdot (\Delta T)^{0.085} \tag{120}$$

In traditional heat exchangers, higher ΔT is favored because heat transfer area is lower, which reduces equipment costs. However, this latent heat exchanger is limited by the rate that liquid droplets shed from the surface. As a consequence, heat flux is nearly independent of ΔT, which is indicated by the near-zero exponent in Equation 119 and shown by the continuous curve in Figure 35.

As ΔT increases, the designed outlet temperature of the vapor compressor must increase, which requires higher compressor outlet pressure, capacity, capital, and operating costs. As ΔT decreases, the designed area of latent heat exchangers must increase to maintain the heat transfer (see Equation 120), which requires higher capital

costs of the heat exchangers. In the design of the vapor-compression system, the compression costs dominate at high ΔT and the heat exchanger costs dominate at low ΔT. A trade-off between these costs was found at ΔT = 0.02 K as shown by the minimum in the continuous curve in Figure 36.

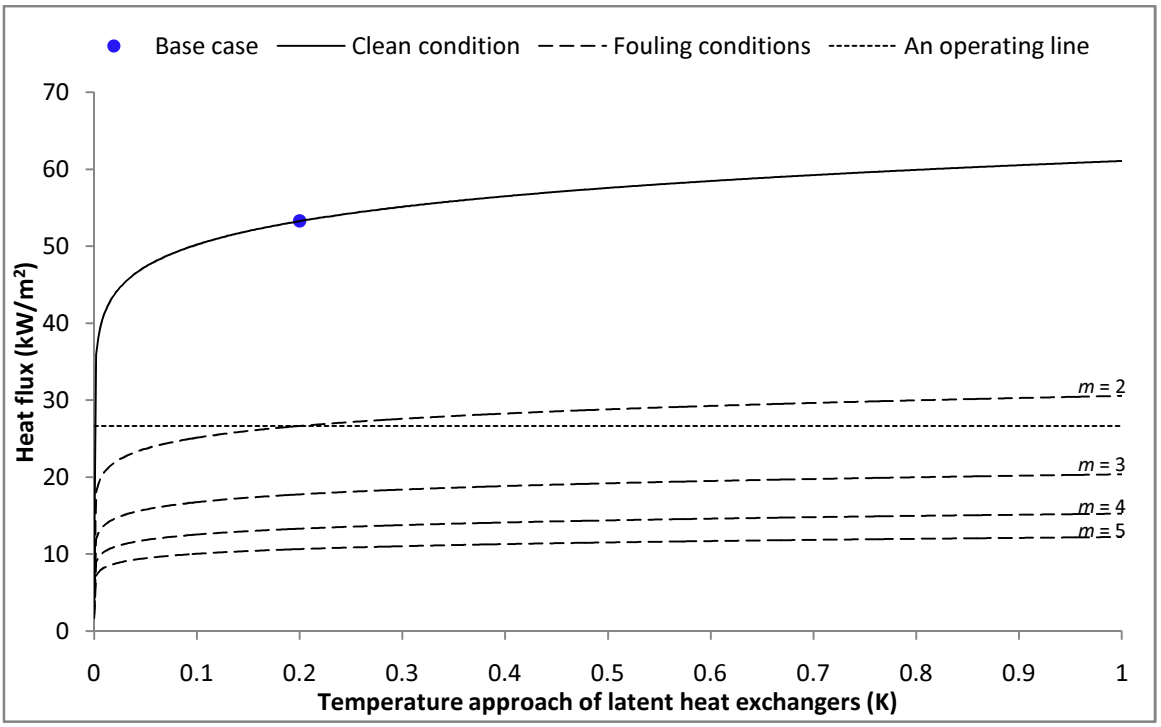

Figure 35. Heat flux of latent heat exchangers with respect to temperature approach at clean and various values of the fouling factor.

Fouling

In practical operation, the overall heat transfer coefficient of the latent heat exchangers decreases over time between maintenance services. The effect of fouling on the overall heat transfer coefficient is assumed to follow Equation 121.

$$U' = U / m \tag{121}$$

where U' is the fouling overall heat transfer coefficient and m is the fouling factor (e.g., m = 2 means overall heat transfer coefficient is reduced twice due to fouling). Figure 35 depicts the heat flux at some values of m.

With fouling, the heat transfer is

$$Q' = U' \cdot A' \cdot \Delta T' \tag{122}$$

where A' is fouling heat transfer area and $\Delta T'$ is the fouling temperature approach.

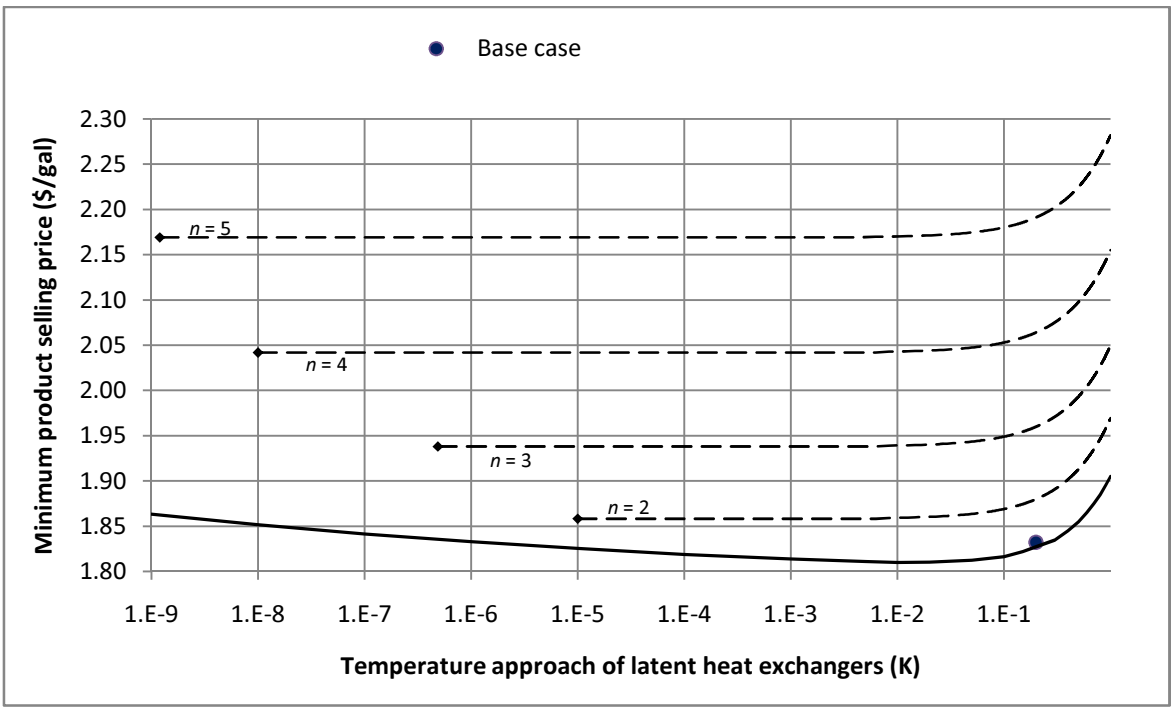

Figure 36. Minimum product selling price with respect to temperature approach at clean condition and various fouling expectation of the latent heat exchangers.

In an operating plant, heat transfer area is not changed (i.e., $A = A'$). To maintain heat transfer (i.e., $Q = Q'$) and avoid reducing vaporization rate as overall heat transfer coefficient decreases from fouling, the latent heat exchangers must be designed with surplus area (i.e., oversized) and heat flux is lowered. (Note: Increasing ΔT without

oversizing does not maintain heat transfer because the heat flux is nearly independent of ΔT as discussed in the previous section).

In the base case, let A_0 be the ideal heat transfer area (i.e., the designed value if no fouling occurs). The heat exchangers are oversized by a factor of n.

$$A' = n \cdot A_0 \tag{123}$$

To maintain heat transfer right after maintenance service is performed (i.e., the heat exchangers are clean), ΔT must be adjusted to a small value such that heat flux reduces by n times as compared to the ideal design.

$$q' = q_0/n \tag{124}$$

where q' is fouling heat flux and q_0 is ideal heat flux. Over time, ΔT increases during operation to keep q constant.

For example, in an ideal scenario where no fouling occurs, the system always operates at the base-case condition where q_0 = 53.3 kW/m^2 and ΔT = 0.2 K. To cope with fouling in a practical scenario, if heat transfer areas are oversized by two times (i.e., n = 2), the system initially operates at $\Delta T = 10^{-5}$ K (see Figure 36) to keep $q = q_0/2$ = 26.6 kW/m^2. Over time as fouling develops, ΔT must increase to keep q constant at this value, which is represented by the horizontal straight operating line in Figure 35. When ΔT is near 1 K, the production cost significantly increases (see Figure 36) because compression energy consumption is higher; therefore, the system should be shut down to clean the heat exchangers. (Note: It is not necessary to manipulate ΔT directly. It assumes a value that is necessary to condense the vapor processed by the compressor; hence, ΔT is a dependent variable determined by independently selecting the compressor speed.)

For higher oversizing factors, the operation period of the system is longer. However, the MPSP must be higher to account for the costs of larger heat exchangers. Figure 36 shows the MPSP for various values of the oversizing factor n.

Cost of latent heat exchangers

Because this technology (dropwise condensation in latent heat exchanger with an extremely high heat transfer coefficient of 240 kW/(m^2·K) has not been applied at a

commercial scale, the coating cost of the plates is uncertain. In the base case, the equipment cost (C) is assumed to be \$155/m^2 of heat transfer area. This sensitivity analysis investigates a wide range of costs from \$100 to \$400/m^2 (Figure 37) assuming ΔT = 0.20 K.

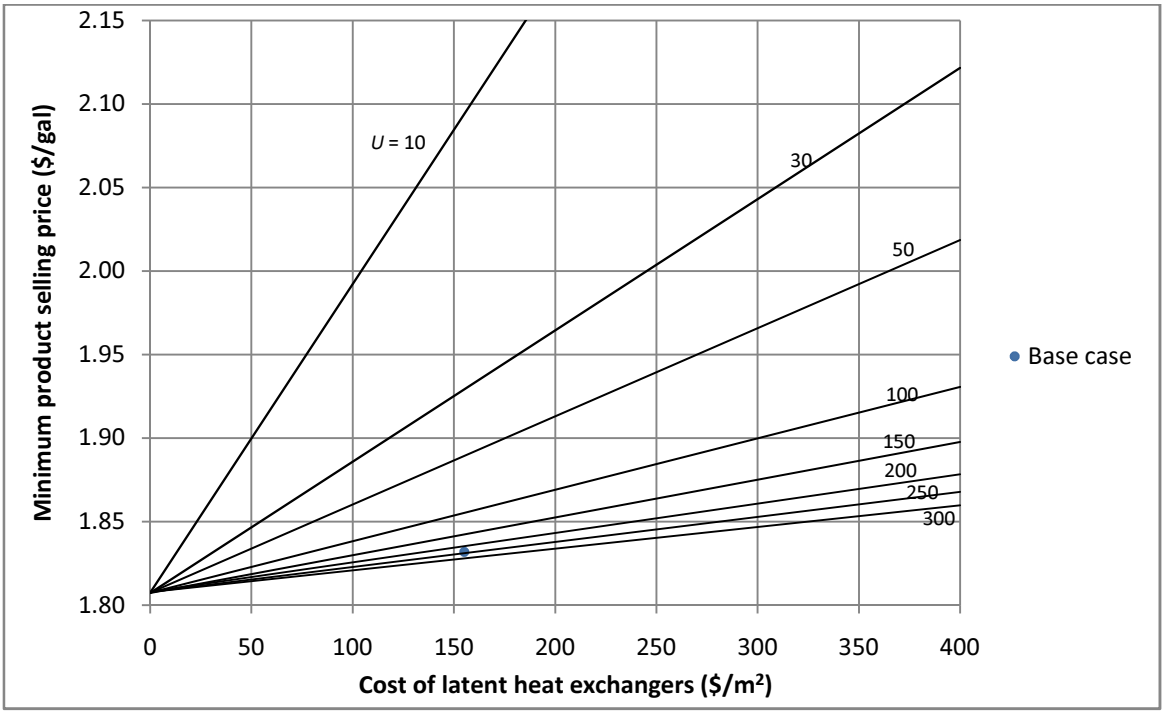

Figure 37. Minimum product selling price with respect to purchased cost of latent heat exchangers at various values of overall heat transfer coefficient U (kW/(m^2·K)) at ΔT = 0.2 K.

At high U, the change of C does not increase MPSP much. For example, at U = 200 kW/(m^2·K), the MPSP increases by only \$0.04/gal as C increases four times, from \$100 to \$400/m^2. However, at low U, an increase of C significantly affects the MPSP. For example, at U = 30 kW/(m^2·K), the MPSP increases by \$0.24/gal for the same four-fold increase of C. The dependence of the MPSP on U and C follows this equation:

$$\text{MPSP} = \frac{0.011847}{U^{0.8061}} C + 1.8072 \quad (125)$$

4.5.3 Sources of hydrogen

The results of the base-case economic analysis shown in Section 4.4.2 reveal that the cost of producing hydrogen from fermentation residue is expensive. In a design in which hydrogen is available from an external source (e.g., nearby petroleum refinery) and the fermentation residue is gasified only for steam and power, the MPSP will be lower if the external hydrogen is inexpensive. However, if the external hydrogen price is expensive, then it is better to produce hydrogen from fermentation residues. Sensitivity analysis of MPSP with respect to external hydrogen prices (Figure 38) shows that the break-even point is $2.44/kg of external hydrogen.

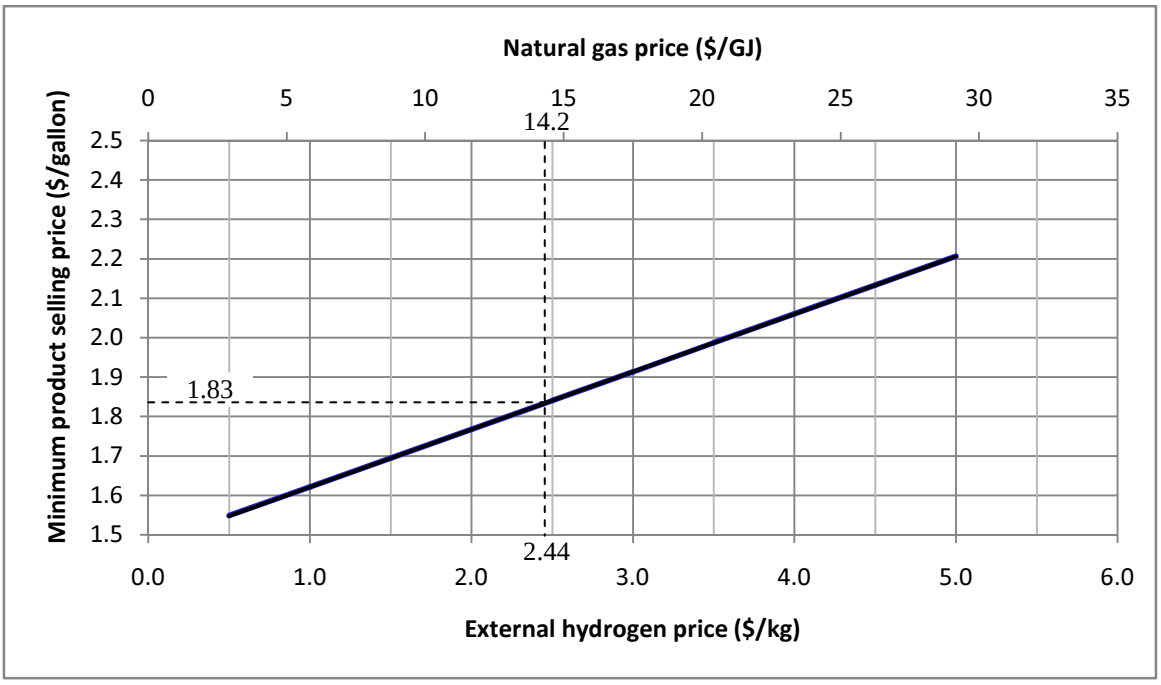

Figure 38. Plot of MPSP versus external hydrogen prices for the case of no hydrogen production.

In another design option in which hydrogen is internally produced from natural gas and the fermentation residue is gasified only for steam and power, the MPSP is lower

than $1.89/gal if natural gas price is less than $14.2/GJ. In the calculation of this case, it was assumed the relationship between hydrogen price and natural gas price is linear.[31]

In other words, the plant is economically favored to produce hydrogen from fermentation residue when external hydrogen and natural gas prices are higher than $2.44/kg and $14.2/GJ, respectively. Otherwise, if those prices are lower than these break points, buying hydrogen or investing in a natural gas reformer is more economical.

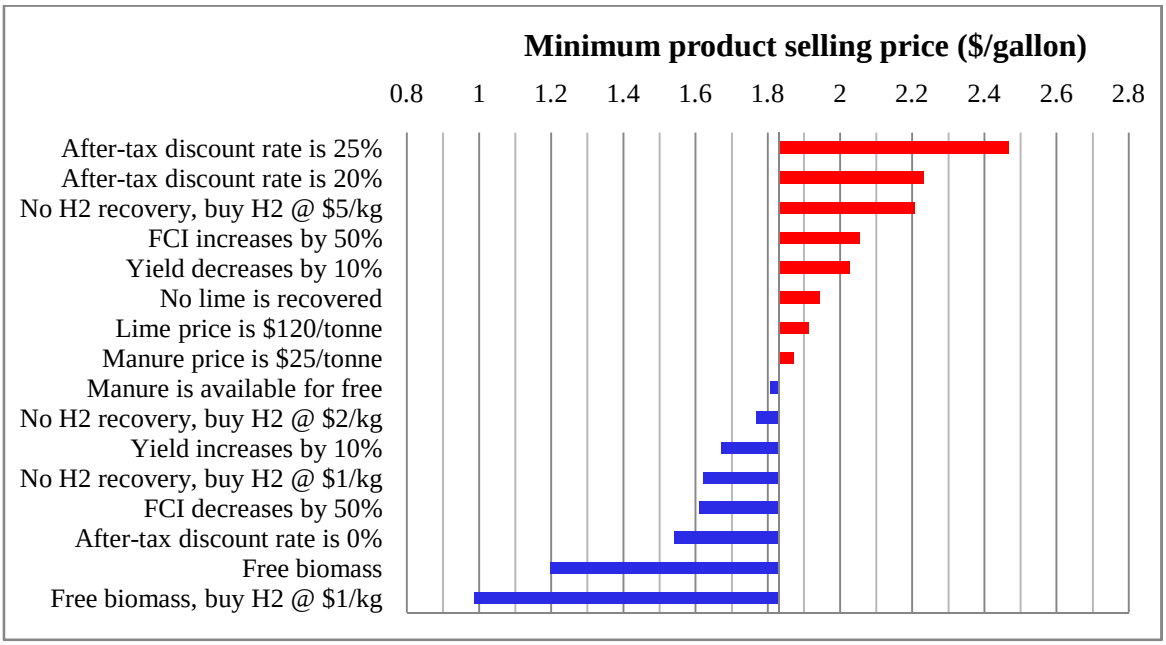

Figure 39. Sensitivity analysis of the key factors on minimum product selling price.

4.5.4 Other sensitivity analyses

Figure 39 shows the sensitivity of the minimum selling price to the following key parameters: after-tax discount rate or return on investment (ROI), overall yields, fixed capital investment, external hydrogen prices, and key raw material prices. If investors expect an ROI of 20% or 25%, the product fuel must be sold for $2.23 or $2.47/gal hydrocarbon, respectively. For an increase of FCI by 50%, the product selling price is $2.06/gal hydrocarbon. A decrease of overall yields by 10% results in a selling price of

$2.03/gal hydrocarbon. If the lime kiln is not employed and pretreatment is fully fed with purchased fresh lime, the selling price increases by $0.11/gal hydrocarbon. By investing in a lime kiln to process the calcium carbonate from ketonization and buying external lime at $120/tonne for make-up demand, the MPSP increases by $0.08/gal hydrocarbon. In the worst-case scenario of manure price, the selling price is not affected much. Unlike the main biomass (sorghum), free manure does not reduce the hydrocarbon selling price significantly.

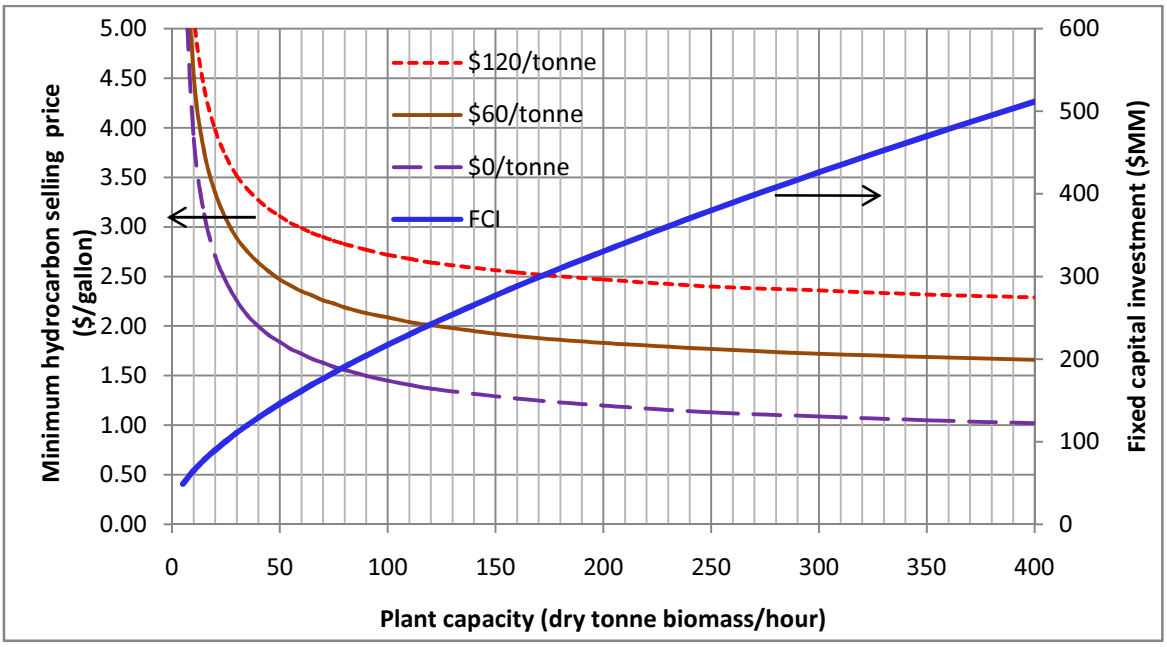

Figure 40. Minimum selling prices and fixed capital investment versus plant capacities using biomass at various prices (sorghum) and $10/dry tonne (manure). Hydrogen is produced by gasification.

Table 14 shows that feedstock costs have high impacts on product price. Figure 40 depicts the effect of feedstock price on the hydrocarbon selling prices. This sensitivity analysis was done for energy sorghum. For other feedstocks with the same volatile solids content as sorghum (91.9% weight), the results are identical. Some feedstocks (e.g., municipal solid waste, food waste) may come with tipping fees whereas sorghum does

not. If such feedstock is delivered for free to the plant gate (i.e., tipping fee is assumed to just cover collecting, sorting, and transporting costs) and the plant uses internal hydrogen, the MPSP is only $1.20/gal hydrocarbon at the base-case capacity (Figure 39). In a reasonable scenario where biomass is available for free at the plant gate and external hydrogen is supplied at $1/kg (the current price based on natural gas costing $5.21/GJ or $5.50/MMBtu), the MPSP of hydrocarbon fuels is $0.99/gal hydrocarbon, as shown in Figure 39.

Figure 40 shows the hydrocarbon selling prices and fixed capital investment with respect to capacity for a plant at various prices of biomass. The FCI curve is represented by a function of capacity to a power of 0.63. At capacities of 300 tonne/h or more and biomass cost of $60/tonne, the MPSP approaches $1.65/gal hydrocarbon.

4.6 Summary

This techno-economic analysis for producing hydrocarbon fuel from lignocellulose via the carboxylate platform was performed by using extensive sources of published data and employing computers for simulation and cost estimation. The following technical advantages of the carboxylate platform were identified: no sterility, no external enzymes, and low capital cost of pretreatment and fermentation. The plant is highly integrated to overcome common challenges in biorefineries, such as lime consumption in pretreatment, calcium carbonate consumption for buffering, water removal for concentrating fermentation product, and hydrogen supplies.

The economic analysis shows that the effects of fermentation operating parameters on process economics can be generalized (Figure 34). This result can be used to quickly estimate the MPSP given any value of the operating parameters. Alternatively, it can quickly target the required parameters to achieve a desired selling price. The economic analysis also shows that the temperature approach of latent heat exchangers is preferred to be as small as 0.20 K. The analysis identified inexpensive feedstock and replacing the crystallizer were keys to significantly lowering the cost.

The process does not need external hydrogen, but it is more economic if external hydrogen is available for less than $2.44/kg, which occurs when natural gas is below $14.2/GJ ($15.0/MMBtu).

The base case with reasonable expectation on technical performances and feedstock cost ($60/dry tonne biomass) requires an MPSP of $1.83/gal hydrocarbon fuel ($1.25/gal equivalent ethanol) at an after-tax discount rate of 10%. In particular, the minimum selling prices of hydrocarbon fuels can be around $1.20/gal ($0.82/gal equivalent ethanol) if municipal solid waste is available for free at the plant gate (200 tonne/h plant, with internal hydrogen production).

4.7 Legal disclaimer

MixAlco^{TM} is a registered trademark of Terrabon, Inc. Unless otherwise noted, inclusion of such trademark in this document does not imply support or endorsement by Terrabon, Inc. Except as expressly referenced in this dissertation, the information, estimates, projections, calculations, and assertions expressed in this dissertation have not been endorsed, approved, or reviewed by any unaffiliated third party, including Terrabon, Inc., and are based on the authors' own independent research, evaluation, and analysis. The views and opinions of the authors expressed herein do not state or reflect those of such third parties, and shall not be construed as the views and opinions of such third parties.

CHAPTER V
CONCLUSIONS

This research developed a complete package of novel tools to systematically design a biorefinery from given feedstocks and desired biofuels. The following tools were proposed.

At first in a synthesis stage, conceptual pathways of converting the feedstocks to the biofuels were synthesized using forward-backward branching approach along with matching and interception steps (Chapter II). This approach can systematically lead to not only familiar pathways but also novel pathways based on known and feasible technologies.

The pathways were then quickly screened and evaluated to globally identify the most economically promising ones in an optimization stage. Application of Bellman's Principle of Optimality (Chapter II) was proposed to significantly reduce the evaluation effort.

After that, the optimal conceptual pathways were assessed in more details. Based on the found pathways, flexible biorefinery configurations were constructed using a novel perspective on design strategy (Chapter III). Operation of partial or whole plant is in idle mode if operating economic efficiency is not favored. This strategy well suits what a plant should be operated in practice in such economic conditions. The new concept can be also applied in another context, e.g., process design with optimum strategy of quality control, where a process is designed such that an off-spec product is discarded (while production is still online).

Finally, detailed design and economic evaluation of the biorefinery configuration was performed (Chapter IV). Although the technical and economic analyses with reliable data were done for the production of hydrocarbon fuels from lignocellulosic biomass via carboxylate platform, the devised framework can be applied to a broad range of biofuel processes. The chapter discussed practical sources of information to perform a techno-economic analysis of a biofuel process, how to simulate a biofuel

process in a process simulation software, and other common technical and economic issues in the design problem of the n^{th} biofuel plant.

All the developed tools were demonstrated in case studies. In general, this research has proposed highly applicable tools and used chemical engineering fundamentals to systematically solve pressing problems in the area of renewable energy.

LITERATURE CITED

1. Huber GW, Iborra S, Corma A. Synthesis of transportation fuels from biomass: Chemistry, catalysts, and engineering. *Chemical Reviews.* 2006;106(9):4044-4098.
2. Kamm B, Kamm M. Biorefineries – Multi-product processes. *Advances in Biochemical Engineering/Biotechnology.* 2007;105:175-204.
3. Fernando S, Adhikari S, Chandrapal C, Murali N. Biorefineries: Current status, challenges, and future direction. *Energy & Fuels.* 2006;20(4):1727-1737.
4. Werpy T, Petersen G. *Top value added chemicals from biomass - Volume I: Results of screening for potential candidates from sugars and synthesis gas.* Richland, WA: Pacific Northwest National Laboratory (PNNL) and National Renewable Energy Laboratory (NREL); August 2004.
5. Holladay JE, Bozell JJ, White JF, Johnson D. *Top value-added chemicals from biomass. Volume II: Results of screening for potential candidates from biorefinery lignin.* Richland, WA: Pacific Northwest National Laboratory; 2007. PNNL-16983.
6. Agnihotri RB, Motard RL. Reaction path synthesis in industrial chemistry. In: Squires RG, Reklaitis GV, eds. *Computer applications to chemical engineering.* Vol 124. Washington, DC: American Chemical Society; 1980:193-206.
7. Nishida N, Stephanopoulos G, Westerberg AW. A review of process synthesis. *AIChE Journal.* 1981;27(3):321-351.
8. Ugi I, Gillespie P. Representation of chemical systems and interconversions by *be* matrices and their transformation properties. *Angewandte Chemie International Edition in English.* 1971;10(12):914-915.
9. Hendrickson JB. Systematic characterization of structures and reactions for use in organic synthesis. *Journal of the American Chemical Society.* 1971;93(25):6847-6854.
10. Corey EJ. Computer-assisted analysis of complex synthetic problems. *Quart. Rev., Chem. Soc.* 1971(25):455-482.
11. Gelernter H, Sridharan N, Hart A, Yen S-C, Fowler F, Shue H-J. The discovery of organic synthetic routes by computer. *New Concepts I.* Vol 41. Berlin: Springer 1973:113-150.
12. Govind R, Powers GJ. A chemical engineering view of reaction path synthesis. In: Wipke WT, Howe WJ, eds. *Computer-Assisted Organic Synthesis.* Vol 61. Washington, DC: American Chemical Society; 1977:81-96.

13. May D, Rudd DF. Development of Solvay clusters of chemical reactions. *Chemical Engineering Science.* 1976;31(1):59-69.

14. Rotstein E, Resasco D, Stephanopoulos G. Studies on the synthesis of chemical reaction paths - I. Reaction characteristics in the (ΔG, T) space and a primitive synthesis procedure. *Chemical Engineering Science.* 1982;37(9):1337-1352.

15. Fornari T, Rotstein E, Stephanopoulos G. Studies on the synthesis of chemical reaction paths - II: Reaction schemes with two degrees of freedom. *Chemical Engineering Science.* 1989;44(7):1569-1579.

16. Crabtree EW, El-Halwagi MM. Synthesis of environmentally acceptable reactions. *AIChE Symposium Series.* 1994;90(303):117-127.

17. Pistikopoulos EN, Stefanis SK, Livingston AG. A methodology for minimum environmental impact analysis. *AIChE Symposium Series.* 1994;90(303):139-150.

18. Buxton A, Livingston AG, Pistikopoulos EN. Reaction path synthesis for environmental impact minimization. *Computers & Chemical Engineering.* 1997;21(Supplement 1):S959-S964.

19. Li M, Hu S, Li Y, Shen J. A hierarchical optimization method for reaction path synthesis. *Industrial & Engineering Chemistry Research.* 2000;39(11):4315-4319.

20. Hu S, Li M, Li Y, Shen J, Liu Z. Reaction path synthesis methodology for waste minimization. *Science in China Series B: Chemistry.* 2004;47(3):206-213.

21. Ng DKS, Pham V, El-Halwagi MM, Jiménez-Gutiérrez A, Spriggs DH. A hierarchical approach to the synthesis and analysis of integrated biorefineries. Paper presented at: 7th International Conference on Foundations of Computer-Aided Process Design (FOCAPD 2009): Design for Energy and the Environment. 2009; Breckenridge, CO.

22. Bao B, Ng DKS, El-Halwagi MM, Tay DHS. Synthesis of technology pathways for an integrated biorefinery. *AIChE Annual Meeting*. Nashville, TN. 2009.

23. Aden A, Ruth M, Ibsen K, Jechura J, Neeves K, et al. *Lignocellulosic biomass to ethanol process design and economics utilizing co-current dilute acid prehydrolysis and enzymatic hydrolysis for corn stover*. Golden, CO: National Renewable Energy Laboratory; 2002. NREL/TP-510-32438.

24. Zhu Y, Jones S. *Techno-economic analysis for the thermochemical conversion of lignocellulosic biomass to ethanol via acetic acid synthesis.* Richland, WA: Pacific Northwest National Laboratory; 2009. PNNL-18483.

25. Phillips SD. Technoeconomic analysis of a lignocellulosic biomass indirect gasification process to make ethanol via mixed alcohols synthesis. *Industrial & Engineering Chemistry Research.* 2007;46(26):8887-8897.

26. Dutta A, Dowe N, Ibsen KN, Schell DJ, Aden A. An economic comparison of different fermentation configurations to convert corn stover to ethanol using Z. mobilis and Saccharomyces. *Biotechnology Progress.* 2010;26(1):64-72.

27. Kazi F, Fortman J, Anex R, Kothandaraman G, Hsu D, et al. *Techno-economic analysis of biochemical scenarios for production of cellulosic ethanol.* Golden, CO: National Renewable Energy Laboratory; 2010. NREL/TP-6A2-46588.

28. Pokoo-Aikins G, Nadim A, Mahalec V, El-Halwagi MM. Design and analysis of biodiesel production from algae grown through carbon sequestration. *Clean Technologies and Environmental Policy.* 2010;12(3):239-254.

29. Myint LL, El-Halwagi MM. Process analysis and optimization of biodiesel production from soybean oil. *Clean Technologies and Environmental Policy.* 2009;11(3):263-276.

30. Pham V, Holtzapple M, El-Halwagi MM. Techno-economic analysis of biomass to fuels conversion via the MixAlco process. *Journal of Industrial Microbiology & Biotechnology.* 2010;37(11):1157-1168.

31. Holtzapple M, Granda C. Carboxylate platform: The MixAlco process part 1: Comparison of three biomass conversion platforms. *Applied Biochemistry and Biotechnology.* 2009;156(1):95-106.

32. Jones S, Zhu Y, Valkenburg C. *Municipal solid waste (MSW) to liquid fuels synthesis. Volume 2: A techno-economic evaluation of the production of mixed alcohols.* Richland, WA: Pacific Northwest National Laboratory; 2009. PNNL-18482.

33. Mohan T, El-Halwagi MM. An algebraic targeting approach for effective utilization of biomass in cogeneration systems through process integration. *Clean Technologies and Environmental Policy.* 2007;9(1):13-25.

34. Qin X, Mohan T, El-Halwagi MM, Cornforth F, McCarl BA. Switchgrass as an alternate feedstock for power generation: Integrated environmental, energy, and economic life cycle analysis. *Clean Technologies and Environmental Policy.* 2006;8(4):233-249.

35. Alvarado-Morales M, Gernaey KV, Woodley JM, Gani R. Synthesis, design and analysis of downstream separation in bio-refinery processes through a group-contribution approach. In: Pierucci S, Ferraris GB, eds. *Computer aided chemical engineering.* Vol 28: 20th European Symposium on Computer Aided Process Engineering (ESCAPE20). 2010:1147-1152.

36. Gosling I. Process simulation and modeling for industrial bioprocessing: Tools and techniques. *Industrial Biotechnology.* 2005;I(2):106-109.

37. Harper PM, Gani R. A multi-step and multi-level approach for computer aided molecular design. *Computers and Chemical Engineering.* 2000;24(2):667-683.

38. Elms RD, El-Halwagi MM. Optimal scheduling and operation of biodiesel plants with multiple feedstocks. *Int. J. Process Systems Engineering.* 2009;1(1):1-28.

39. Pokoo-Aikins G, Heath A, Mentzer RA, Mannan MS, Rogers WJ, El-Halwagi MM. A multi-criteria approach to screening alternatives for converting sewage sludge to biodiesel. *Loss Prevention in the Process Industries.* 2010;23(3):412-420.

40. Kasra S. *Entropy analysis as a tool for optimal sustainable use of biorefineries*. Boras, Sweden: School of Engineering, University College of Boras; 2007.

41. Sammons Jr NE, Yuan W, Eden MR, Aksoy B, Cullinan HT. Optimal biorefinery resource utilization by combining process and economic modeling. *Chemical Engineering Research and Design.* 2008;86(7):800-808.

42. Villegas JD, Gnansounou E. Techno-economic and environmental evaluation of lignocellulosic biochemical refineries: Need for a modular platform for integrated assessment (MPIA). *Journal of Scientific & Industrial Research.* 2008;67:1017-1030.

43. Ng DKS. Automated targeting for the synthesis of an integrated biorefinery. *Chemical Engineering Journal.* 2010;162(1):67-74.

44. Bellman RE. *Dynamic programming*. Princeton, NJ: Princeton University Press; 1957.

45. Denardo EV. *Dynamic programming: Models and applications*. Mineola, NY: Dover Publications; 2003.

46. Goyal HB, Seal D, Saxena RC. Bio-fuels from thermochemical conversion of renewable resources: A review. *Renewable and Sustainable Energy Reviews.* 2008;12(2):504-517.

47. Blommel PG, Cortright RD. Production of conventional liquid fuels from sugars. 2008. http://www.virent.com/BioForming/Virent_Technology_Whitepaper.pdf. Accessed March 3rd, 2011.

48. Piccolo C, Bezzo F. A techno-economic comparison between two technologies for bioethanol production from lignocellulose. *Biomass and Bioenergy.* 2009;33(3):478-491.

49. Schmittinger P. *Chlorine: Principles and industrial practice*. 1st ed. Weinheim, Germany: Wiley-VCH; 2000.

50. Hamelinck C, Hooijdonk G, Faaij A. Ethanol from lignocellulosic biomass: Techno-economic performance in short-, middle-and long-term. *Biomass and Bioenergy.* 2005;28(4):384-410.

51. Gassner M, Maréchal F. Thermo-economic process model for thermochemical production of synthetic natural gas (SNG) from lignocellulosic biomass. *Biomass and Bioenergy.* 2009;33(11):1587-1604.

52. U.S. Environmental Protection Agency. Landfill methane outreach program: Potential benefits gained by landfill owners/operators from landfill gas energy; 2002:1-2.

53. Gray EE. Appendix H: Technologies for biofuels production. In: *Renewable fuels roadmap and sustainable biomass feedstock supply for New York.* Albany, NY: Antares Group, Inc.; 2010.

54. Hamelinck CN, Faaij APC. Future prospects for production of methanol and hydrogen from biomass. *Journal of Power Sources.* 2002;111(1):1-22.

55. Carey FA, Sundberg RJ. Advanced organic chemistry - Part B: Reactions and synthesis (5th edition). *Advanced organic chemistry*. New York, NY: Springer - Verlag; 2007:639.

56. Chang NS. *The kinetic studies of enzymatic cellulose hydrolysis and catalytic ketone hydrogenation*. College Station, TX: Chemical Engineering, Texas A&M University; 1994.

57. Kiff B, Schreck D, Inventors; Union Carbide Corporation, assignee. Production of ethanol from acetic acid. US patent 4421939. 12/20/1983, 1983.

58. Bechtel. *Task 4.2 Commercial applications - Economics of MTBE via mixed alcohol*: Prepared for Air Products and Chemicals, Inc.;1998. Available from DOE Scientific and Technical Information (OSTI).

59. Kowalewicz A. Methanol as a fuel for spark ignition engines: A review and analysis. *Journal of Automobile Engineering.* 1993;207(D1):43-52.

60. Granda C, Holtzapple M, Luce G, Searcy K, Mamrosh D. Carboxylate platform: The MixAlco process part 2: Process economics. *Applied Biochemistry and Biotechnology.* 2009;156(1):107-124.

61. Pham V, Granda C, Holtzapple M, El-Halwagi M. Techno-economic analysis of biomass to fuel via the MixAlco process. *AIChE 2010 Spring Meeting*. San Antonio, Texas. 2010.

62. Pfromm PH, Amanor-Boadu V, Nelson R, Vadlani P, Madl R. Bio-butanol vs. bio-ethanol: A technical and economic assessment for corn and switchgrass fermented by yeast or *Clostridium acetobutylicum*. *Biomass and Bioenergy*. 2010;34(4):515-524.

63. DOL. Producer Price Index for chemical and allied products. Department of Labor, Bureau of Labor Statistics; 2010. http://data.bls.gov/PDQ/servlet/SurveyOutputServlet?series_id=WPU06&data_tool=XGtable. Accessed September 1st, 2010.

64. Pistikopoulos E. Uncertainty in process design and operations. *Computers & Chemical Engineering.* 1995;19:553-563.

65. Bernardo F, Saraiva P, Pistikopoulos E. Process design under uncertainty: Robustness criteria and value of information. *Computer Aided Chemical Engineering.* 2003;16:175-208.

66. Taguchi G. *Introduction to quality engineering: Designing quality into products and processes*. Tokyo, Japan: Asian Productivity Organization; 1986.

67. Rudd DF, Watson CCm. *Strategy of process engineering*. New York: John Wiley & Sons; 1968.

68. Grossmann IE, Halemane KP, Swaney RE. Optimization strategies for flexible chemical processes. *Computers & Chemical Engineering.* 1983;7(4):439-462.

69. Halemane KP, Grossmann IE. Optimal process design under uncertainty. *AIChE Journal.* 1983;29(3):425-433.

70. Grossmann IE, Sargent RWH. Optimum design of chemical plants with uncertain parameters. *AIChE Journal.* 1978;24(6):1021 - 1028.

71. Swaney RE, Grossmann IE. An index for operational flexibility in chemical process design. Part I: Formulation and theory. *AIChE Journal.* 1985;31(4):621-630.

72. Swaney RE, Grossmann IE. An index for operational flexibility in chemical process design. Part II: Computational algorithms. *AIChE Journal.* 1985;31(4):631-641.

73. Grossmann IE, Floudas CA. Active constraint strategy for flexibility analysis in chemical processes. *Computers & Chemical Engineering.* 1987;11(6):675-693.

74. Pistikopoulos EN, Grossmann IE. Optimal retrofit design for improving process flexibility in linear systems. *Computers & Chemical Engineering.* 1988;12(7):719-731.

75. Pistikopoulos E, Grossmann I. Optimal retrofit design for improving process flexibility in nonlinear systems - I. Fixed degree of flexibility. *Computers & Chemical Engineering.* 1989;13(9):1003-1016.

76. Pistikopoulos E, Grossmann I. Optimal retrofit design for improving process flexibility in nonlinear systems - II. Optimal level of flexibility. *Computers & Chemical Engineering.* 1989;13(10):1087-1096.

77. Pistikopoulos EN, Grossmann IE. Stochastic optimization of flexibility in retrofit design of linear systems. *Computers & Chemical Engineering.* 1988;12(12):1215-1227.

78. Straub D, Grossmann I. Integrated stochastic metric of flexibility for systems with discrete state and continuous parameter uncertainties. *Computers & Chemical Engineering.* 1990;14(9):967-985.

79. Straub DA, Grossmann IE. Design optimization of stochastic flexibility. *Computers & Chemical Engineering.* 1993;17(4):339-354.

80. Pistikopoulos E, Ierapetritou M. Novel approach for optimal process design under uncertainty. *Computers & Chemical Engineering.* 1995;19(10):1089-1110.

81. Grossmann IE, Straub DA. Recent developments in the evaluation and optimization of flexible chemical processes. In: Puigjaner L, Espuna A, eds. *Computer-oriented process engineering*. Amsterdam, Neitherland: Elsevier; 1991.

82. USDA. Price received by farmers for corn by month - United States. National Agricultural Statistics Service. U.S. Department of Agriculture; 2011. http://www.nass.usda.gov/Charts_and_Maps/graphics/data/pricecn.txt. Accessed May 23rd, 2011.

83. USDA. Corn: U.S. cold storage stocks by month and year from January 2008 to April 2011. National Agricultural Statistics Service. U.S. Department of Agriculture; 2011. http://www.nass.usda.gov/Charts_and_Maps/Crops_Cold_ Storage/corn.asp. Accessed May 22nd, 2011.

84. Theoretical ethanol yield calculator. Energy efficiency & renewable energy; 2011. http://www1.eere.energy.gov/biomass/ethanol_yield_calculator.html. Accessed May 24th, 2011.

85. Lindo. *Lingo user's guide* [computer program]. Version 11. Chicago, IL: LINDO Systems Inc.; 2010.

86. Agler MT, Wrenn BA, Zinder SH, Angenent LT. Waste to bioproduct conversion with undefined mixed cultures: The carboxylate platform. *Trends in biotechnology.* 2011;29(2):70-78.

87. Holtzapple M, Davison R, Ross M, Aldrett-Lee S, Nagwani M, et al. Biomass conversion to mixed alcohol fuels using the MixAlco process. *Applied Biochemistry and Biotechnology.* 1999;79(1):609-631.

88. Lau MH, Richardson JW, Outlaw JL, Holtzapple MT, Ochoa RF. The economics of ethanol from sweet sorghum using the MixAlco process. 2006. http://www.afpc.tamu.edu/pubs/2/446/RR%2006-2.pdf. Accessed August 11, 2006.

89. Pham V, Holtzapple M, El-Halwagi M. Techno-economic analysis of biomass to fuel conversion via the MixAlco process. *Journal of Industrial Microbiology and Biotechnology.* 2010:1-12.

90. Aspentech. *Aspen Plus* [computer program]. Version 7. Cambridge, MA; 2010.

91. Aspentech. *Aspen Process Economic Analyzer* [computer program]. Cambridge, MA; 2010.

92. Wooley RJ, Putsche V. *Development of an ASPEN PLUS physical property database for biofuels components*. Golden, CO: National Renewable Energy Laboratory; 1996.

93. Wooley R, Putsche V. *Development of an ASPEN PLUS physical property database for biofuels components.* Golden, CO: National Renewable Energy Laboratory; 1996.

94. Linnhoff B. Pinch analysis: A state-of-the-art overview: Techno-economic analysis. *Chemical Engineering Research & Design.* 1993;71(5):503-522.

95. El-Halwagi M. *Process integration.* San Diego, CA: Academic Press; 2006.

96. Wright MM, Daugaard DE, Satrio JA, Brown RC. Techno-economic analysis of biomass fast pyrolysis to transportation fuels. *Fuel.* 2010;89(Supplement 1):S2-S10.

97. Walas SM. *Chemical process equipment: Selection and design.* Boston: Butterworths; 1988.

98. Peters MS, Timmerhaus KD, West RE. *Plant design and Economics for chemical engineers*. 5th ed. New York: McGraw-Hill; 2003.

99. Chemical Engineering's Plant Cost Index. Chemical Engineering; 2011. Accessed January 2011.

100. Rapier R. *Volatile fatty acid fermentation of lime-treated biomass by rumen microorganisms*. College Station: Chemical Engineering, Texas A&M University; 1995.

101. Lara JR, Holtzapple MT. Experimental investigation of dropwise condensation on hydrophobic heat exchangers part I: Dimpled-sheets. *Desalination.* In Press, Corrected Proof.

102. Lara JR, Holtzapple M. Experimental investigation of dropwise condensation on hydrophobic heat exchangers. Part 2: Effect of coatings and surface geometry. Manuscript.

103. Chang NS. *The kinetics studies of enzymatic cellulose hydrolysis and catalytic ketone hydrogenation* [PhD. dissertation]. College Station, Texas: Chemical Engineering, Texas A&M; 1994.

104. Capareda S. College Station, Texas; 2010. Personal communication.

105. Palmisano A, Barlaz M. *Microbiology of solid waste*. Boca Raton, FL: CRC Press; 1996.

106. Sims B. Terrabon Achieves Production Milestone at Texas Demo Facility. *Biorefining.* 2011. http://www.biorefiningmagazine.com/articles/5278/terrabon-achieves-production-milestone-at-texas-demo-facility. Accessed January 27, 2011.

107. AspenTech. Aspen Plus: System management. Version 11.1. Cambridge, MA; 2001:4.1 - 4.9.

108. Holtzapple M. Cellulose. In: Caballero B, Trugo LC, Finglas PM, eds. *Encyclopedia of food science, food technology, and nutrition*. 2nd ed. London, England: Academic; 2003.

109. Holtzapple M. Lignin. In: Caballero B, Trugo LC, Finglas PM, eds. *Encyclopedia of food science, food technology, and nutrition*. 2nd ed. London, England: Academic; 2003:3535 - 3542.

110. Short W, Packey DJ, Holt T. *A manual for the economic evaluation and energy efficiency and renewable energy technologies.* Golden, CO: National Renewable Energy Laboratory; 1995.

111. Garrett D. *Chemical engineering economics.* New York: Van Nostrand Reinhold; 1989.

112. Seider W, Seader J, Lewin D. *Product and process design principles: Synthesis, analysis, and evaluation*. New York: Wiley; 2004.

113. Spot prices for crude oil and petroleum products. U.S. Energy Information Administration. http://tonto.eia.doe.gov/dnav/pet/pet_pri_spt_s1_m.htm. Accessed February 12th, 2011.

114. Domke SB, Aiello-Mazzarri C, Holtzapple MT. Mixed acid fermentation of paper fines and industrial biosludge. *Bioresour. Technol.* 2003;91(1):41-51.

115. Thanakoses P, Black AS, Holtzapple MT. Fermentation of corn stover to carboxylic acids. *Biotechnol. Bioeng.* 2003;83(2):191-200.

116. Agbogbo FK, Holtzapple MT. Fermentation of rice straw/chicken manure to carboxylic acids using a mixed culture of marine mesophilic microorganisms. *Appl. Biochem. Biotechnol.* 2006;129-132:997-1014.

117. Fu Z, Holtzapple M. Fermentation of sugarcane bagasse and chicken manure to calcium carboxylates under thermophilic conditions. *Applied Biochemistry and Biotechnology.* 2010;162(2):561-578.

APPENDIX A

INPUT DATA FOR THE CASE STUDY OF BIOREFINERY DESIGN WITH AN OPTIMUM LEVEL OF FLEXIBILITY

Table 17. Input data for raw material composition (%).

Index	Name	CELLULOSE	XYLAN	LIGNIN	HYDROGEN	WATER
1	Biomass 1	35	7.5	7.5	0	50
2	Biomass 2	25	10	15	0	50
3	Hydrogen	0	0	0	100	0

Table 18. Input data for raw material availabilities (tonne/h).

Index	Name	Scenario					
		1	2	3	4	5	6
1	Biomass 1	300	300	300	300	300	300
2	Biomass 2	450	450	450	**250**	450	450
3	Hydrogen	3	3	3	3	3	3

Table 19. Input data for raw material costs ($/tonne).

Index	Name	Scenario					
		1	2	3	4	5	6
1	Biomass 1	30	30	**90**	30	30	30
2	Biomass 2	5	5	**40**	5	5	5
3	Hydrogen	4,000	**200**	4,000	4,000	4,000	4,000

Table 20. Input data for product demand (tonne/h).

Index	Name	Scenario					
		1	2	3	4	5	6
1	Mixed alcohols	60	60	60	60	60	**120**
2	Lime	30	30	30	30	30	**60**

Table 21. Input data for product prices ($/tonne).

Index	Name	Scenario					
		1	2	3	4	5	6
1	Mixed alcohols	686	686	686	686	686	686
2	Lime	70	70	70	70	70	70

Table 22. Input data for capital costs of equipment.

Index	Equipment	CAPCOEF	SCALE	SIZECOEF	Characteristic size
1	Pretreatment	15.21	0.682	9.00	Total pile volume (1,000 m^3)
2	Fermentation	90.99	0.668	9.00	Total pile volume (1,000 m^3)
3	Vapor compression system	2,714	0.612	0.11	Total latent heat transfer area (1,000m^2)
4	Crystallization	1,274	0.612	0.80	Water vaporization rate (tonne/h)
5	Ketonization	3,064	0.544	0.43	Carboxylate salt rate (tonne/h)
6	Hydrogenation	3,863	0.538	0.30	Ketone rate (tonne/h)
7	Gasification	1,643	0.694	1.50	Inlet solid rate (tonne/h)
8	Cogeneration	170.8	0.694	6.80	Inlet gas rate (tonne/h)
9	Water-gas shift	4,596	0.694	0.57	Inlet carbon monoxide rate (tonne/h)
10	Pressure swing adsorption	798.6	0.694	62.0	Inlet gas rate (tonne/h)
11	Lime kiln	78.44	0.600	1.80	Calcium carbonate rate (tonne/h)

Table 23. Data for operating costs of equipment.

Index	Equipment	OPCOEF	Characteristic flow rate (tonne/h)
1	Pretreatment	38	Wet biomass rate
2	Fermentation	74	Wet biomass rate
3	Vapor compression system	71	Salt solution (excluding contaminants) rate from fermentation
4	Crystallization	67	Salt solution (excluding contaminants) rate from fermentation
5	Ketonization	27.9	Salt solution (excluding contaminants) rate from fermentation
6	Hydrogenation	20.6	Ketone rate
7	Gasification	201	Inlet solid rate
8	Cogeneration	-12.7	Inlet gas rate
9	Water-gas shift	8.8	Inlet carbon monoxide rate
10	Pressure swing adsorption	0.8	Inlet gas rate
11	Lime kiln	46	Calcium carbonate rate

Table 24. Yield matrices (Scenario 1/Scenario 5 if yield is varied).

		Inlet components									
	Outlet components	CELLULOSE	XYLAN	LIGNIN	CARBO	KETONE	HYDRO	SYNGAS	WATER	ALCOHOL	LIME
Equipment 1: Pretreatment	CELLULOSE	1	0	0	0	0	0	0	0	0	0
	XYLAN	0	1	0	0	0	0	0	0	0	0
	LIGNIN	0	0	1	0	0	0	0	0	0	0
	CARBO	0	0	0	1	0	0	0	0	0	0
	KETONE	0	0	0	0	1	0	0	0	0	0
	HYDRO	0	0	0	0	0	1	0	0	0	0
	SYNGAS	0	0	0	0	0	0	1	0	0	0
	WATER	0	0	0	0	0	0	0	1	0	0
	ALCOHOL	0	0	0	0	0	0	0	0	1	0
	LIME	0	0	0	0	0	0	0	0	0	0
Equipment 2: Fermentation	CELLULOSE	**0.5 / 0.6**	0	0	**0.5 / 0.4**	0	0	0	0	0	0
	XYLAN	0	**0.4/0.52**	0	**0.6/0.48**	0	0	0	0	0	0
	LIGNIN	0	0	1	0	0	0	0	0	0	0
	CARBO	0	0	0	1	0	0	0	0	0	0
	KETONE	0	0	0	0	1	0	0	0	0	0
	HYDRO	0	0	0	0	0	1	0	0	0	0
	SYNGAS	0	0	0	0	0	0	1	0	0	0
	WATER	0	0	0	0	0	0	0	1	0	0
	ALCOHOL	0	0	0	0	0	0	0	0	1	0
	LIME	0	0	0	0	0	0	0	0	0	1

Table 24 continued.

		Inlet components									
Outlet components		CELLULOSE	XYLAN	LIGNIN	CARBO	KETONE	HYDRO	SYNGAS	WATER	ALCOHOL	LIME
Equipment 3: Vapor compression system	CELLULOSE	1	0	0	0	0	0	0	0	0	0
	XYLAN	0	1	0	0	0	0	0	0	0	0
	LIGNIN	0	0	1	0	0	0	0	0	0	0
	CARBO	0	0	0	1	0	0	0	0	0	0
	KETONE	0	0	0	0	1	0	0	0	0	0
	HYDRO	0	0	0	0	0	1	0	0	0	0
	SYNGAS	0	0	0	0	0	0	1	0	0	0
	WATER	0	0	0	0	0	0	0	0.3	0	0
	ALCOHOL	0	0	0	0	0	0	0	0	1	0
	LIME	0	0	0	0	0	0	0	0	0	1
Equipment 4: Crystallization	CELLULOSE	1	0	0	0	0	0	0	0	0	0
	XYLAN	0	1	0	0	0	0	0	0	0	0
	LIGNIN	0	0	1	0	0	0	0	0	0	0
	CARBO	0	0	0	1	0	0	0	0	0	0
	KETONE	0	0	0	0	1	0	0	0	0	0
	HYDRO	0	0	0	0	0	1	0	0	0	0
	SYNGAS	0	0	0	0	0	0	1	0	0	0
	WATER	0	0	0	0	0	0	0	0	0	0
	ALCOHOL	0	0	0	0	0	0	0	0	1	0
	LIME	0	0	0	0	0	0	0	0	0	1

Table 24 continued.

		Inlet components									
Outlet components		CELLULOSE	XYLAN	LIGNIN	CARBO	KETONE	HYDRO	SYNGAS	WATER	ALCOHOL	LIME
Equipment 5: Ketonization	CELLULOSE	1	0	0	0	0	0	0	0	0	0
	XYLAN	0	1	0	0	0	0	0	0	0	0
	LIGNIN	0	0	1	0	0	0	0	0	0	0
	CARBO	0	0	0	0	0.46	0	0.30	0	0	0.24
	KETONE	0	0	0	0	1	0	0	0	0	0
	HYDRO	0	0	0	0	0	1	0	0	0	0
	SYNGAS	0	0	0	0	0	0	1	0	0	0
	WATER	0	0	0	0	0	0	0	1	0	0
	ALCOHOL	0	0	0	0	0	0	0	0	1	0
	LIME	0	0	0	0	0	0	0	0	0	1
Equipment 6: Hydrogenation	CELLULOSE	1	0	0	0	0	0	0	0	0	0
	XYLAN	0	1	0	0	0	0	0	0	0	0
	LIGNIN	0	0	1	0	0	0	0	0	0	0
	CARBO	0	0	0	1	0	0	0	0	0	0
	KETONE	0	0	0	0	0	0	0	0	1	0
	HYDRO	0	0	0	0	0	0	0	0	1	0
	SYNGAS	0	0	0	0	0	0	1	0	0	0
	WATER	0	0	0	0	0	0	0	1	0	0
	ALCOHOL	0	0	0	0	0	0	0	0	1	0
	LIME	0	0	0	0	0	0	0	0	0	1

Table 24 continued.

		Inlet components									
Outlet components		CELLULOSE	XYLAN	LIGNIN	CARBO	KETONE	HYDRO	SYNGAS	WATER	ALCOHOL	LIME
Equipment 7: Gasification	CELLULOSE	0	0	0	0	0	0	0.4	0	0	0
	XYLAN	0	0	0	0	0	0	0.4	0	0	0
	LIGNIN	0	0	0	0	0	0	0.4	0	0	0
	CARBO	0	0	0	1	0	0	0	0	0	0
	KETONE	0	0	0	0	1	0	0	0	0	0
	HYDRO	0	0	0	0	0	1	0	0	0	0
	SYNGAS	0	0	0	0	0	0	1	0	0	0
	WATER	0	0	0	0	0	0	0	1	0	0
	ALCOHOL	0	0	0	0	0	0	0	0	1	0
	LIME	0	0	0	0	0	0	0	0	0	1
Equipment 8: Cogeneration	CELLULOSE	1	0	0	0	0	0	0	0	0	0
	XYLAN	0	1	0	0	0	0	0	0	0	0
	LIGNIN	0	0	1	0	0	0	0	0	0	0
	CARBO	0	0	0	1	0	0	0	0	0	0
	KETONE	0	0	0	0	1	0	0	0	0	0
	HYDRO	0	0	0	0	0	1	0	0	0	0
	SYNGAS	0	0	0	0	0	0	1	0	0	0
	WATER	0	0	0	0	0	0	0	1	0	0
	ALCOHOL	0	0	0	0	0	0	0	0	1	0
	LIME	0	0	0	0	0	0	0	0	0	1

Table 24 continued.

		Inlet components									
Outlet components		CELLULOSE	XYLAN	LIGNIN	CARBO	KETONE	HYDRO	SYNGAS	WATER	ALCOHOL	LIME
Equipment 9: Water-gas shift	CELLULOSE	1	0	0	0	0	0	0	0	0	0
	XYLAN	0	1	0	0	0	0	0	0	0	0
	LIGNIN	0	0	1	0	0	0	0	0	0	0
	CARBO	0	0	0	1	0	0	0	0	0	0
	KETONE	0	0	0	0	1	0	0	0	0	0
	HYDRO	0	0	0	0	0	1	0	0	0	0
	SYNGAS	0	0	0	0	0	0	0.60	0	0	0
	WATER	0	0	0	0	0	0	0	1	0	0
	ALCOHOL	0	0	0	0	0	0	0	0	1	0
	LIME	0	0	0	0	0	0	0	0	0	1
Equipment 10: Pressure swing	CELLULOSE	1	0	0	0	0	0	0	0	0	0
	XYLAN	0	1	0	0	0	0	0	0	0	0
	LIGNIN	0	0	1	0	0	0	0	0	0	0
	CARBO	0	0	0	1	0	0	0	0	0	0
	KETONE	0	0	0	0	1	0	0	0	0	0
	HYDRO	0	0	0	0	0	1	0	0	0	0
	SYNGAS	0	0	0	0	0	0.05	0.95	0	0	0
	WATER	0	0	0	0	0	0	0	1	0	0
	ALCOHOL	0	0	0	0	0	0	0	0	1	0
	LIME	0	0	0	0	0	0	0	0	0	1

Table 24 continued.

		Inlet components									
Outlet components		CELLULOSE	XYLAN	LIGNIN	CARBO	KETONE	HYDRO	SYNGAS	WATER	ALCOHOL	LIME
Equipment 11: Lime kiln	CELLULOSE	1	0	0	0	0	0	0	0	0	0
	XYLAN	0	1	0	0	0	0	0	0	0	0
	LIGNIN	0	0	1	0	0	0	0	0	0	0
	CARBO	0	0	0	1	0	0	0	0	0	0
	KETONE	0	0	0	0	1	0	0	0	0	0
	HYDRO	0	0	0	0	0	1	0	0	0	0
	SYNGAS	0	0	0	0	0	0	1	0	0	0
	WATER	0	0	0	0	0	0	0	1	0	0
	ALCOHOL	0	0	0	0	0	0	0	0	1	0
	LIME	0	0	0	0	0	0	0	0	0	1

APPENDIX B

LINGO MODEL FOR THE CASE STUDY OF BIOREFINERY DESIGN WITH AN OPTIMUM LEVEL OF FLEXIBILITY

```
SETS:
! Three raw materials: two lignocellulosic sources and external H2;
      RAW /1..3/;
! Two products: mixed alcohols and Lime;
      PRODUCT /1..2/;
! Ten main components;
      COMPONENT /CELLULOSE, XYLAN, LIGNIN, CARBOX, KETONE, HYDRO,
                 SYNGAS, WATER, ALCOHOL, LIME/;
! Eleven processing units. See the end of the model for the list of
equipment with assigned indices;
      EQUIPMENT /1..11/: CAPCOEF, SCALE, MSIZE, SIZECOEF, OPCOEF;
! Six scenarios;
      SCENARIO /1..6/: PROB;

! Derived sets from two sets;
      RAW_SCENARIO (RAW, SCENARIO): COST, SUPPLY, AVAIL;
      PRODUCT_SCENARIO (PRODUCT, SCENARIO): PRICE, DEMAND, PROD;
      EQUIPMENT_SCENARIO (EQUIPMENT, SCENARIO): SIZE, TFLOW, Y;

! Derived sets from three sets;
      RAW_COMP (RAW, COMPONENT): FRACTION;
      RAW_SCEN_COMP (RAW, SCENARIO, COMPONENT): CONTENT;
      EQUI_SCEN_COMP (EQUIPMENT, SCENARIO, COMPONENT): FIN, FOUT,
                                                       WASTE;
      EQUI_SCEN_COMP_COMP (EQUIPMENT, SCENARIO, COMPONENT, COMPONENT):
            YIELD;
ENDSETS

DATA:
! Data are imported from a spreadsheet;
      CAPCOEF, OPCOEF, SCALE, SIZECOEF, PROB, COST, AVAIL, PRICE,
      DEMAND, FRACTION, YIELD = @OLE('Data.xlsx');
! Results are exported to a spreadsheet;
      @OLE('Data.xlsx') = Y, TFLOW, SIZE, MSIZE, SUPPLY, PROD, FIN,
      FOUT;
ENDDATA

! Maximum profit ($1,000/year);
MAX = @SUM(SCENARIO(p): PROB(p)*(         ! Expected value of revenue;
       8*@SUM(PRODUCT(k):PRICE(k,p)*PROD(k,p))  ! Sale income;
      -8*@SUM(RAW(i):COST(i,p)*SUPPLY(i,p))     ! Raw materials costs;
        -@SUM(EQUIPMENT(j):OPCOEF(j)*TFLOW(j,p))! Operating costs;
   -22*8*@SUM(EQUIPMENT(j):@SUM(COMPONENT(m): WASTE(j,p,m))))) ! Waste;
    - @SUM(EQUIPMENT(j):CAPCOEF(j)*MSIZE(j)^SCALE(j))/7;!Capital costs;

! Raw availability;
```

```
      @FOR(RAW_SCENARIO: SUPPLY <= AVAIL);
! Production limitation;
      @FOR(PRODUCT_SCENARIO: PROD <= DEMAND);
! Mass balance through equipment;
      @FOR(EQUI_SCEN_COMP(j,p,m):
      FOUT(j,p,m)=@SUM(COMPONENT(n):FIN(j,p,n)*YIELD(j,p,n,m)));
! Total inlet flow rate;
      @FOR(EQUIPMENT_SCENARIO(j,p):
      TFLOW(j,p)=@SUM(COMPONENT(m):FIN(j,p,m)));
! Mass balance between equipment (define process structure);
      @FOR(SCENARIO(p):
      ! Raw contents;
            @FOR(RAW_COMP(i,m):
            CONTENT(i,p,m) = FRACTION (i,m)*SUPPLY(i,p));
      ! Raw - Pretreatment;
            @FOR(COMPONENT(m): @SUM(RAW(i)|i#LE#2:
            CONTENT(i,p,m)) = FIN(1,p,m));
      ! Pretreatment - Fermentation;
            @FOR(COMPONENT(m): FOUT(1,p,m) = FIN(2,p,m));
      ! Fermentation - Vapor compression system & Gasification;
            @FOR(COMPONENT(m)|m#GE#4:  FOUT(2,p,m) = FIN(3,p,m));
            @FOR(COMPONENT(m)|m#LT#4:  FOUT(2,p,m) = FIN(7,p,m) +
                                                     WASTE(2,p,m));
            @FOR(COMPONENT(m)|m#GE#4:           0 = FIN(7,p,m));
            @FOR(COMPONENT(m)|m#LT#4:           0 = FIN(3,p,m));
      ! Vapor compression system - Crystallization;
            @FOR(COMPONENT(m): FOUT(3,p,m) = FIN(4,p,m));
      ! Crystallization - Ketonization;
            @FOR(COMPONENT(m): FOUT(4,p,m) = FIN(5,p,m));
      ! Ketonization & Pressure swing absorption - Hydrogenation & Lime
      kiln;
            FOUT(5,p,10) = FIN (11,p,10);
            FOUT(5,p,7) = FIN (11,p,7);
            @FOR(COMPONENT(m)|(m#LE#9)#AND#(m#NE#7): 0 = FIN (11,p,m));
            FOUT(5,p,6) + FOUT (10,p,6) + SUPPLY(3,p) = FIN(6,p,6);
            @FOR(COMPONENT(m)|m#NE#6: FOUT(5,p,m) = FIN(6,p,m) +
                                                    FIN (11,p,m));
            FOUT (10,p,6) + SUPPLY(3,p) = 0.055*FOUT(5,p,5);
            ! H2 consumption;
      ! Gasification - Cogeneration;
            @FOR(COMPONENT(m): FOUT(7,p,m) = FIN(8,p,m));
      ! Cogeneration - Water-gas shift;
            @FOR(COMPONENT(m): FOUT(8,p,m) = FIN(9,p,m));
      ! Water-gas shift - Pressure swing absorption;
            @FOR(COMPONENT(m): FOUT(9,p,m) = FIN(10,p,m));
      ! Final products;
            PROD(1,p) = FOUT(6,p,9);
            PROD(2,p) = FOUT(11,p,10);
      );
! Sizing contraints;
      @FOR(EQUIPMENT_SCENARIO(j,p):
      ! Sizes in a scenario;
            SIZE(j,p)=SIZECOEF(j)*TFLOW(j,p);
      ! Designed sizes;
```

```
            MSIZE(j) >= SIZE(j,p);
      ! Operational mode;
            0.5*Y(j,p)*MSIZE(j) <= SIZE(j,p);
            SIZE(j,p) <= 10000*Y(j,p);
            Y(j,p) <= 10*MSIZE(j);
            @BIN(Y(j,p));
      );
END

! List of equipment:
    Index   Name
      1.    Pretreatment
      2.    Fermentation
      3.    Vapor compression system
      4.    Crystallization
      5.    Ketonization
      6.    Hydrogenation
      7.    Gasification
      8.    Cogeneration
      9.    Water-gas shift
      10.   Pressure swing absorption
      11.   Lime kiln;
```

APPENDIX C

SOLUTIONS FOR THE CASE STUDY OF BIOREFINERY DESIGN WITH AN OPTIMUM LEVEL OF FLEXIBILITY

Figure 41. A snapshot of the Lingo solver status report for the case study.

Table 25. Results on raw materials, products, and waste (tonne/h).

Raw materials and products		Scenarios					
Name	Index	1	2	3	4	5	6
Raw materials name							
Lignocellulosic biomass 1	1	0	0	0	168	0	0
Lignocellulosic biomass 2	2	450	450	0	250	450	450
Hydrogen	3	0.41	0.41	0	0.60	0	0.41
Product name							
Mixed alcohols	1	40.4	40.4	0	40.4	32.3	40.4
Lime	2	19.8	19.8	0	19.8	15.8	19.8
Waste		0	142	0	0	18	0

Table 26. Results on operational mode (Y).

Processing units		Scenarios					
Name	Index	1	2	3	4	5	6
Pretreatment	1	1	1	0	1	1	1
Fermentation	2	1	1	0	1	1	1
Vapor compression system	3	1	1	0	1	1	1
Crystallization	4	1	1	0	1	1	1
Ketonization	5	1	1	0	1	1	1
Hydrogenation	6	1	1	0	1	1	1
Gasification	7	1	0	0	1	1	1
Cogeneration	8	1	0	0	1	1	1
Water-gas shift	9	1	0	0	1	1	1
Pressure swing absorption	10	1	0	0	1	1	1
Lime kiln	11	1	1	0	1	1	1

Table 27. Results on total flow rate (TFLOW).

Processing units		Scenarios					
Name	Index	1	2	3	4	5	6
Pretreatment	1	450	450	0	418	450	450
Fermentation	2	450	450	0	418	450	450
Vapor compression system	3	308	308	0	292	292	308
Crystallization	4	151	151	0	146	134	151
Ketonization	5	83	83	0	83	67	83
Hydrogenation	6	40	40	0	40	32	40
Gasification	7	142	0	0	126	140	142
Cogeneration	8	57	0	0	50	56	57
Water-gas shift	9	57	0	0	50	56	57
Pressure swing absorption	10	34	0	0	30	34	34
Lime kiln	11	45	45	0	45	36	45

Table 28. Results on sizes (SIZE and MSIZE).

Processing units		Size in every scenarios						Design size
Name	Index	1	2	3	4	5	6	
Pretreatment	1	4,050	4,050	0	3,764	4,050	4,050	4,050
Fermentation	2	4,050	4,050	0	3,764	4,050	4,050	4,050
Vapor compression system	3	34	34	0	32	32	34	34
Crystallization	4	121	121	0	117	107	121	121
Ketonization	5	36	36	0	36	29	36	36
Hydrogenation	6	12	12	0	12	10	12	12
Gasification	7	213	0	0	189	211	213	213
Cogeneration	8	386	0	0	342	382	386	386
Water-gas shift	9	32	0	0	29	32	32	32
Pressure swing absorption	10	2,109	0	0	1,873	2,089	2,109	2,109
Lime kiln	11	81	81	0	81	65	81	81

Table 29. Results on inlet components flow rate (FIN).

Index	Equipment	Scenario	Components										Total
			CELLULOSE	XYLAN	LIGNIN	CARBOX	KETONE	HYDRO	SYNGAS	WATER	ALCOHOL	LIME	
1	Pretreatment	1	112.5	45	67.5	0	0	0	0	225	0	0	450
		2	112.5	45	67.5	0	0	0	0	225	0	0	450
		3	0	0	0	0	0	0	0	0	0	0	0
		4	121.4	38	50.1	0	0	0	0	209	0	0	418
		5	112.5	45	67.5	0	0	0	0	225	0	0	450
		6	112.5	45	67.5	0	0	0	0	225	0	0	450
2	Fermentation	1	112.5	45	67.5	0	0	0	0	225	0	0	450
		2	112.5	45	67.5	0	0	0	0	225	0	0	450
		3	0	0	0	0	0	0	0	0	0	0	0
		4	121.4	38	50.1	0	0	0	0	209	0	0	418
		5	112.5	45	67.5	0	0	0	0	225	0	0	450
		6	112.5	45	67.5	0	0	0	0	225	0	0	450
3	Vapor compression system	1	0	0	0	83.25	0	0	0	225	0	0	308
		2	0	0	0	83.25	0	0	0	225	0	0	308
		3	0	0	0	0	0	0	0	0	0	0	0
		4	0	0	0	83.25	0	0	0	209	0	0	292
		5	0	0	0	66.6	0	0	0	225	0	0	292
		6	0	0	0	83.25	0	0	0	225	0	0	308
4	Crystallization	1	0	0	0	83.25	0	0	0	67.5	0	0	151
		2	0	0	0	83.25	0	0	0	67.5	0	0	151
		3	0	0	0	0	0	0	0	0	0	0	0
		4	0	0	0	83.25	0	0	0	62.7	0	0	146
		5	0	0	0	66.6	0	0	0	67.5	0	0	134
		6	0	0	0	83.25	0	0	0	67.5	0	0	151

Table 29 continued.

Index	Equipment	Scenario	Components										Total
			CELLULOSE	XYLAN	LIGNIN	CARBOX	KETONE	HYDRO	SYNGAS	WATER	ALCOHOL	LIME	
5	Ketonization	1	0	0	0	83.25	0	0	0	0	0	0	83
		2	0	0	0	83.25	0	0	0	0	0	0	83
		3	0	0	0	0	0	0	0	0	0	0	0
		4	0	0	0	83.25	0	0	0	0	0	0	83
		5	0	0	0	66.6	0	0	0	0	0	0	67
		6	0	0	0	83.25	0	0	0	0	0	0	83
6	Hydrogenation	1	0	0	0	0	38.3	2.11	0	0	0	0	40
		2	0	0	0	0	38.3	2.11	0	0	0	0	40
		3	0	0	0	0	0	0	0	0	0	0	0
		4	0	0	0	0	38.3	2.11	0	0	0	0	40
		5	0	0	0	0	30.6	1.68	0	0	0	0	32
		6	0	0	0	0	38.3	2.11	0	0	0	0	40
7	Gasification	1	56.25	18	67.5	0	0	0	0	0	0	0	142
		2	0	0	0	0	0	0	0	0	0	0	0
		3	0	0	0	0	0	0	0	0	0	0	0
		4	60.68	15.0	50.1	0	0	0	0	0	0	0	126
		5	49.52	23.4	67.5	0	0	0	0	0	0	0	140
		6	56.25	18	67.5	0	0	0	0	0	0	0	141
8	Cogeneration	1	0	0	0	0	0	0	56.7	0	0	0	57
		2	0	0	0	0	0	0	0	0	0	0	0
		3	0	0	0	0	0	0	0	0	0	0	0
		4	0	0	0	0	0	0	50.3	0	0	0	50
		5	0	0	0	0	0	0	56.2	0	0	0	56
		6	0	0	0	0	0	0	56.7	0	0	0	57

Table 29 continued.

Index	Equipment	Scenario	Components										Total
			CELLULOSE	XYLAN	LIGNIN	CARBOX	KETONE	HYDRO	SYNGAS	WATER	ALCOHOL	LIME	
9	Water-gas shift	1	0	0	0	0	0	0	56.7	0	0	0	57
		2	0	0	0	0	0	0	0	0	0	0	0
		3	0	0	0	0	0	0	0	0	0	0	0
		4	0	0	0	0	0	0	50.3	0	0	0	50.
		5	0	0	0	0	0	0	56.2	0	0	0	56
		6	0	0	0	0	0	0	56.7	0	0	0	57
10	Pressure swing absorption	1	0	0	0	0	0	0	34.0	0	0	0	34
		2	0	0	0	0	0	0	0	0	0	0	0
		3	0	0	0	0	0	0	0	0	0	0	0
		4	0	0	0	0	0	0	30.2	0	0	0	30
		5	0	0	0	0	0	0	33.7	0	0	0	34
		6	0	0	0	0	0	0	34.02	0	0	0	34
11	Lime kiln	1	0	0	0	0	0	0	25.2	0	0	19.8	45
		2	0	0	0	0	0	0	25.2	0	0	19.8	45
		3	0	0	0	0	0	0	0	0	0	0	0
		4	0	0	0	0	0	0	25.2	0	0	19.8	45
		5	0	0	0	0	0	0	20.1	0	0	15.8	36
		6	0	0	0	0	0	0	25.2	0	0	19.8	45

Table 30. Results on outlet component flow rates (FOUT).

Index	Equipment	Scenario	Components										Total
			CELLULOSE	XYLAN	LIGNIN	CARBOX	KETONE	HYDRO	SYNGAS	WATER	ALCOHOL	LIME	
1	Pretreatment	1	112.5	45	67.5	0	0	0	0	225	0	0	450
		2	112.5	45	67.5	0	0	0	0	225	0	0	450
		3	0	0	0	0	0	0	0	0	0	0	0
		4	121.4	38	50.1	0	0	0	0	209	0	0	418
		5	112.5	45	67.5	0	0	0	0	225	0	0	450
		6	112.5	45	67.5	0	0	0	0	225	0	0	450
2	Fermentation	1	56.25	18	67.5	83.25	0	0	0	225	0	0	450
		2	56.25	18	67.5	83.25	0	0	0	225	0	0	450
		3	0	0	0	0	0	0	0	0	0	0	0
		4	60.68	15	50.1	83.25	0	0	0	209	0	0	418
		5	67.5	23	67.5	66.6	0	0	0	225	0	0	450
		6	56.25	18	67.5	83.25	0	0	0	225	0	0	450
3	Vapor compression system	1	0	0	0	83.25	0	0	0	67.5	0	0	151
		2	0	0	0	83.25	0	0	0	67.5	0	0	151
		3	0	0	0	0	0	0	0	0	0	0	0
		4	0	0	0	83.25	0	0	0	62.7	0	0	146
		5	0	0	0	66.6	0	0	0	67.5	0	0	134
		6	0	0	0	83.25	0	0	0	67.5	0	0	151
4	Crystallization	1	0	0	0	83.25	0	0	0	0	0	0	83
		2	0	0	0	83.25	0	0	0	0	0	0	83
		3	0	0	0	0	0	0	0	0	0	0	0
		4	0	0	0	83.25	0	0	0	0	0	0	83
		5	0	0	0	66.6	0	0	0	0	0	0	67
		6	0	0	0	83.25	0	0	0	0	0	0	83

Table 30 continued.

Index	Equipment	Scenario	Components										Total
			CELLULOSE	XYLAN	LIGNIN	CARBOX	KETONE	HYDRO	SYNGAS	WATER	ALCOHOL	LIME	
5	Ketonization	1	0	0	0	0	38.3	0	25.2	0	0	19.8	83
		2	0	0	0	0	38.3	0	25.2	0	0	19.8	83
		3	0	0	0	0	0	0	0	0	0	0	0
		4	0	0	0	0	38.3	0	25.2	0	0	19.8	83
		5	0	0	0	0	30.6	0	20.1	0	0	15.8	67
		6	0	0	0	0	38.3	0	25.2	0	0	19.8	83
6	Hydrogenation	1	0	0	0	0	0	0	0	0	40.4	0	40
		2	0	0	0	0	0	0	0	0	40.4	0	40
		3	0	0	0	0	0	0	0	0	0	0	0
		4	0	0	0	0	0	0	0	0	40.4	0	40
		5	0	0	0	0	0	0	0	0	32.3	0	32
		6	0	0	0	0	0	0	0	0	40.4	0	40
7	Gasification	1	0	0	0	0	0	0	56.7	0	0	0	57
		2	0	0	0	0	0	0	0	0	0	0	0
		3	0	0	0	0	0	0	0	0	0	0	0
		4	0	0	0	0	0	0	50.3	0	0	0	50
		5	0	0	0	0	0	0	56.2	0	0	0	56
		6	0	0	0	0	0	0	56.7	0	0	0	57
8	Cogeneration	1	0	0	0	0	0	0	56.7	0	0	0	57
		2	0	0	0	0	0	0	0	0	0	0	0
		3	0	0	0	0	0	0	0	0	0	0	0
		4	0	0	0	0	0	0	50.3	0	0	0	50
		5	0	0	0	0	0	0	56.2	0	0	0	56
		6	0	0	0	0	0	0	56.7	0	0	0	57

Table 30 continued.

Index	Equipment	Scenario	Components										Total
			CELLULOSE	XYLAN	LIGNIN	CARBOX	KETONE	HYDRO	SYNGAS	WATER	ALCOHOL	LIME	
9	Water-gas shift	1	0	0	0	0	0	0	34.0	0	0	0	34
		2	0	0	0	0	0	0	0	0	0	0	0
		3	0	0	0	0	0	0	0	0	0	0	0
		4	0	0	0	0	0	0	30.2	0	0	0	30
		5	0	0	0	0	0	0	33.7	0	0	0	34
		6	0	0	0	0	0	0	34.0	0	0	0	34
10	Pressure-swing absorption	1	0	0	0	0	0	1.70	32.3	0	0	0	34
		2	0	0	0	0	0	0	0	0	0	0	0
		3	0	0	0	0	0	0	0	0	0	0	0
		4	0	0	0	0	0	1.51	28.7	0	0	0	30
		5	0	0	0	0	0	1.68	32.0	0	0	0	34
		6	0	0	0	0	0	1.70	32.3	0	0	0	34
11	Lime kiln	1	0	0	0	0	0	0	25.2	0	0	19.8	45
		2	0	0	0	0	0	0	25.2	0	0	19.8	45
		3	0	0	0	0	0	0	0	0	0	0	0
		4	0	0	0	0	0	0	25.2	0	0	19.8	45
		5	0	0	0	0	0	0	20.1	0	0	15.8	36
		6	0	0	0	0	0	0	25.2	0	0	19.8	45

VITA

Name:	Viet Pham
Address:	Department of Chemical Engineering, Texas A&M University, 3122 TAMU, College Station, TX 77843
Email Address:	viet.pham@ymail.com
Education:	B.E., Chemical Engineering, University of Technology at Ho Chi Minh City, Vietnam, 2002 M.S., Chemical Engineering, Texas A&M University, 2007 Ph.D., Chemical Engineering, Texas A&M University, 2011